RODOLFO CAMPOS ZANIN

PERFIL DE LIBERAÇÃO DE COMPOSTOS DE AROMA EM CAFÉ SOLÚVEL E CAPPUCCINO ADICIONADOS DE MICROCÁPSULAS DE ÓLEO DE CAFÉ TORRADO

Londrina
2019

RODOLFO CAMPOS ZANIN

PERFIL DE LIBERAÇÃO DE COMPOSTOS DE AROMA EM CAFÉ SOLÚVEL E CAPPUCCINO ADICIONADOS DE MICROCÁPSULAS DE ÓLEO DE CAFÉ TORRADO

Tese apresentada ao Curso de Doutorado em Ciência de Alimentos da Universidade Estadual de Londrina – Paraná, como requisito parcial à obtenção do título de Doutor em Ciência de Alimentos.

Orientador: Prof. Dr. Fabio Yamashita

Coorientadora: Prof. Dr[a] Louise Emy Kurozawa

Londrina
2019

Ficha de identificação da obra elaborada pelo autor, através do Programa de Geração Automática do Sistema de Bibliotecas da UEL

ZANIN, RODOLFO CAMPOS .

PERFIL DE LIBERAÇÃO DE COMPOSTOS DE AROMA EM CAFÉ SOLÚVEL E CAPPUCCINO ADICIONADOS DE MICROCÁPSULAS DE ÓLEO DE CAFÉ TORRADO / RODOLFO CAMPOS ZANIN. - Londrina, 2019.

129 f. : il.

Orientador: FABIO YAMASHITA.
Coorientador: LOUISE EMY KUROZAWA.

Tese (Doutorado em Ciência de Alimentos) - Universidade Estadual de Londrina, Centro de Ciências Agrárias, , 2019.

Inclui bibliografia.

1. MICROENCAPSULAÇÃO - Tese. 2. SPRAY DRYING - Tese. 3. AROMA - Tese. 4. CAFÉ - Tese. I. YAMASHITA, FABIO . II. EMY KUROZAWA, LOUISE . III. Universidade Estadual de Londrina. Centro de Ciências Agrárias. . IV. Título.

RODOLFO CAMPOS ZANIN

PERFIL DE LIBERAÇÃO DE COMPOSTOS DE AROMA EM CAFÉ SOLÚVEL E CAPPUCCINO ADICIONADOS DE MICROCÁPSULAS DE ÓLEO DE CAFÉ TORRADO

Tese apresentada ao Curso de Doutorado em Ciência de Alimentos da Universidade Estadual de Londrina - Paraná, como requisito parcial à obtenção do título de Doutor em Ciência de Alimentos.

BANCA EXAMINADORA

_____

Orientador Prof. Dr Fabio Yamashita
Universidade Estadual de Londrina - UEL

_____

Prof. Dr Carlos Raimundo Ferreira Grosso
Universidade Estadual de Campinas - UNICAMP

_____

Profa. Dra. Josiane Alessandra Vignoli
Universidade Estadual de Londrina - UEL

_____

Profa. Dra. Lyssa Setsuko Sakanaka
Universidade Tecnológica Federal do Paraná - UTFPR

_____

Profa. Dra. Marianne Ayumi Shirai
Universidade Tecnológica Federal do Paraná - UTFPR

Londrina, 07 de junho de 2019

DEDICATÓRIA

*A **Deus**, por me capacitar no desenvolvimento desse trabalho, por me dar forças em continuar mesmo diante das dificuldades, e por colocar pessoas excepcionais no meu caminho.*

*À minha esposa, **Caroline Prado Almeida Zanin**, pelo companheirismo e compreensão.*

*Aos meus pais, **Maurício e Elenice**, que de forma grata e grandiosa agradeço todo amor e dedicação depositados em mim por toda a minha vida.*

AGRADECIMENTOS

Agradeço a Deus pelo dom da vida, saúde e pela capacidade para a realização desse trabalho.

O meu muito obrigado a minha esposa **Carol** pelo carinho e incentivo e principalmente pela compreensão nos momentos de ausência.

A minha família, **pai, mãe, Isabella, Clenilson, Felipe, Lívia e Clara** que são minha fortaleza e sempre estiveram ao meu lado dando força e acreditando no meu potencial. Obrigado por sempre me proporcionar uma excelente formação. A vocês dedico esse trabalho.

Ao meu orientador **Dr Fábio Yamashita** e coorientadora **Drª Louise Emy Kurozawa**, pela excelente e grandiosa orientação, pela paciência e partilha de conhecimentos, obrigado pela confiança, dedicação e incentivo durante esses anos.

Ao meu supervisor **Dr. Chahan Yeretzian** pela oportunidade da experiência de trabalhar no Coffee Excellence Center na Zurich University of Applied Scinece (ZHAW), e aos outros integrantes do laboratório **Samo Smrke, Anja Rahn, Giulia, Patrick, Mizue, Sebastian, Marco Wellinger** pela ajuda na execução do trabalho.

Aos professores, em especial **Profª Marta** e **Profª Elza**, e equipe técnica do Departamento de Ciência de Alimentos pelos conhecimentos e experiências compartilhadas.

Aos membros da banca pela contribuição na análise e sugestões para a melhoria do trabalho.

Ao Conselho Nacional de Desenvolvimento Científico e Tecnológico (CNPq) e Coordenação de Aperfeiçoamento de Pessoal de Nível Superior - CAPES pelo suporte financeiro.

A **Marcelo Viegas** (Café Iguaçú) pela concessão das amostras de óleo de café torrado, realização das análises cromatográficas e contribuição intelectual que enriqueceram o trabalho.

Aos amigos e colegas de turma e de laboratório, **Mariah Benine, Fernanda Henrique, Bruna Yoshida, Ariana Justus, Heloísa Falcão, Cíntia Handa, Julyene Francisco, Bruna Gerônimo, Bruna Böger, Rafael Carvalho, Marcela Guelfi**, pelo carinho e ajuda e por contribuírem para um ambiente mais alegre e prazeroso.

Aos amigos da Meise house (Suíça) que foram minha família por 6 meses do qual vou sempre me lembrar: **Raphael Gnehm, Michel, Valentina, Jan, Yoshua, Jannis, Mischka, Aska, Rafael, Adrian, Patricia, Alex e Nina**.

“Hoje ainda almejamos saber por que estamos aqui e de onde viemos. O desejo profundo da humanidade pelo conhecimento é justificativa suficiente para nossa busca contínua.”

Stephen Hawking

ZANIN, Rodolfo Campos. **Perfil de liberação de compostos de aroma em café solúvel e cappuccino adicionados de microcápsulas de óleo de café torrado**. 2019. 128 f. Tese (Doutorado em Ciência de Alimentos) - Universidade Estadual de Londrina, Londrina, 2019.

RESUMO

O café coado (torrado e moído) é a forma de preparo mais apreciada pelos consumidores devido à sua característica de aroma, apesar disso as formas instantâneas de café, p. ex. café solúvel e o cappuccino instantâneo vêm ganhando espaço no mercado, principalmente por sua praticidade, e são responsáveis pelo aumento do consumo de café fora das residências. Porém, o aroma destes produtos é menos intenso que o do café torrado e moído tradicional uma vez que, para a obtenção desses produtos instantâneos, as altas temperaturas durante o processamento provoca perda considerável de compostos de aroma. A microencapsulação do óleo de café torrado, fração que contém a maior concentração destes compostos, é interessante pois estas microcápsulas podem ser aplicadas como ingrediente em produtos de café visando intensificar a sensação de aroma nesses produtos. Diante disso, o objetivo deste trabalho foi microencapsular óleo de café por *spray drying* utilizando o ultrassom como método de emulsificação, e aplicar as microcápsulas como ingrediente em produtos instantâneos de café a fim de se aumentar a intensidade aromática nesses produtos. Óleo de café torrado foi utilizado como material de recheio, e como material de parede foi utilizado o amido modificado (OSA - anidrido octenil succínico). As emulsões foram obtidas pelo método de ultrassom e um Delineamento Centro Composto Rotacional (DCCR) foi aplicado a fim de se avaliar os efeitos da potência (W) e temperatura (°C) de ultrassom nas características das emulsões e nas microcápsulas. Foram analisadas as mudanças no balanço da composição aromática nas emulsões, no interior e na superfícies das microcápsulas. O perfil de liberação dos aromas a partir das microcápsulas adicionadas em café solúvel e cappuccino instantâneo foi monitorado em tempo real durante o preparo da bebida por PTR-ToF-MS. De modo geral, foram obtidas emulsões altamente estáveis com gotículas de diâmetro submicron (< 2 μm) e distribuição monomodal, e o DCCR foi eficiente na avaliação dos efeitos dos parâmetros do ultrassom nas emulsões e nas micropartículas. O aparato construído permitiu o monitoramento da dinâmica de liberação de voláteis de aroma durante o preparo da bebida, e os perfis de tempo-intensidade foram correlacionados com suas propriedades físico-químicas. O agrupamento dos compostos de aroma em suas classes e a avaliação da composição do aroma de café demostrou que mudanças profundas ocorreram nesse balanço quando o óleo é emulsionado no material de parede e, posteriormente, submetido a microencapsulação no *spray drying*. As microcápsulas obtidas foram adicionadas em café solúvel e cappuccino instantâneo, e o perfil de liberação mostrou que essa adição provocou o aumento da intensidade na maioria dos aromas, principalmente no cappuccino uma vez que este produto apresenta uma concentração menor de café em sua composição, contudo o perfil de liberação não foi alterado. Esse trabalho compreendeu um estudo abrangente acerca da emulsificação por ultrassom e microencapsulação de óleo de café, e demonstrou a importância dessa tecnologia em aumentar as característica de aroma em produtos instantâneos.

Palavras-chave: Aroma de café. Emulsão. Ultrassom. Café solúvel. Cappuccino instantâneo. PTR-ToF-MS.

ZANIN, Rodolfo Campos. **Release profile of aroma compounds in soluble coffee and cappuccino added with microcapsules of roasted coffee oil.** 2019. 128 p. Thesis (Doctoral Degree in Food Science) - Universidade Estadual de Londrina, Londrina, 2019.

ABSTRACT

Filter coffee (roasted and ground coffee) is the most popular form of coffee preparation because of its aroma feature, nevertheless instant coffees, i.e. soluble coffee and instant cappuccino, are gaining market space, mainly because of their convenience, and are responsible for the increase in the consumption of coffee outside the residences. However, the aroma of these products is less intense than traditional roast and ground coffee since, in order to obtain such instant products, high temperatures applied during processing cause considerable losses of aroma compounds. The microencapsulation of the roasted coffee oil, the fraction that contains the highest concentration of these compounds, is interesting since these microcapsules can be applied as an ingredient in coffee products in order to enhance the aroma sensation in these products. Therefore, the aim of this work was to microencapsulate coffee oil by spray drying using ultrasound as emulsification method and to apply the microcapsules as an ingredient in instant coffee products in order to increase the aroma intensity in these products. Roasted coffee oil was used as core material, and modified starch (OSA - octenyl succinic anhydride) was used as wall material. The emulsions were obtained by the ultrasound-assisted method and a Central Composite Rotational Design (CCRD) was applied in order to evaluate the effects of ultrasound power (W) and temperature (°C) on the characteristics of the emulsions and microcapsules. The changes in the balance of the flavor composition in the emulsions, in the interior and on the surfaces of the microcapsules were evaluated. The flavor release profile from the microcapsules added in soluble coffee and instant cappuccino was monitored in real time during the brew preparation. In general, highly stable emulsions were obtained with submicron (< 2 μm) diameter droplets and monomodal droplet size distribution, and CCRD was efficient in evaluating the effects of ultrasound parameters on emulsions and microparticles. The sampling setup was efficient in monitoring the dynamics of aroma volatiles release during the brew preparation, and the time-intensity profiles were correlated with their physicochemical properties. By grouping the aroma compounds into their chemical classes and the evaluation of the coffee aroma composition showed that great changes occurred in this balance during the emulsification in the wall material and subsequently submitted to microencapsulation by spray drying. The microcapsules obtained were added in soluble coffee and instant cappuccino, and the release profile showed that this addition resulted in an increase in intensity in most flavors, especially in instant cappuccino since this product has a lower concentration of coffee in its composition. However, the release profile did not present any change. This work comprised a comprehensive study on ultrasonic-assisted emulsification and microencapsulation of roasted coffee oil and highlighted the importance of this technology in increasing the aroma characteristic in instant coffee products.

Keywords: Coffee aroma. Emulsion. Ultrasound. Soluble coffee. Instant cappuccino. PTR-ToF-MS.

LISTA DE FIGURAS

CAPÍTULO 1

CAPÍTULO 2

CAPÍTULO 3

CAPÍTULO 4

CAPÍTULO 5

LISTA DE TABELAS

CAPÍTULO 1

CAPÍTULO 2

CAPÍTULO 3

CAPÍTULO 4

CAPÍTULO 5

SUMÁRIO

1 INTRODUÇÃO GERAL

O café representa um dos produtos que mais colaboram para o crescimento da economia brasileira correspondendo cerca de 5,74% das exportações do agronegócio em 2018 (BRASIL, 2019), com 2,1 milhões de toneladas exportadas e receita de mais de US$ 5,1 bilhões (CECAFE, 2019). O Brasil ainda ocupa posição de liderança quando se trata de produção e exportação de café, com mais de 3,75 milhões de toneladas produzidas (ICO, 2019a), e o segundo lugar em consumo per capita de café atrás apenas dos EUA, tendo entre 2017 e 2018 cerca de 1,3 milhões de toneladas de café (ICO, 2019b).

A preferência do consumidor brasileiro se concentra no café torrado e moído, pois cerca de 80% do café consumido no país é dessa forma. Os atributos sensoriais de sabor e aroma bastante característicos dessa bebida são os principais fatores que contribuem para essa preferência (EUROMONITOR INTERNATIONAL, 2017). Por esse motivo, as propriedades sensoriais da bebida de café são objeto de pesquisa há vários anos, e devido ao aumento do consumo e critérios de qualidade na opção de compra, o interesse no estudo do seu sabor e aroma impulsionou as pesquisas nesse campo tanto de pesquisadores quanto das indústrias.

Há uma forte tendência pela procura por maior qualidade de café por parte dos consumidores despertada pela maior disponibilidade de informações a respeito do café: conhecimento dos benefícios do consumo da bebida para a saúde, diferentes produtos de café como por exemplo cafés *premium* e as cápsulas, divulgação de concursos de qualidade, o que significa que os consumidores estão buscando produtos inovadores e estão mais atentos às diferenciações quanto à região de produção, certificações, sabores, etc (EUROMONITOR INTERNATIONAL, 2017).

Os produtos instantâneos de café apresentam uma intensidade de aroma menor do que o café torrado e moído tradicionais. Tal fato prejudica o crescimento do consumo desse tipo de produto, visto que o aroma é um dos principais atributos do café. Assim, diversas metodologias vêm sendo desenvolvidas e aperfeiçoadas a fim de se melhorar as características sensoriais destes produtos (FLAMENT, 2002; SANZ et al., 2002; ZELLER et al., 2014).

Uma alternativa interessante é a microencapsulação que consiste num processo no qual compostos de interesse, na forma de gás, líquido ou sólido, são envolvidos por um material de parede que protege contra as condições do ambiente e permite sua liberação controlada durante o armazenamento. Os métodos mais empregados para a obtenção dessas

microcápsulas são por *spray drying*, *spray chilling*, coacervação complexa e gelificação iônica (BAKRY et al., 2016; RÉ, 1998; UHLEMANN; SCHLEIFENBAUM; BERTRAM, 2002).

Trata-se de uma metodologia relevante para a veiculação de aromas em produtos de café, por exemplo cafés instantâneos: solúvel, cappuccino, etc, pois protege os compostos de aroma contra fatores externos e minimiza perdas durante o armazenamento, garantindo a presença desses compostos em concentrações suficientes para causar o impacto sensorial desejado na bebida (REINECCIUS, 2004; SOBEL; VERSIC; GAONKAR, 2014; ZELLER et al., 2014; DORDEVIC et al., 2014).

O óleo de café, produto que pode ser obtido pela prensagem dos grãos de café torrado e que representa a fração mais rica em compostos de aroma (FLAMENT, 2002), foi utilizado como material de recheio para microencapsulação em estudos anteriores como potencial veículo de aroma de café (FRASCARELI et al., 2012a, 2012b; FREIBERGER et al., 2015; GETACHEW; CHUN, 2016; RODRIGUES; GROSSO, 2008).

Na avaliação do impacto do aroma na aceitação de um produto é necessária a compreensão do perfil de liberação dos aroma durante seu preparo e consumo, isto é, como a liberação dos aroma se altera em função do tempo. Já são disponíveis comercialmente equipamentos que permitem o monitoramento da emissão de compostos voláteis em tempo real. Uma dessas tecnologias é a PTR-MS (*Proton Transfer Reaction Mass Spectrometry* ou Reação de Transferência de Prótons acoplada a Espectrometria de Massas) em que os compostos são diretamente injetados e detectados sem que ocorra qualquer separação ou preparo de amostra como ocorre na cromatografia gasosa. É uma técnica que tem alta sensibilidade e resolução e os compostos são detectados em frações de segundos (BLAKE; MONKS; ELLIS, 2009; ELLIS; MAYHEW, 2014a; JORDAN et al., 2009).

A aplicação da microencapsulação de ingredientes vem aumentando uma vez que os consumidores estão dispostos a dispensar mais recursos em produtos nos quais ingredientes sensíveis e promotores de saúde foram adicionados (SOBEL; VERSIC; GAONKAR, 2014). Devido à maior exigência destes consumidores em relação à qualidade dos alimentos, a oferta de produtos com melhor característica sensorial pode representar um diferencial para as empresas produtoras.

2 OBJETIVOS

2.1 Objetivo Geral

Microencapsular óleo de café torrado pelo método de *spray drying* utilizando o ultrassom como método de emulsificação e aplicar as microcápsulas como ingrediente em produtos instantâneos de café a fim de se melhorar as características sensoriais desses produtos.

2.2 Objetivos Específicos

- Analisar os efeitos da temperatura e potência do ultrassom nas características da emulsão do óleo de café com o material de parede;
- Estudar como as características da emulsão afetam a retenção de compostos voláteis;
- Avaliar a composição de voláteis retidos na emulsão, no interior e exterior das microcápsulas;
- Determinar os perfis de liberação do aroma de café durante o preparo da bebida contendo as microcápsulas utilizando metodologia de análise em tempo real.

CAPÍTULO 1 – REVISÃO BIBLIOGRÁFICA

1. AROMA DE CAFÉ

O aroma do café torrado representa uma das principais características sensoriais da bebida, sendo este um dos parâmetros que levam a preferência do consumo por esse produto (SHIBAMOTO, 2015). Esse atributo inclui uma mistura complexa de compostos voláteis produzidos durante a torra, com características sensorialmente apreciadas (BUFFO; CARDELLI-FREIRE, 2004), e sua composição depende basicamente do local de cultivo do café, cultivar, processamento pós-colheita, tipo de preparo da bebida e grau de torra (BHUMIRATANA; ADHIKARI; IV, 2011).

É durante a torra que ocorrem as transformações de cor e sabor e a formação do aroma de café. O mecanismo de formação destes compostos voláteis é bastante complexo e envolve uma série de interações entre os componentes do grão e entre as rotas envolvidas na formação. Dentre essas transformações, destacam-se as reações de Maillard e de degradação de Strecker; degradação de aminoácidos, da trigonelina, do ácido quínico, de pigmentos, de lipídios menores como os diterpenos e de interações entre produtos intermediários (BUFFO; CARDELLI-FREIRE, 2004; SEMMELROCH; BLANK; GROSCHT, 1995). Por essa razão a composição dos precursores de aroma são relevantes e impactam diretamente na composição aromática do café torrado (DE MARIA et al., 1994).

O óleo é a fração mais rica em compostos voláteis e é obtido através da prensagem do grão de café torrado, representando cerca de 10% de massa do grão torrado, (BUFFO; CARDELLI-FREIRE, 2004; FLAMENT, 2002). O óleo de café contém em torno de 35 compostos ativos responsáveis pelo aroma global da bebida (CALLIGARIS et al., 2009; HURTADO-BENAVIDES; DORADO; SÁNCHEZ-CAMARGO, 2016) e, por isso, é utilizado para conferir aroma de café em diversos produtos.

Os estudos a respeito desses compostos de aroma de café tiveram início há 35 anos e foi possível com os desenvolvimentos da cromatografia gasosa e espectrometria de massas (BUFFO; CARDELLI-FREIRE, 2004; SHIBAMOTO, 2015). Cerca de 900 compostos foram identificados como integrantes da fração volátil de café torrado, porém poucos compostos são os que efetivamente contribuem para o aroma do produto (BUFFO; CARDELLI-FREIRE, 2004; CZERNY; MAYER; GROSCH, 1999; FLAMENT, 2002; SEMMELROCH; BLANK; GROSCHT, 1995; SEMMELROCH; GROSCH, 1996). Dentre

esses compostos, frequentemente descritos como compostos chave para o aroma de café, incluem: tióis, pirazinas, acetaldeído, piridinas, pirimidinas, tiofenos, oxazois e tiazóis (CZERNY; MAYER; GROSCH, 1999; SEMMELROCH; BLANK; GROSCHT, 1995; SEMMELROCH; GROSCH, 1996; FLAMENT, 2002; SHIBAMOTO, 2015). As principais classes de compostos pelo aroma são listadas na Tabela 1.

Tabela 1. Classe de compostos voláteis identificados em café torrado.

Classes de compostos voláteis identificados em café torrado
Compostos Sulfurados
Tióis
Sulfeto de hidrogênio
Tiofenos (ésteres, aldeídos e cetonas)
Triazóis (alquil, alcóxi e derivados de acetal)
Pirazinas
Pirazina
Derivados de tiol e furfurílico
Derivados alquila (principalmente metil e dimetil)
Piridinas
Derivados metil, etil, acetil e vinil
Pirróis
Alquila, acila e derivados de furfurilo
Oxazol
Furanos
Aldeídos, cetonas, ésteres, alcoóis, ácidos, tióis, sulfetos e combinação com pirazinas e pirrol
Aldeídos e cetonas
Aromáticos e alifáticos
Fenóis

Fonte: Buffo; Cardelli-Freire (2004).

Um grande problema enfrentado pelas indústrias produtoras de café solúvel é a sensação de aroma deste produto, menos intenso quando comparado ao café torrado e moído tradicional (BASSOLI, 2006; POLLIEN; KREBS; CHAINTREAU, 1997; ZELLER et al., 2014). Por ser obtido através de tratamentos térmicos para remoção de água, por exemplo, tecnologia de *spray drying* na qual o extrato concentrado de café é pulverizado em câmaras de

secagem em altas temperaturas, grande parte dos voláteis é perdida (BASSOLI et al., 1993). Ainda que tenham ocorrido melhoras na tecnologia de produção de café solúvel e dos métodos de recuperação de aroma, há grande diferença tanto na composição como na concentração destes compostos no café solúvel (ZELLER et al., 2014; POLLIEN; KREBS; CHAINTREAU, 1997; SANZ et al., 2002).

Algumas alternativas foram desenvolvidas a fim de se garantir a preservação dos compostos aromáticos ou para impedir e mascarar sabores não característicos (*off-flavors*), formados pela oxidação dos componentes do óleo em cafés solúveis ou produtos de café tais como a adição de vapor de voláteis ao produto logo depois de embalado (CLINTON; PLAINS; PITCHON, 1962), extração do óleo de café torrado e posterior adição ao produto final (KLEIN; RABEN; HERRERA, 1968), extração criogênica do aroma e retorno ao produto (PATEL, 1974) e a microencapsulação do óleo (FREIBERGER et al., 2015; ZELLER et al., 2014).

Como se trata de um dos atributos que mais afeta a decisão de compra e a qualidade de bebida de café, a indústria produtora deve estar apta a entender e desenvolver metodologias que garantam a permanência ou o retorno dos compostos de aroma ao produto final a fim de se melhorar a qualidade e, assim, ganhar destaque no mercado (BHUMIRATANA; ADHIKARI; IV, 2011; SUNARHARUM; WILLIAMS; SMYTH, 2014).

2. MICROENCAPSULAÇÃO

Microencapsulação é nome dado ao processo de empacotamento de substâncias de interesse em estruturas sólidas pequenas, com a finalidade de proteger contra as condições do ambiente externo. Esse processo consiste no envolvimento de uma ou um conjunto de substâncias bioativas numa matriz polimérica (GHARSALLAOUI et al., 2007; SHAHIDI; HAN, 1993). São classificadas de acordo com o diâmetros de suas partículas em nano (< 0,2 μm), micro (0,2 a 5000 μm), ou macropartículas (> 5000 μm) (RÉ, 1998).

Existem diversos termos para se referir ao material que se deseja preservar, tais como: núcleo, material de recheio, agente ativo, fase interna, etc. Da mesma forma, o material de empacotamento que envolve o que está no interior da microcápsula pode ser denominado de material de parede, carreador, parede, fase externa, etc. Contudo, os termos material de recheio e material de parede são bastante utilizados (GHARSALLAOUI et al., 2007; THIES, 2007; SHAHIDI; HAN, 1993). Existem dois principais tipos de microcápsulas em relação à disposição do material de recheio na microcápsula: (a) quando o recheio se concentra no interior

da microcápsula ou (b) quando o recheio está disperso como pequenas gotículas na parede (YE; GEORGES; SELOMULYA, 2018) (Figura 1).

F**igura 1.** Exemplos de microcápsulas: (a) recheio no interior da partícula; (b) recheio disperso na parede da partícula.

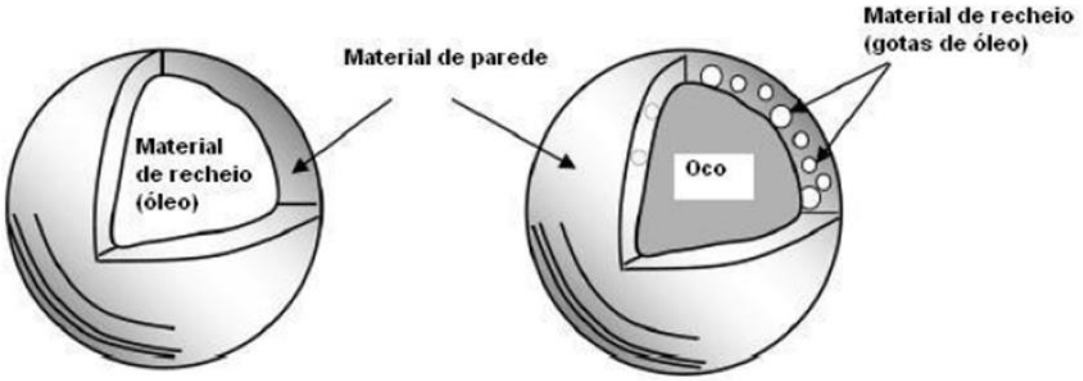

Fonte: Jafari et al., 2008.

As diferenças entre os dois tipos de microcápsulas ocorrem pela diferença na razão entre a taxa de evaporação da água e a velocidade de movimentação dos solutos. Quando a razão é baixa durante a evaporação da água, ou seja, a velocidade de movimentação dos solutos é alta em comparação com a taxa de evaporação da água, os solutos migram para o interior da cápsula que sofre um encolhimento, resultando em uma partícula densa. Por outro lado, quando a evaporação predomina, característico de soluções viscosas, a remoção rápida de água promove a concentração dos solutos na superfície da cápsula e formação quase instantânea de uma membrana, formando uma microcápsula oca (SCHIFFTER; LEE, 2007; VICENTE et al., 2013).

A liberação do material de recheio pode ocorrer por vários mecanismos que vai desde a fragmentação física da parede à sua degradação química ou enzimática (YE; GEORGES; SELOMULYA, 2018).

Segundo Shahidi e Han (1993), as razões para a aplicação da microencapsulação na indústria de alimentos são: reduzir a reatividade do material encapsulado com fatores ambientais; diminuir a taxa de transferência do material de recheio para o ambiente; facilitar o manuseio; controlar a liberação do recheio; mascarar sabores e diluir o material de recheio no momento da utilização em quantidades muito pequenas.

Nos últimos anos houve um aumento no número de publicações tratando desse tema em alimentos. Os materiais de recheio são os mais diversos e incluem óleos

(CARVALHO; SILVA; HUBINGER, 2014; KARADENIZ; SAHIN; SUMNU, 2018; PILETTI et al., 2019), vitaminas (ABBAS et al., 2012; JANNASARI et al., 2019), aromas (PELLICER et al., 2018; SOOTTITANTAWAT et al., 2005a), corantes (FANG et al., 2019; CAI et al., 2019), óleos essenciais (BARANAUSKIENE et al., 2006; BARANAUSKIENÉ et al., 2007), compostos fenólicos (LUCA et al., 2014), edulcorantes (ROCHA-SELMI et al., 2013) e microrganismos (BRINQUES; AYUB, 2011; WANG et al., 2019).

Muitos trabalhos sugerem o uso de diferentes tipos de materiais de parede, com propriedades adequadas para cada tipo de aplicação ou material de recheio, entretanto, para a aplicação em alimentos, esses materiais devem ser reconhecidamente seguros (GRAS – *Generally Recognized As Safe*). Com isso, vários materiais de parede aplicados na área cosmética e farmacêutica são restritos quando utilizados na área de alimentos (CORTÉS-ROJAS; SOUZA; OLIVEIRA, 2014; DIAS; FERREIRA; BARREIRO, 2015; MARTINS et al., 2014).

Por consequência, a escolha do material de parede adequado é o primeiro passo para o sucesso do processo de microencapsulação, pois deve apresentar as propriedades de barreira adequadas e não ser tóxico (DIAS; FERREIRA; BARREIRO, 2015), além disso, é desejável que apresente propriedades como: baixa viscosidade mesmo a altas concentrações, boas propriedades emulsificantes, facilidade manipulação, livre de solvente orgânico, máxima proteção do material de recheio do ambiente externo e boa redispersão no local e momento desejado (SHAHIDI; HAN, 1993; YE; GEORGES; SELOMULYA, 2018).

Em vista disso, os materiais mais comumente utilizados como materiais de parede são polissacarídeos (amidos e derivados, dextrinas e celulose), exsudatos de plantas (galactomananas, pectina), gomas extraídas de algas marinhas (carragena e alginato), polissacarídeos extraídos de outras fontes (xantana, gelana, quitosana), proteínas e lipídeos (BAE; LEE, 2008; BARANAUSKIENÉ et al., 2007; DIAS; FERREIRA; BARREIRO, 2015; RODRIGUES; GROSSO, 2008; VAIDYA; BHOSALE; SINGHAL, 2006). Porém, nenhum material de parede apresenta todas as propriedades requeridas e, por essa razão, são feitas formulações com dois ou mais tipos de materiais a fim de se aproveitar as características de cada um (Tabela 2) (MADENE et al., 2006; FANG; BHANDARI, 2010).

Tabela 2. Características dos principais materiais de parede utilizados na microencapsulação

Material de parede	Característica
Maltodextrina (DE < 20)	Formação de filme
Amido modificado	Bom emulsificante
Goma arábica	Emulsificante, formação de filme
Celulose modificada	Formação de filme
Gelatina	Emulsificante, formação de filme
Ciclodextrina	Encapsulante, emulsificante
Lecitina	Emulsificante
Proteína de soro de leite	Bom emulsificante
Gordura hidrogenada	Barreira ao oxigênio e água

Fonte: Madene et al., 2006.

A obtenção das microcápsulas pode ocorrer por diferentes métodos tais como *spray drying*, *spray chilling*, coacervação complexa, gelificação iônica e extrusão. A seleção do método é feita de acordo com o tipo de material de recheio, aplicação das microcápsulas, tamanho das partículas, propriedades físico-químicas do recheio e do material de parede, mecanismo de liberação, escala de produção e custo (DIAS; FERREIRA; BARREIRO, 2015; ZUIDAM; SHIMONI, 2010).

Atualmente as principais indústrias que contribuem para o desenvolvimento da microencapsulação são as farmacêuticas e a de cosméticos; a indústria de alimentos contribui pouco para o desenvolvimento de técnicas e disponibilidade desses produtos. A possibilidade de incorporação de aditivos ativos sensíveis em alimentos, bem como da conveniência da comercialização de produtos em pó, sua estabilidade química e microbiológica além da redução dos custos de transporte, desperta o interesse no desenvolvimento e aplicação de materiais microencapsulados em alimentos (FORNY; MARABI; PALZER, 2011; GOUIN, 2004; UBBINK; KRÜGER, 2006; MARTINS et al., 2014).

Apesar do interesse das indústrias de alimentos na utilização de produtos microencapsulados, existem entraves tais como o tempo requerido para o desenvolvimento e padronização das metodologias, uma vez que quase sempre necessitam de adaptações para a aplicação de interesse (GOUIN, 2004; UBBINK; KRÜGER, 2006). Daí a necessidade de se conseguir viabilizar o uso da microencapsulação em grande escala considerando as restrições e requisitos industriais (MADENE et al., 2006).

2.1 *SPRAY DRYING*

A técnica de *spray drying* é uma operação unitária de secagem utilizada na indústria de alimentos cujo objetivo é a conservação dos produtos pela redução da umidade e atividade de água. Por esse motivo, é garantida a segurança microbiológica do alimento, se evita a ocorrência de reações químicas e enzimáticas indesejáveis e ainda permite a obtenção de produtos com características específicas, como o leite em pó e o café solúvel (GHARSALLAOUI et al., 2007; GOUIN, 2004).

Trata-se de uma das técnicas mais antigas e mais aplicadas na microencapsulação de substâncias bioativas (GHARSALLAOUI et al., 2007; RÉ, 1998; REINECCIUS, 2004; ZUIDAM; SHIMONI, 2010) devido à tecnologia já bem estabelecida e equipamento disponível, processo de operação econômico, flexível e contínuo, boa recuperação e fluidez das partículas (MURUGESAN; ORSAT, 2012).

Nesse sentido, várias publicações dizem respeito à utilização de *spray drying* como método de microencapsulação em alimentos. Os trabalhos tem foco principal no estudo dos efeitos dos parâmetros operacionais do *spray dryer* (temperatura de ar de entrada, temperatura de saída, vazão etc.) (BENCHABANE, 2007; FRASCARELI et al., 2012a; VICENTE et al., 2013), utilização de diferentes materiais de parede (FANG et al., 2019; CAI et al., 2019; BAE; LEE, 2008; BARANAUSKIENÉ et al., 2007; ORDOÑEZ; HERRERA, 2014; RODRIGUES; GROSSO, 2008; SHEN; QUEK, 2014; VAIDYA; BHOSALE; SINGHAL, 2006) e dos métodos de formação, propriedades e composição da emulsão (REN et al., 2018; CERVANTES-MARTÍNEZ et al., 2014; KELLY et al., 2014; LIU et al., 2001; SILVA et al., 2016; SOOTTITANTAWAT et al., 2005b); sobre as características das microcápsulas. Além disso, o tipo de material a ser microencapsulado é muito diverso e incluem β-caroteno (FANG et al., 2019), óleos (BARANAUSKIENÉ et al., 2007; CARVALHO; SILVA; HUBINGER, 2014; FRASCARELI et al., 2012a), aromas (BARANAUSKIENE et al., 2006), ácidos graxos (LOUGHRILL et al., 2019), compostos fenólicos (SUN; CAMERON; BAI, 2019), pigmentos (CAI et al., 2019), microrganismos (WANG et al., 2019), etc.

A produção de microcápsulas por essa tecnologia é similar ao processo de secagem convencional, exceto pela preparação do material a ser atomizado no *spray dryer*. Nessa etapa, a mistura a ser atomizada é preparada dispersando o material a ser encapsulado (recheio), geralmente hidrofóbico, numa solução aquosa do material de parede. A solução é homogeneizada com ou sem adição de emulsificante dependendo das propriedades

emulsificantes do material de parede e, posteriormente atomizada na câmara de secagem (GHARSALLAOUI et al., 2007; FANG; BHANDARI, 2010; CAL; SOLLOHUB, 2010).

Na Figura 2 é apresentado um modelo de spray dryer.

Figura 2. Modelo de *spray dryer* de bancada.

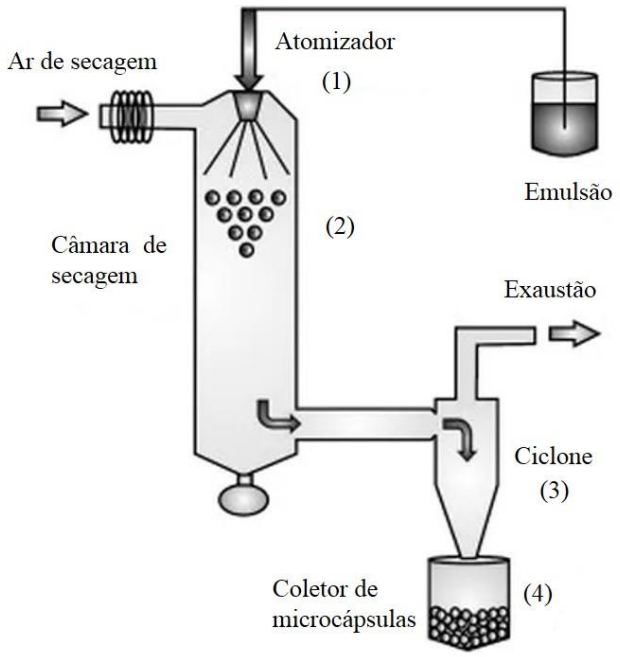

O processo de secagem pode ser dividido em quatro estágios principais: 1) atomização; 2) contato com o ar de secagem; 3) secagem do material e 4) separação do produto do ar.

Anteriormente à secagem propriamente dita, é necessário a obtenção de uma dispersão ou emulsão estável. Para material de recheio hidrofílico, este pode ser solubilizado juntamente com o material de parede. Já para recheio hidrofóbico, é necessária a formação de uma emulsão óleo/água estável e, por isso, é importante a seleção de materiais de parede que assegurem a estabilidade da emulsão e tenham boas propriedades de barreira (RÉ, 1998; SHEN; QUEK, 2014; FANG; BHANDARI, 2010).

A etapa de atomização se refere à pulverização do material de alimentação dentro da câmara de secagem e formação de gotículas muito pequenas. Uma atomização eficiente produz gotículas pequenas e uniformes, que favorecem o aquecimento e a transferência de calor e massa durante a secagem (VICENTE et al., 2013). Essa formação de partículas e sua dispersão na câmara de secagem promove um aumento muito grande da superfície de contato, e a secagem ocorre em frações de segundos (RÉ, 1998).

A temperatura de secagem e o tempo de contato do material com o ar de secagem são importantes, pois determinam a taxa e a intensidade da secagem. O tempo de residência de cada gotícula dentro da câmara de secagem depende do fluxo de ar de entrada e as dimensões da câmara que deve permitir o bom escoamento do produto para evitar sua deposição nas paredes da câmara. A taxa de aquecimento depende do tamanho das gotículas, da temperatura e velocidade do ar e de atomização (CAL; SOLLOHUB, 2010).

A secagem do material é um processo simultâneo de transferência de calor e de massa. Enquanto o calor do ar é transferido para as gotículas por convecção e promove a elevação da temperatura do material, ocorre a migração da água do interior da gotícula para a superfície e sua evaporação contínua, à temperatura constante de bulbo úmido. No momento em que o conteúdo de água da gotícula atinge um valor crítico, forma-se uma crosta na superfície e decréscimo da taxa de secagem, e cessa quando a temperatura da gotícula se iguala a temperatura do ar de secagem (FLEMING, 1921; GHARSALLAOUI et al., 2007; PAPADAKIS; KING, 1988). O resultado é a obtenção de uma partícula seca e porosa, a microcápsula (GHARSALLAOUI et al., 2007; MAHDAVI et al., 2014), que é separada do ar úmido e coletada na parte inferior do equipamento por meio de um ciclone (Figura 2) (GHARSALLAOUI et al., 2007; WOO et al., 2009).

A utilização do *spray drying* é especialmente indicada para compostos sensíveis à altas temperaturas como aromas, enzimas e microrganismos, pois a secagem ocorre na superfície de forma quase instantânea, a partir do contato do material com o ar de secagem, e o interior da microcápsula permanece na temperatura de bulbo úmido, pela absorção do calor do ar pela água da superfície (RÉ, 1998; REINECCIUS, 2004; JAFARI et al., 2008a; FLEMING, 1921).

2.2 MICROENCAPSULAÇÃO DE AROMAS

O aroma, do ponto de vista sensorial, trata-se de um estímulo químico, causado pela interação de compostos ativos de aroma com as células olfativas na mucosa olfatória da cavidade nasal e que, por meio de receptores, enviam essa informação ao cérebro onde o aroma é reconhecido e discriminado (DUTCOSKY, 2011; TOURNIER; SULMONT-ROSSE; GUICHARD, 2007). Por outro lado, do ponto de vista químico, esse atributo consiste numa mistura complexa de compostos voláteis e moléculas orgânicas de baixa massa molecular, na sua grande maioria lipofílicas embora algumas moléculas sejam solúveis em água, que

apresentam-se na forma de gás ou líquida classificadas em álcoois, hidrocarbonetos, aldeídos, cetonas, ésteres, ácidos, etc (VOILLEY; ETIÉVANT, 2006; ZUIDAM; SHIMONI, 2010).

O aroma é um atributo importante na escolha do produto alimentício, portanto é importante manter as características aromáticas dos alimentos até o consumo. Tal manutenção pode ser alcançada pela tecnologia de microencapsulação (MADENE et al., 2006; REINECCIUS, 2004; VOILLEY; ETIÉVANT, 2006; ZUIDAM; HEINRICH, 2010).

Contudo, a microencapsulação de aromas representa um desafio uma vez que deve reter as características desejadas de aroma, uma mistura complexa de compostos com diferentes estruturas, solubilidades, pressão de vapor e estabilidade, sem que provoque alterações químicas desses compostos. Por isso, se deve considerar essa diversidade de componentes na escolha do método e da tecnologia de microencapsulação (THIES, 2007). Da mesma forma, a técnica deve ser escolhida levando-se em conta as propriedades do produto final, grau de estabilidade durante o processamento e estocagem, propriedades de liberação, máxima eficiência de encapsulação e custo (MADENE et al., 2006).

Os benefícios da microencapsulação de aromas incluem facilidade de manipulação pela conversão do óleo líquido para a forma de pó; maior estabilidade do produto final e durante o processo (menor evaporação, degradação e reação com os componentes do alimento); segurança (reduz a inflamabilidade do óleo, menor manipulação do óleo concentrado); ajuste do aroma (quantidade de óleo microencapsulado e tamanho de partícula), liberação controlada do aroma ou retenção e para mascarar aromas indesejáveis (LAOKULDILOK et al., 2015; GHARSALLAOUI et al., 2007; UHLEMANN; SCHLEIFENBAUM; BERTRAM, 2002).

As microcápsulas que carregam os aromas devem garantir a estabilidade desses compostos desde sua obtenção até o consumo. Essa estabilidade pode ser comprometida a partir do momento em que são adicionadas a um produto, na qual é submetido a processos que causam a ruptura da parede da cápsula e liberação do material de recheio, por exemplo, cisalhamento e altas temperaturas. Outros fatores, como luz, oxigênio, calor e umidade, afetam a estabilidade dos aromas e, portanto, o material de parede deve ser uma barreira eficiente contra essas condições (FRASCARELI et al., 2012b; THIES, 2007).

Dentre os métodos disponíveis para a microencapsulação de ingredientes alimentícios, o de *spray drying* é o mais antigo e mais utilizado método para encapsular óleos e aromas (SAIFULLAH et al., 2019). Há estudos sobre a encapsulação por *spray drying* de aroma de menta (BARANAUSKIENÉ et al., 2007), aroma de morango (PELLICER et al.,

2018), aroma de extrato de café (RODRIGUES; GROSSO, 2008), aroma de canela (VAIDYA; BHOSALE; SINGHAL, 2006), mentol (SOOTTITANTAWAT et al., 2005a), flavors hidrofóbicos (LIU et al., 2001) e limoneno (ORDOÑEZ; HERRERA, 2014).

Durante a secagem por *spray drying* mais de 90% da água é evaporada e os compostos mais voláteis que a água são retidos quando se utilizam condições ótimas de secagem. Contudo, não seria esperado que compostos voláteis fossem retidos por *spray drying* dado às altas temperaturas empregadas no processo (REINECCIUS, 2004; ZUIDAM; HEINRICH, 2010). A teoria mais aceita para explicar essa retenção é a da difusão seletiva, que é baseada nas diferenças dos coeficientes de difusão da água e dos compostos voláteis durante o processo de secagem. No momento do contato do material de alimentação com o ar quente, as gotículas começam a secar a partir da superfície e, conforme a umidade das gotículas é reduzida, há uma redução nos coeficientes de difusão da água e dos compostos voláteis. Os coeficientes de difusão dos voláteis são reduzidos de forma muito mais acentuada que o coeficiente de difusão da água. Por esse motivo, a água é continuamente removida a uma taxa considerável enquanto que a perda de voláteis é bem menor. Ao atingir determinado teor de umidade, a superfície passa a agir como uma membrana semipermeável que permite a passagem de água, mas não a dos voláteis, retendo esses compostos de forma eficiente (THIJSSEN; RULKENS, 1968).

Durante a microencapsulação por *spray drying*, foram determinados os três estágios que mais influenciam a perda de voláteis: 1) na atomização, 2) logo após a formação da gotícula, mas antes da temperatura atingir o ponto de evaporação da água e 3) quando atinge o ponto de evaporação da água, mas antes da formação da estrutura final da cápsula (KING, 1995; REINECCIUS, 2004).

Na atomização há uma grande área superficial, turbulência e fluxo de ar, que promove grande evaporação de compostos voláteis, já que há pouca barreira à transferência de massa. No próximo estágio, logo após a formação da gotícula, ocorre rápida evaporação de água e os voláteis se difundem junto a ela a partir da superfície para o ar aquecido. Neste estágio, há perda máxima de voláteis que depois decresce pela formação da barreira na superfície. E, por último, a formação e colapso de bolhas de vapor de água ao atingir seu ponto de evaporação, que carregam voláteis para o meio exterior, favorecendo suas perdas (KING, 1995; REINECCIUS, 2004).

A fim de se reduzir a perda dos compostos de interesse, os parâmetros que mais influenciam a retenção de voláteis devem ser otimizados, tais como: conteúdo de sólidos, massa

molecular e volatilidade dos compostos, tipo e massa molecular do material de parede, concentração dos voláteis, viscosidade do material de alimentação, tipo de atomização, velocidade do ar de secagem, temperatura de entrada e de saída, umidade relativa do ar de entrada, tamanho das gotículas da fase dispersa da emulsão e da partícula atomizada e temperatura do ar de secagem (KING, 1995; REINECCIUS, 2004).

Ainda que a técnica de *spray drying* seja a tecnologia predominante para a microencapsulação de aromas, tecnologias alternativas como o método físico-químico da coacervação complexa são metodologias potenciais na produção de microcápsulas de aromas (THIES, 2007).

Pela flexibilidade e versatilidade, a coacervação complexa possibilita a formação de microcápsulas de tamanhos variados, desde poucos mícrons a cápsulas com milímetros de diâmetro, possibilita maior quantidade de recheio e não se empregam altas temperaturas. O produto obtido pode estar na forma de pó seco ou solução aquosa e, quando na forma de solução, suporta manipulação e tensões durante processamentos subsequentes pela menor rigidez do material da parede, além de permitir a coencapsulação de dois ou mais ingredientes ativos (SAIFULLAH et al., 2019; SANTOS et al., 2015; JUN-XIA; HAI-YAN; JIAN, 2011; THIES, 2007).

Mesmo em menor número, quando comparado aos trabalhos a respeito de microencapsulação de aromas por *spray drying*, a utilização da coacervação complexa para microencapsulação de aromas foi empregada, por exemplo, para microencapsular aroma de alecrim (KOUPANTSIS; PAVLIDOU; PARASKEVOPOULOU, 2014), aroma de baunilha (SHADDEL et al., 2018), limoneno, mentol (LECLERCQ; HARLANDER; REINECCIUS, 2009), aroma de laranja (JUN-XIA; HAI-YAN; JIAN, 2011) e aroma de bolo (YEO et al., 2005).

3 EMULSÃO

Emulsões são sistemas coloidais heterogêneos na qual um líquido imiscível está completamente difuso num outro, na forma de pequenas gotículas esféricas, com diâmetros variando de 0,1 a 100 μm (ARAÚJO, 2012; MCCLEMENTS, 1999; SILVA et al., 2016; WALSTRA, 2003).

Trata-se de um complexo termodinamicamente instável, pois as moléculas presentes na fase dispersa tendem a se fundir umas às outras ao se chocarem, podendo levar a

completa separação de fase. Contudo, é possível obter emulsões estáveis pela adição de moléculas conhecidas como emulsificantes que ,em geral, são moléculas de características anfifílicas, que ficam adsorvidas à superfície das gotículas durante a homogeneização formando uma membrana que previne a agregação e desestabilização do sistema (ARAÚJO, 2012; MCCLEMENTS, 1999).

Todavia, a preparação de emulsões com a utilização de emulsificantes deve ser realizada de forma cuidadosa considerando a toxicidade de alguns emulsificantes. Em vista disso, a substituição dos emulsificantes por biopolímeros, como polissacarídeos e proteínas ou a combinação dos dois, que apresentam propriedades emulsificantes, tem sido aplicado com sucesso na preparação de emulsões estáveis (RAMAKRISHNAN et al., 2018; SHAO et al., 2019; BARANAUSKIENÉ et al., 2007; RODRIGUES; GROSSO, 2008; JAFARI; HE; BHANDARI, 2007; BOUYER et al., 2012; SILVA et al., 2015).

Esses sistemas são convenientemente classificados de acordo com a distribuição das duas fases, isto é, quando gotículas de óleo estão dispersas em fase aquosa, denominada dispersante, o sistema é tipo óleo/água (O/A); por outro lado, se gotas de água estão dispersas em óleo, o sistema é do tipo água/óleo (A/O) (ARAÚJO, 2012; MCCLEMENTS, 1999).

Como a maioria dos compostos de aroma está na forma líquida e são insolúveis em água, esses compostos são microencapsulados a partir da sua emulsificação com a solução aquosa do material de parede, resultando numa emulsão O/A. Esse tipo de emulsão é muito utilizado na área de alimentos, uma vez que são veículos que permitem alta retenção de ingredientes ativos (RÉ, 1998; JAFARI et al., 2008b; SILVA et al., 2015).

A emulsificação envolve ao menos três eventos principais: 1) a ruptura das gotas em gotículas menores durante a homogeneização; 2) adsorção do emulsificante, se necessário, na interface das gotículas e 3) coalescência das gotículas não adsorvidas pelo emulsificante (MCCLEMENTS, 1999).

A homogeneização é a etapa responsável pela conversão dos dois líquidos imiscíveis numa emulsão, podendo envolver um ou vários passos. O instrumento mecânico responsável pelo processo, o homogeneizador, fornece a energia necessária para que ocorra a ruptura das gotas da fase dispersa (MCCLEMENTS, 1999). Exemplos de homogeneizadores incluem agitadores de altas velocidades, ultrassom, microfluidização, homogeneizadores por membranas, dentre outros (SILVA et al., 2015, 2016; JAFARI; HE; BHANDARI, 2007; MCCLEMENTS, 1999).

A formação de uma emulsão se dá por meio da homogeneização primária na qual resulta em gotas relativamente grandes, que favorece a ruptura posterior das gotas e reduz a coalescência; e/ou homogeneização secundária, com redução do diâmetro das gotículas a partir de uma emulsão pré-formada (TRUJILLO-CAYADO et al., 2018; DOMIAN et al., 2015; POLAVARAPU et al., 2011; SHEN et al., 2010). Em alguns casos, não há necessidade do uso dos dois tipos de homogeneização, já que alguns homogeneizadores são capazes de produzir emulsões com gotículas muito pequenas (ARAÚJO, 2012; MCCLEMENTS, 1999).

Na tecnologia de microencapsulação, emulsões são sistemas muito utilizados, sendo o primeiro passo na preparação do material, onde o recheio é incorporado à solução do material de parede (AGHBASHLO et al., 2012; BASTOS et al., 2012; CARVALHO; SILVA; HUBINGER, 2014; RÉ, 1998; SILVA et al., 2016). As gotículas da fase dispersa devem ser pequenas (< 2 µm) para se aumentar a estabilidade e prevenir a coalescência dessas gotículas (RÉ, 1998; JAFARI et al., 2008; SILVA et al., 2015). Teor de sólidos, viscosidade e método de emulsificação são outros parâmetros da emulsão que afetam significativamente a eficiência de microencapsulação (JAFARI et al., 2008a).

A utilização de metodologias que permitem a obtenção de emulsões em escala submícron tem sido empregada a fim de aumentar a estabilidade e aumentar a retenção de compostos de interesse (SOOTTITANTAWAT et al., 2005b). A tecnologia do ultrassom tem sido aplicada em diversos estudos com a intenção de melhorar as características de emulsões em comparação com os métodos de agitação convencionais (CONSOLI et al., 2017; FERNANDES et al., 2016; JAFARI; HE; BHANDARI, 2007; SILVA et al., 2015, 2016).

Portanto a emulsão, compreendendo a primeira etapa do processo de microencapsulação, além de interferir diretamente na eficiência de encapsulação, deve ser cuidadosamente formada. Uma emulsão estável favorece a retenção de voláteis e, consequentemente, menos material terá que ser adicionado ao produto para se atingir o aroma desejado e, consequentemente, haverá menos óleo na superfície susceptível à oxidação e formação de *off-flavors* (JAFARI et al., 2008a).

3.1 EMULSIFICAÇÃO POR ULTRASSOM

A produção de emulsões pelo método de ultrassom faz uso de aplicação de ondas ultrassônicas de alta intensidade (frequência > 20 kHz) que geram altas tensões de cisalhamento

e gradientes de pressão no material, que rompem as gotículas da emulsão principalmente pelo efeito da cavitação (MCCLEMENTS, 1999).

Este efeito da cavitação é verificado em fluidos que são submetidos a inúmeras oscilações de pressão. Com o aumento de pressão, o líquido é comprimido e posteriormente expandido quando há o decréscimo da pressão. Com a contínua compressão/expansão ocorre a formação de bolhas de cavitação que, no momento de nova compressão, explodem gerando intensas ondas que deformam e rompem as gotas em gotículas menores. Em paralelo com esse fenômeno há aumento da temperatura e pressão associado à propagação dessas ondas (JAFARI; HE; BHANDARI, 2007; WALSTRA, 2003; MCCLEMENTS, 1999).

O aumento de temperatura, resultado da dissipação de energia mecânica, afeta a eficiência da emulsificação. Temperaturas mais altas reduzem a viscosidade da dispersão e a tensão superficial, facilitando a ruptura das gotículas (GAIKWAD; PANDIT, 2008; MCCLEMENTS, 1999). Por outro lado, o aumento da temperatura pode comprometer a atividade emulsificante dos biopolímeros e facilitar a coalescência das gotículas pelo aumento da frequência de colisões, prejudicando a estabilidade da emulsão (FLOURY et al., 2003; JAFARI; HE; BHANDARI, 2007).

Os parâmetros que afetam a eficiência do método de ultrassom na obtenção de emulsões incluem a intensidade da potência de radiação, pressão hidrostática, fração óleo/água, posição da ponteira ultrassônica, o tempo de exposição e a frequência das ondas (GAIKWAD; PANDIT, 2008; JAFARI; HE; BHANDARI, 2007; MCCLEMENTS, 1999; MONGENOT; CHARRIER; CHALIER, 2000; ABISMAIL et al., 1999; MAHDI JAFARI; HE; BHANDARI, 2006).

O diâmetro das gotículas pode ser reduzido pelo aumento da intensidade das ondas e do tempo de exposição a esse método de homogeneização. O aumento da potência de radiação do ultrassom causa maiores amplitudes de pressão e, por isso, a cavitação é mais intensa, o que favorece o colapso das gotas. No entanto, há de se considerar que excesso de processamento afetam a estabilidade da emulsão, causando a coalescência das gotículas e aumento significativo da temperatura (JAFARI et al., 2008b; GAIKWAD; PANDIT, 2008; JAFARI; HE; BHANDARI, 2007; MCCLEMENTS, 1999; MONGENOT; CHARRIER; CHALIER, 2000).

Dos métodos disponíveis na geração das ondas ultrassônicas, o que utiliza transdutores piezoelétricos é um dos mais utilizados em escala industrial e laboratorial, pela possibilidade de se trabalhar com pequenos volumes de amostra. Nesse método, um cristal

piezoelétrico é localizado no interior de transdutores ultrassônicos. Uma corrente elétrica de alta intensidade é aplicada a esse transdutor que causa a oscilação do cristal, que gera as ondas ultrassônicas. Essas ondas são direcionadas ao topo do transdutor, que as espalham para o líquido ao redor e geram os gradientes de pressão e cisalhamento responsáveis pela ruptura das gotas (MCCLEMENTS, 1999).

Em vista do exposto, essa tecnologia oferece vantagens em relação às outras tecnologias disponíveis para a produção de emulsões, como a possibilidade de se obter partículas da fase dispersa em escala submícron e com distribuição estreita de tamanho de partículas, emulsões mais estáveis, dispensa a adição de surfactantes para a estabilização do sistema e a energia necessária para a formação da emulsão é que aquela necessária por outros métodos (CHANDRAPALA et al., 2012; CHEMAT; KHAN, 2011; ABISMAIL et al., 1999; CHENDKE; FOGLER, 1975).

Assim, dado que a estabilidade da emulsão é influenciada principalmente pelo diâmetro das gotículas da fase dispersa, a utilização das chamadas tecnologias emergentes, na qual se inclui o ultrassom, com o objetivo de se obter emulsões mais estáveis é extensamente empregada (AGUIAR et al., 2016; CONSOLI et al., 2017; FERNANDES et al., 2016; REN et al., 2018; JAFARI; HE; BHANDARI, 2006; SILVA et al., 2015, 2016), uma vez que a emulsificação é uma das etapas mais importantes no processo de microencapsulação, que afeta diretamente a encapsulação de compostos de interesse (AGUIAR et al., 2016; SILVA et al., 2016; SOOTTITANTAWAT et al., 2005b; MONGENOT; CHARRIER; CHALIER, 2000).

4 REAÇÃO DE TRANSFERÊNCIA DE PRÓTONS ACOPLADA A ESPECTROMETRIA DE MASSAS (*PROTON TRANSFER REACTION MASS SPECTROMETRY – PTR-MS)*

Compostos orgânicos voláteis (VOC) correspondem a uma série de moléculas orgânicas e inorgânicas provenientes das mais diferentes fontes: plantas, animais, poluição ambiental etc. A detecção desses VOC é importante em alimentos, uma vez que os compostos voláteis afetam o sabor e o aroma do alimento, além de ser um indicador da qualidade do produto (DUTCOSKY, 2011; ELLIS; MAYHEW, 2014a; TAYLOR; LINFORTH, 1998).

A técnica mais utilizada para análise de VOC é a cromatografia gasosa, que é capaz de detectar concentrações muito baixas. Embora seja uma técnica útil para identificação e quantificação de compostos de aroma, ela apresenta algumas limitações, na qual a mais

notável é a resolução temporal, isto é, não permite o monitoramento da concentração dos compostos em função do tempo. Além disso, a cromatografia gasosa demanda tempo para preparação de amostra, que por vezes precisa ser pré-concentrada, além de colunas de separação específicas (BIASIOLI et al., 2011a; BLAKE; MONKS; ELLIS, 2009; DEWULF; VAN LANGENHOVE; WITTMANN, 2002).

A técnica de Reação de Transferência de Prótons Acoplada à Espectrometria de Massas (PTR-MS - *Proton Transfer Reaction - Mass Spectrometry*) apresenta diversas vantagens comparada às metodologias tradicionalmente empregadas na análise de compostos voláteis em amostras complexas, tal como a cromatografia gasosa (DEWULF; VAN LANGENHOVE; WITTMANN, 2002). A PTR-MS é mais rápida pois as variações dependentes do tempo que ocorrem no método de espaço-livre (*headspace* - HS), podem ser monitoradas em frações de segundos e em alta resolução; não necessita de preparos de amostras morosos com a manipulação com solventes e utilização de fibras de adsorção e dessorção. Além disso, devido à pequena fragmentação, esta técnica permite reproduzir o mesmo perfil do espectro de massa obtido por HS e possibilita a conversão do sinal da intensidade do espectro de massas em concentração obtida pelo método HS (YERETZIAN; JORDAN; LINDINGER, 2003).

A técnica PTR-MS utiliza o H_3O^+ como doador de prótons dado que a maioria das moléculas orgânicas tem afinidade por prótons superior a este íon, consequentemente, a transferência de prótons ocorre quase que inteiramente às demais moléculas orgânicas. Tal reação provoca apenas uma ionização suave (RH^+) com pouca ou nenhuma fragmentação. Característica importante quando se trata de análises de misturas complexas, uma vez que, quando ocorre intensa fragmentação, tende a levar a uma identificação equivocada do composto ou um espectro de massas confuso e sem valor analítico (ELLIS; MAYHEW, 2014b).

O aparato de um PTR-MS (*Proton Transfer Reaction - Mass Spectrometry*) com espectrômetro de massas ToF (*Time-of-Flight*) está ilustrado de forma simplificada na Figura 3, na qual se utiliza um espectrômetro de massas por tempo de voo.

Figura 3. Esquema de um equipamento PTR-ToF-MS. © IONICON.

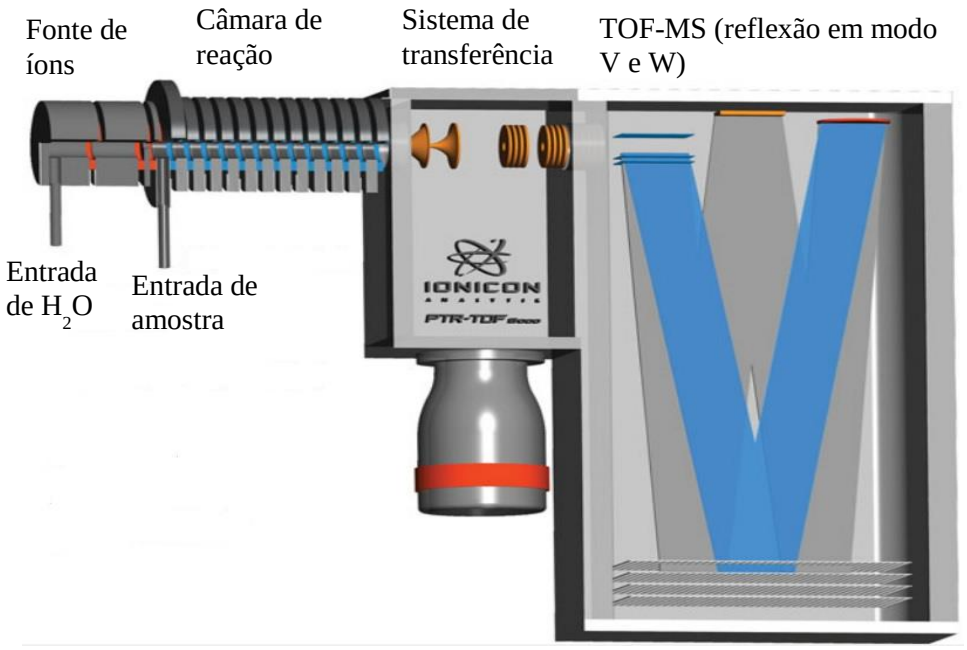

O equipamento de PTR-MS é composto por cinco partes principais:

1. Uma fonte de íons H_3O^+ (produzida a partir de H_2O) gera íons livres de contaminações, que vão reagir com o analito;
2. A câmara de reação é o local onde ocorre múltiplas colisões entre íons e moléculas que resulta na transferência de prótons dos íons H_3O^+ para os analitos.
3. Os íons formados atravessam o sistema de transferência para o espectrômetro de massas;
4. No espectrômetro de massas os íons são separados de acordo com a razão massa/carga (*m/z*).
5. O detector promove a aquisição dos sinais eletrônicos dos íons.

A utilização do ToF como espectrômetro de massa apresenta algumas vantagens em relação a outros detectores: teoricamente faixa de *m/z* ilimitada, alta resolução, rápida transição de íons, espectro de massas completo como todos os íons formados sendo detectados (CAPPELLIN et al., 2010; ELLIS; MAYHEW, 2014b; JORDAN et al., 2009).

No entanto, uma das principais vantagens do uso do PTR-ToF-MS é a possibilidade do monitoramento de VOC em tempo real (ELLIS; MAYHEW, 2014a; LINDINGER et al., 2008), que fornece informações de processos dinâmicos de formação e liberação de VOC, permitindo verificar mudanças rápidas de concentração de compostos voláteis e liberação *in vivo* (BIASIOLI et al., 2011b; GLÖESS et al., 2014; ROMANO et al., 2014; YERETZIAN et al., 2002).

A técnica PTR-ToF-MS tem sido empregada na análise de VOCs nas áreas mais diversas da ciência de alimentos, tais como: monitoramento da liberação de VOCs de tomate

durante a mastigação (FARNETI et al., 2013), discriminação de vinhos quanto à origem e cultura da fermentação malolática (CAMPBELL-SILLS et al., 2016), composição de VOCs em leites submetidos a diferentes processos de produção (LIU et al., 2018), influência das propriedades da manga na liberação e percepção de aroma (BONNEAU et al., 2018), avaliação do efeito da origem do cacau e na composição aromática de chocolates (ACIERNO et al., 2019), perfil aromático de especiarias (SILVIS et al., 2019) e mudança da composição aromática durante a fermentação de cervejas (RICHTER et al., 2018).

Na ciência do café, em razão da complexidade de aromas formados durante a torra de café bem como liberados durante o preparo de bebidas, essa técnica foi empregada no monitoramento da formação de VOCs durante a torra de cafés (GLÖESS et al., 2014), dinâmica de extração de VOCs de cápsulas de café espresso (SÁNCHEZ-LÓPEZ; ZIMMERMANN; YERETZIAN, 2014), efeito da temperatura e pressão de água na cinética de extração de VOCs durante o preparo de café espresso (LÓPEZ et al., 2016), além do uso da PTR-ToF-MS como ferramenta de discriminação entre espécies (COLZI et al., 2017).

Trata-se, portanto, de uma ferramenta emergente útil no monitoramento de processos dinâmicos complexos e que ocorrem num tempo curto, na detecção de traços por apresentar alta sensibilidade, além da versatilidade pelos diferentes usos principalmente na ciência de alimentos.

REFERÊNCIAS

ABBAS, S.; WEI, C. D., HAYAT, K.; XIAOMING, Z. Ascorbic Acid: Microencapsulation Techniques and Trends - A Review. **Food Reviews International**, v. 28, p. 343–374, 2012.

ABISMAIL, B.; CANSELIER, J. P; WILHELM, A. M.; DELMAS, H.; GOURDON, C. Emulsification by ultrasound- drop size distribution and stability.pdf. **Ultrasonics Sonochemistry**, v. 6, p. 75–83, 1999.

ACIERNO, V.; LIU, N.; ALEWIJN, M.; STIEGER, M.; RUTH, S. M. V. Which cocoa bean traits persist when eating chocolate? Real-time nosespace analysis by PTR-QiToF-MS. **Talanta**, v. 195, p. 676–682, 2019.

AGHBASHLO, M.; MOBLI, H.; MADADLOU, A.; RAFIEE, S. The correlation of wall material composition with flow characteristics and encapsulation behavior of fish oil emulsion. **Food Research International**, v. 49, n. 1, p. 379–388, 2012.

AGUIAR, A. C.; SILVA, L. P.; REZENDE, C. A.; BARBERO, G. F.; MARTÍNEZ, J. Encapsulation of pepper oleoresin by supercritical fluid extraction of emulsions. **Journal of Supercritical Fluids**, v. 112, p. 37–43, 2016.

ARAÚJO, J. M. A. Emulsão/Emulsificantes. In: **Química de Alimentos - Teoria e Prática**. 5. ed. [s.l.] UFV, 2012. p. 244–287.

BAE, E. K.; LEE, S. J. Microencapsulation of avocado oil by spray drying using whey protein and maltodextrin. **Journal of microencapsulation**, v. 25, n. 8, p. 549–560, 2008.

BAKRY, A. M.; ABBAS, S.; ALI, B.; MAJEED, H.; ABOUELWAFA, M. Y.; MOUSA, A.; LIANG, L. Microencapsulation of Oils: A Comprehensive Review of Benefits, Techniques, and Applications. **Comprehensive Reviews in Food Science and Food Safety**, v. 15, n. 1, p. 143–182, 2016.

BARANAUSKIENE, R.; VENSKUTONIS, P. R.; DEWETTINCK, K.; VERHÉ, R. Properties of oregano (Origanum vulgare L.), citronella (Cymbopogon nardus G.) and marjoram (Majorana hortensis L.) flavors encapsulated into milk protein-based matrices. **Food Research International**, v. 39, n. 4, p. 413–425, 2006.

BARANAUSKIENÉ, R.; BYLAITÉ, E.; ZUKAUSKAITÉ, J.; VENSKUTONIS, R. Flavor retention of peppermint (*Mentha piperita L.*) essential oil spray-dried in modified starches during encapsulation and storage. **Journal of Agricultural and Food Chemistry**, v. 55, n. 8, p. 3027–3036, 2007.

BASSOLI, D. G. **Impacto Aromático Dos Componentes Voláteis Do Café Solúvel : Impacto Aromático Dos Componentes Voláteis Do Café Solúvel :** [s.l.] Universidade Estadual de Londrina, 2006.

BENCHABANE, S.; SUBIRADE, M.; VANDENBERG, G. W. Production of BSA-loaded alginate microcapsules: Influence of spray dryer parameters on the microcapsule characteristics and BSA release. **Journal of Microencapsulation,** v. 24, n. 6, p. 647–658, 2007.

BHUMIRATANA, N.; ADHIKARI, K.; IV, E. C. Evolution of sensory aroma attributes from coffee beans to brewed coffee. **LWT - Food Science and Technology**, v. 44, p. 2185–2192, 2011.

BIASIOLI, F. YERETZIAN, C.; GASPERI, F.; MÄRK, T. D. PTR-MS monitoring of VOCs and BVOCs in food science and technology. **TrAC - Trends in Analytical Chemistry**, v. 30, n. 7, p. 968–977, 2011a.

BIASIOLI, F.; YERETZIAN, C.; MÄRK, T. D.; DEWULF, J.; VAN LANGENHOVE, H. Direct-injection mass spectrometry adds the time dimension to (B)VOC analysis. **TrAC - Trends in Analytical Chemistry**, v. 30, n. 7, p. 1003–1017, 2011b.

BLAKE, R. S.; MONKS, P. S.; ELLIS, A. M. Proton-Transfer Reaction Mass Spectrometry. **Chemical Reviews**, v. 44, p. 861–896, 2009.

BONNEAU, A.; BOULANGER, R.; LEBRUN, M.; MARAVAL, I.; VALETTE, J.; GUICHARD, E.; GUNATA, Z. Impact of fruit texture on the release and perception of aroma compounds during in vivo consumption using fresh and processed mango fruits. **Food Chemistry**, v. 239, p. 806–815, 2018.

BOUYER, E.; MEKHLOUFI, G.; ROSILIO, V.; GROSSIORD, J. L.; AGNELY, F. Proteins, polysaccharides, and their complexes used as stabilizers for emulsions: Alternatives to synthetic surfactants in the pharmaceutical field? **International Journal of Pharmaceutics**, v. 436, p. 359-378, 2012.

BRASIL. Ministério da Agricultura, Pecuária e Abastecimento. Disponível em: http://indicadores.agricultura.gov.br/index.htm. Acesso em: 12 mar. 2019.

BRINQUES, G. B.; AYUB, M. A. Z. Effect of microencapsulation on survival of Lactobacillus plantarum in simulated gastrointestinal conditions, refrigeration, and yogurt. **Journal of Food Engineering**, v. 103, n. 2, p. 123–128, 2011.

BUFFO, R. A.; CARDELLI-FREIRE, C. Coffee flavour: An overview. **Flavour and Fragrance Journal**, v. 19, n. 2, p. 99–104, 2004.

CAL, K.; SOLLOHUB, K. Spray drying technique. I: Hardware and process parameters. **Journal of Pharmaceutical Sciences**, v. 99, n. 2, p. 575–586, 2010.

CALLIGARIS, S.; MUNARI, M.; ARRIGHETTI, G.; BARBA, L. Insights into the physicochemical properties of coffee oil. **European Journal of Lipid Science and Technology**, v. 111, n. 12, p. 1270–1277, 2009.

CAMPBELL-SILLS, H.; CAPOZZI, V.; ROMANO, A.; CAPPELLIN, L.; SPANO, G.; BRENIAUX, M.; LUCAS, P.; BIASIOLI, F. Advances in wine analysis by PTR-ToF-MS: Optimization of the method and discrimination of wines from different geographical origins and fermented with different malolactic starters. **International Journal of Mass Spectrometry**, v. 397–398, p. 42–51, 2016.

CAPPELLIN, L.; BIASIOLI, F.; FABRIS, A.; SCHUHFRIED, E.; SOUKOULIS, C.; MÄRK, T. D.; GASPERI, F. Improved mass accuracy in PTR-TOF-MS: Another step towards better compound identification in PTR-MS. **International Journal of Mass Spectrometry**, v. 290, n. 1, p. 60–63, 2010.

CARVALHO, A. G. S.; SILVA, V. M.; HUBINGER, M. D. Microencapsulation by spray drying of emulsified green coffee oil with two-layered membranes. **Food Research International**, v. 61, p. 236–245, 2014.

CECAFE – Conselho dos Exportadores de café do Brasil. Disponível em: https://www.cecafe.com.br/publicacoes/relatorio-de-exportacoes/. Acesso em: 12 mar. 2019.

CERVANTES-MARTÍNEZ, C. V.; MEDINA-TORRES, L.; GONZÁLEZ-LAREDO, R. F.; CALDERAS, F.; SÁNCHEZ-OLIVARES, G.; HERRERA-VALENCIA, E. E.; INFANTE, J. A. G.; ROCHA-GUZMAN, N. E.; RODRÍGUEZ-RAMÍREZ, J. Study of spray drying of the Aloe vera mucilage (Aloe vera barbadensis Miller) as a function of its rheological properties. **LWT - Food Science and Technology**, v. 55, n. 2, p. 426–435, 2014.

CHANDRAPALA, J.; OLIVER, C.; KENTISH, S.; ASHOKKUMAR, M. Ultrasonics in food processing. **Ultrasonics Sonochemistry**, v. 19, n. 5, p. 975–983, 2012.
CHEMAT, F.; ZILL-E-HUMA; KHAN, M. K. Applications of ultrasound in food technology: Processing, preservation and extraction. **Ultrasonics Sonochemistry**, v. 18, n. 4,

p. 813–835, 2011.

CHENDKE, P. K.; FOGLER, H. S. Macrosonics in industry: 4. Chemical Processing. **Ultrasonics**, v. 13, p. 31–37, 1975.

CLINTON, W. P.; PLAINS, M.; PITCHON, E. **Producing a stable coffee aroma product**, 1962.

COLZI, I.; TAITI, C.; MARONE, E.; MAGNELLI, S.; GONNELLI, C.; MANCUSO, S. Covering the different steps of the coffee processing : Can headspace VOC emissions be exploited to successfully distinguish between Arabica and Robusta? **Food Chemistry**, v. 237, p. 257–263, 2017.

CONSOLI, L.; FURTADO, G. F.; CUNHA, R. L.; HUBINGER, M. D. High solids emulsions produced by ultrasound as a function of energy density. **Ultrasonics Sonochemistry**, v. 38, p. 772–782, 2017.

CORTÉS-ROJAS, D. F.; SOUZA, C. R. F.; OLIVEIRA, W. P. Encapsulation of eugenol rich clove extract in solid lipid carriers. **Journal of Food Engineering**, v. 127, p. 34–42, 2014.

CZERNY, M.; MAYER, F.; GROSCH, W. Sensory study on the character impact odorants of roasted Arabica coffee. **Journal of Agricultural and Food Chemistry**, v. 47, n. 2, p. 695–699, 1999.

DE MARIA, C. A. B.; TRUGO, L. C.; MOREIRA, R. F. A.; WERNECK, C. C. Composition of green coffee fractions and their contribution to the volatile profile formed during roasting. **Food Chemistry**, v. 50, n. 2, p. 141–145, 1994.

DEWULF, J.; VAN LANGENHOVE, H.; WITTMANN, G. Analysis of volatile organic compounds using gas chromatography. **Trends in Analytical Chemistry**, v. 21, n. 02, p. 637–646, 2002.

DIAS, M. I.; FERREIRA, I. C. F. R.; BARREIRO, M. F. Microencapsulation of bioactives for food applications. **Food & function**, v. 6, p. 1035–1052, 2015.

DOMIAN, E.; BRYNDA-KOPYTOWASKA, A.; CENKIER, J.; SWIRYDOW, E. Selected properties of microencapsulated oil powders with commercial preparations of maize OSA starch and trehalose. **Journal of Food Engineering**, v. 152, p. 72–84, 2015.

DORDEVIC, V.; BALANC, B.; BELSCAK-CVITANOVIC, A.; LECIV, S.; TRIFKOVIC, K.; KALUSEVIC, A.; KOSTIC, I.; KOMES, D.; BUGARSKI, B.; NEDOVIC, V. Trends in Encapsulation Technologies for Delivery of Food Bioactive Compounds. **Food Engineering Reviews**, v. 7, n. 4, p. 452–490, 2014.

DUTCOSKY, S. D. Os receptores sensoriais - elementos de avaliação sensorial. In: **Análise Sensorial de Alimentos**. 3. ed. Curitiba: Champagnat, 2011. p. 29–40.

ELLIS, A. M.; MAYHEW, C. A. Background. In: **Proton Transfer Reaction Mass Spectrometry. Principles and Applications**. 1. ed. West Sussex: CRC Press LLC, 2014. p. 2–23.

ELLIS, A. M.; MAYHEW, C. A. Experimental: Components and Principles. In: **Proton Transfer Reaction Mass Spectrometry. Principles and Applications**. 1. ed. West Sussex: CRC Press LLC, 2014. p. 49–109.

EUROMONITOR INTERNATIONAL. Disponível em: http://consorciopesquisacafe.com.br/arquivos/consorcio/consumo/tendencias_do_mercado_cafe_2017.pdf. Acesso em: 20 mar. 2019.

FANG, S.; ZHAO, X.; LIU, Y.; LIANG, X.; YANG, Y. Fabricating multilayer emulsions by using OSA starch and chitosan suitable for spray drying: Application in the encapsulation of β-carotene. **Food Hydrocolloids**, v. 93, p. 102-110, 2019.

FANG, Z.; BHANDARI, B. Encapsulation of polyphenols - a review. **Trends in Food Science & Technology**, v. 21, n. 10, p. 510–523, 2010.

FARNETI, B.; ALGARRA, ALARCÓN, A. A.; CRISTESCU, S. M.; COSTA, G.; HARREN, F. J. M.; HOLTHUYSEN, N. T. E.; WOLTERING, E. J. Aroma volatile release kinetics of tomato genotypes measured by PTR-MS following artificial chewing. **Food Research International**, v. 54, n. 2, p. 1579–1588, 2013.

FERNANDES, R. V. B.; BORGES, S. V.; SILVA, E. K.; SILVA, Y. F.; SOUZA, H. J B.; CARMO, E. L.; OLIVEIRA, C. R.; YOSHIDA, M. I.; BOTREL, D. A. Study of ultrasound-assisted emulsions on microencapsulation of ginger essential oil by spray drying. **Industrial Crops and Products**, v. 94, p. 413–423, 2016.

FLAMENT, I. From the raw bean to the roast coffee. In: FLAMENT, I. (Ed.). . **Coffee Flavour Chemistry**. Chichester: John Wiley & Sons, 2002. p. 37–52.

FLEMING, R. S. The Spray Process of Drying. **Industrial and Engineering Chemistry**, v. 13, n. 5, p. 447–449, 1921.

FORNY, L.; MARABI, A.; PALZER, S. Wetting, disintegration and dissolution of agglomerated water soluble powders. **Powder Technology**, v. 206, n. 1–2, p. 72–78, 2011.

FRASCARELI, E. C.; SILVA, V. M.; TONON, R. V.; HUBINGER, M. D. Effect of process conditions on the microencapsulation of coffee oil by spray drying. **Food and Bioproducts Processing**, v. 90, n. 3, p. 413–424, 2012a.

FRASCARELI, E. C.; SILVA, V. M.; TONON, R. V.; HUBINGER, M. D. Determination of critical storage conditions of coffee oil microcapsules by coupling water sorption isotherms and glass transition temperature. **International Journal of Food Science and Technology**, v. 47, n. 5, p. 1044–1054, 2012b.

FREIBERGER, E. B.; KAUFMANN, K. C.; BONA, E.; ARAÚJO, P. H. H.; SAYER, C.; LEIMANN, F. V.; GONÇALVES, O. H. Encapsulation of roasted coffee oil in biocompatible nanoparticles. **LWT - Food Science and Technology**, v. 64, n. 1, p. 381–389, 2015.

GAIKWAD, S. G.; PANDIT, A. B. Ultrasound emulsification : Effect of ultrasonic and physicochemical properties on dispersed phase volume and droplet size. **Ultrasonics Sonochemistry**, v. 15, p. 554–563, 2008.

GETACHEW, A. T.; CHUN, B. S. Optimization of coffee oil flavor encapsulation using response surface methodology. **LWT - Food Science and Technology**, v. 70, p. 126–134, 2016.

GHARSALLAOUI, A.; ROUDAUT, G.; CHAMBIN, O.; VOILLEY, A.; SAUREL, R. Applications of spray-drying in microencapsulation of food ingredients: An overview. **Food Research International**, v. 40, n. 9, p. 1107–1121, 2007.

GLÖESS, A. N.; VIETRI, A.; WIELAND, F.; SMRKE, S.; SCHÖNBÄCHLER, B.; LÓPEZ, J. A. S.; PETROZZI, S.; BONGERS, S.; KOZIOROWSKI, T.; YERETZIAN, C. Evidence of different flavour formation dynamics by roasting coffee from different origins: On-line analysis with PTR-ToF-MS. **International Journal of Mass Spectrometry**, v. 365–366, p. 324–337, 2014.

GOUIN, S. Microencapsulation: Industrial appraisal of existing technologies and trends. **Trends in Food Science and Technology**, v. 15, n. 7–8, p. 330–347, 2004.

HURTADO-BENAVIDES, A.; DORADO, D. A.; SÁNCHEZ-CAMARGO, A. D. P. Study of the fatty acid profile and the aroma composition of oil obtained from roasted Colombian coffee beans by supercritical fluid extraction. **Journal of Supercritical Fluids**, v. 113, p. 44–52, 2016.

ICO - International Coffee Organization a. Disponível em: http://www.ico.org/prices/po-production.pdf. Acesso em: 12 mar. 2019.

ICO - International Coffee Organization b. Disponível em: http://www.ico.org/prices/new-consumption-table.pdf. Acesso em: 12 mar. 2019.

JAFARI, S. M.; ASSADPOOR, E.; HE, Y.; BHANDARI, B. Encapsulation Efficiency of Food Flavours and Oils during Spray Drying. **Drying Technology**, v. 26, n. 7, p. 816–835, 2008a.

JAFARI, S. M.; ASSADPOOR, E.; HE, Y.; BHANDARI, B. Re-coalescence of emulsion droplets during high-energy emulsification. **Food Hydrocolloids**, v. 22, n. 7, p. 1191–1202, 2008b.

JAFARI, S. M.; HE, Y.; BHANDARI, B. Production of sub-micron emulsions by ultrasound and microfluidization techniques. **Journal of Food Engineering**, v. 82, n. 4, p. 478–488, 2007.

JANNASARI, N.; FATHI, M.; MOSHTAGHIAN, S. J.; ABBASPOURRAD, A. Microencapsulation of vitamin D using gelatin and cress seed mucilage: Production, characterization and in vivo study. **International Journal of Biological Macromolecules**, v. 129, p. 972–979, 2019.

JORDAN, A.; HAIDACHER, S.; HANEL, G.; HARTUNGEN, E.; MÄRK, L. SEEHAUSER, H.; SCHOTTKOWSKY, R.; SULZER, P.; MÄRK. A high resolution and high sensitivity proton-transfer-reaction time-of-flight mass spectrometer (PTR-TOF-MS). **International Journal of Mass Spectrometry**, v. 286, n. 2–3, p. 122–128, 2009.

JUN-XIA, X.; HAI-YAN, Y.; JIAN, Y. Microencapsulation of sweet orange oil by complex coacervation with soybean protein isolate/gum Arabic. **Food Chemistry**, v. 125, n. 4, p. 1267–1272, 2011.

KARADENIZ, M.; SAHIN, S.; SUMNU, G. Enhancement of storage stability of wheat germ oil by encapsulation. **Industrial Crops and Products**, v. 114, n. July 2017, p. 14–18, 2018.

KELLY, G. M.; O'MAHONY, J. A.; KELLY, A. L.; O'CALLAGHAN, D. J. Physical characteristics of spray-dried dairy powders containing different vegetable oils. **Journal of Food Engineering**, v. 122, n. 1, p. 122–129, 2014.

KING, C. J. Spray Drying: Retention of Volatile Compounds Revisited. **Drying Technology**, v. 13, n. 5–7, p. 1221–1240, 1 jan. 1995.

KLEIN, P.; RABEN, I.; HERRERA, W. R. **Aromatization of instant coffee**, 1968.

KOUPANTSIS, T.; PAVLIDOU, E.; PARASKEVOPOULOU, A. Flavour encapsulation in milk proteins - CMC coacervate-type complexes. **Food Hydrocolloids**, v. 37, p. 134–142, 2014.

LAOKULDILOK, N.; THAKEOW, P.; KOPERMSUB, P.; UTAMA-ANG, N. Optimisation of microencapsulation of turmeric extract for masking flavour. **Food Chemistry**, v. 194, p. 695–704, 2015.

LECLERCQ, S.; HARLANDER, K. R.; REINECCIUS, G. A. Formation and characterization of microcapsules by complex coacervation with liquid or solid aroma cores. **Flavour and Fragrance Journal**, v. 24, n. 1, p. 17–24, 2009.

LINDINGER, C.; LABBE, D.; POLLIEN, P.; RYTZ, A.; JUILLERAT, M. A.; YERETZIAN, C.; BLANK, I. When Machine Tastes Coffee: Instrumental Approach to Predict Sensory Profile of Espresso Coffee. **Analytical Chemistry**, v. 80, n. 5, p. 1574–1581, 2008.

LIU, N.; KOOT, A.; HETTINGA, K.; JONG, J.; RUTH, S. M. Portraying and tracing the impact of different production systems on the volatile organic compound composition of milk by PTR-(Quad)MS and PTR-(ToF)MS. **Food Chemistry**, v. 239, p. 201–207, 2018.

LIU, X.-D. ATARASHI, T.; FURUTA, T.; YOSHII, H.; AISHIMA, S.; OHKAWARA, M.; LINKO, P. Microencapsulation of Emulsified Hydrophobic Flavors By Spray Drying. **Drying Technology**, v. 19, n. 7, p. 1361–1374, 2001.

LÓPEZ, J. A. S.; WELLINGER, M.; GLOESS, A. N.; ZIMMERMANN, R.; YERETZIAN, C. Extraction kinetics of coffee aroma compounds using a semi-automatic machine: On-line analysis by PTR-ToF-MS. **International Journal of Mass Spectrometry**, v. 401, p. 22–30, 2016.

LOUGHRILL, E.; THOMPSON, S.; OWUSU-WARE, S.; SNOWDEN, M. J.; DOUDOUMIS, D.; ZAND, N.. Controlled release of microencapsulated docosahexaenoic acid (DHA) by spray–drying processing. **Food Chemistry**, v. 286, p. 368–375, 2019.

LUCA, A. CILEK, B.; HASIRCI, V.; SAHIN, S.; SUMNU, G. Storage and Baking Stability of Encapsulated Sour Cherry Phenolic Compounds Prepared from Micro- and Nano-Suspensions. **Food and Bioprocess Technology**, v. 7, n. 1, p. 204–211, 2014.

MADENE, A.; JACQUOT, M.; SCHER, J.; DESEBRY. Flavour encapsulation and controlled release - A review. **International Journal of Food Science and Technology**, v. 41, n. 1, p. 1–21, 2006.

MAHDAVI, S. A. JAFARI, S. M.; GHORBANI, M.; ASSADPOOR, E. Spray-Drying Microencapsulation of Anthocyanins by Natural Biopolymers: A Review. **Drying Technology**, v. 32, n. 5, p. 509–518, 2014.

MAHDI JAFARI, S.; HE, Y.; BHANDARI, B. Nano-emulsion production by sonication and microfluidization - A comparison. **International Journal of Food Properties**, v. 9, n. 3, p. 475–485, 2006.

MARTINS, I. M.; BARREIRO, M. F.; COELHO, M.; RODRIGUES, A. E. Microencapsulation of essential oils with biodegradable polymeric carriers for cosmetic applications. **Chemical Engineering Journal**, v. 245, p. 191–200, 2014.

MCCLEMENTS, D. J. **Food Emulsions**. Boca Raton: CRC Press LLC, 1999.

MONGENOT, N.; CHARRIER, S.; CHALIER, P. Effect of ultrasound emulsification on cheese aroma encapsulation by carbohydrates. **Journal of Agricultural and Food Chemistry**, v. 48, n. 3, p. 861–867, 2000.

MURUGESAN, R.; ORSAT, V. Spray Drying for the Production of Nutraceutical Ingredients-A Review. **Food and Bioprocess Technology**, v. 5, n. 1, p. 3–14, 2012.

ORDOÑEZ, M.; HERRERA, A. Morphologic and stability cassava starch matrices for encapsulating limonene by spray drying. **Powder Technology**, v. 253, p. 89–97, 2014.

PAPADAKIS, S. E.; KING, C. J. Air temperature and humidity profiles in spray drying. 1. Features predicted by the particle source in cell model. **Industrial & Engineering Chemistry Research**, v. 27, n. 11, p. 2111–2116, 1988.

PATEL, J. M. **Cryogenic aromatization of instant coffee**, 1974.

PELLICER, J. A.; FORTEA, M. I.; TRABAL, J.; RODRÍGUEZ-LÓPEZ, M. I.; CARAZO-DÍAZ, C.; GABALDÓN, J. A.; NÚÑEZ-DELICADO, E. Optimization of the microencapsulation of synthetic strawberry flavour with different blends of encapsulating agents using spray drying. **Powder Technology**, v. 338, p. 591–598, 2018.

PILETTI, R. ZANETTI, M.; JUNG, G.; MELLO, J. M. M.; DALCANTON, F.; SOARES, C.; RIELLA, H. G.; FIORI, M. A. Microencapsulation of garlic oil by β-cyclodextrin as a thermal protection method for antibacterial action. **Materials Science and Engineering C**, v. 94, p. 139–149, 2019.

POLAVARAPU, S. OLIVER, C. M.; AJLOUNI, S.; AUGUSTIN, M. A. Physicochemical characterisation and oxidative stability of fish oil and fish oil-extra virgin olive oil

microencapsulated by sugar beet pectin. **Food Chemistry**, v. 127, n. 4, p. 1694–1705, 2011.

POLLIEN, P.; KREBS, Y.; CHAINTREAU, A. **Comparison of a brew and an instant coffee using a new GC-olfactometric method**. ASIC-17eme Colloque Scientifique International sur le Cafè. 1997. Disponível em: <%5C%5CRobsrv-05%5Creference manager%5CArticles%5C5177.pdf>

RAMAKRISHNAN, Y.; ADZAHAN, N. M.; YUSOF, Y. A.; MUHAMMAD, K. Effect of wall materials on the spray drying efficiency, powder properties and stability of bioactive compounds in tamarillo juice microencapsulation. **Powder Technology**, v. 328, p. 406–414, 2018.

RÉ, M. I. Microencapsulation by spray drying. **Drying Technology**, v. 16, n. 6, p. 1195–1236, 1998.

REN, X.; HOU, T.; LIANG, Q.; ZHANG, X.; HU, D.; XU, B.; CHEN, X.; CHALAMAIAH, M.; MA, H. Effects of frequency ultrasound on the properties of zein-chitosan complex coacervation for resveratrol encapsulation. **Food Chemistry**, v. 279, p. 223–230, 2018.

REINECCIUS, G. A. The spray drying of food flavors. **Drying Technology**, v. 22, n. 6, p. 1289–1324, 2004.

RICHTER, T. M.; SILCOCK, P.; ALGARRA, A.; EYRES, G. T.; CAPOZZI, V.; BREMER, P. J.; BIASIOLI, F. Evaluation of PTR-ToF-MS as a tool to track the behavior of hop-derived compounds during the fermentation of beer. **Food Re**, v. 111, p. 582–589, 2018.

ROCHA-SELMI, G. A.; BOZZA, F. T.; THOMAZINI, M.; BOLINI, H. M. A.; FÁVARO-TRINDADE, C. S. Microencapsulation of aspartame by double emulsion followed by complex coacervation to provide protection and prolong sweetness. **Food Chemistry**, v. 139, n. 1–4, p. 72–78, 2013.

RODRIGUES, R. A F.; GROSSO, C. R. F. Cashew gum microencapsulation protects the aroma of coffee extracts. **Journal of microencapsulation**, v. 25, n. 1, p. 13–20, 2008.

ROMANO, A.; CAPPELLIN, L.; TING, V.; APREA, E.; NAVARINI, L.; GASPERI, F.; BIASIOLI, F. Nosespace analysis by PTR-ToF-MS for the characterization of food and tasters : The case study of coffee. **International Journal of Mass Spectrometry**, v. 365–366, p. 20–27, 2014.

SAIFULLAH, M.; SHISHIR, M. R. I.; FERDOWSI, R.; RAHMAN, M. R. T.; VUONG, Q. V. Micro and nano encapsulation, retention and controlled release of flavor and aroma compounds: A critical review. **Trends in Food Science and Technology**, v. 86, p. 230–251, 2019.

SÁNCHEZ-LÓPEZ, J. A.; ZIMMERMANN, R.; YERETZIAN, C. Insight into the time-resolved extraction of aroma compounds during espresso coffee preparation: Online monitoring by PTR-ToF-MS. **Analytical Chemistry**, v. 86, n. 23, p. 11696–11704, 2014.

SANTOS, M. G.; BOZZA, F. T.; THOMAZINI, M.; FAVARO-TRINDADE, C. S. Microencapsulation of xylitol by double emulsion followed by complex coacervation. **Food**

Chemistry, v. 171, p. 32–39, 2015.

SANZ, C.; CZERNY, M.; CID, C.; SCHIEBERLE, P. Comparison of potent odorants in a filtered coffee brew and in an instant coffee beverage by aroma extract dilution analysis (AEDA). **European Food Research and Technology**, v. 214, n. 4, p. 299–302, 2002.

SCHIFFTER, H.; LEE, G. Single-Droplet Evaporation Kinetics and Particle Formation in an Acoustic Levitator. Part 2: Drying Kinetics and Particle Formation from Microdroplets of Aqueous Mannitol, Trehalose, or Catalase. **Journal of pharmaceutical sciences**, v. 96, n. 9, p. 2284–2295, 2007.

SEMMELROCH, P.; BLANK, I.; GROSCHT, W. Determination of Potent Odourants in Roasted Coffee by Stable Isotope Dilution Assays. **Flavour and Fragrance Journal**, v. 10, p. 1–7, 1995.

SEMMELROCH, P.; GROSCH, W. Studies on character impact odorants of coffee brews. **Journal of Agricultural and Food Chemistry**, v. 44, n. 2, p. 537–543, 1996.

SHAHIDI, F.; HAN, X. Q. Encapsulation of Food Ingredients. **Critical Reviews in Food Science and Nutrition**, v. 33, n. 6, p. 501–547, 1993.

SHAO, P.; XUAN, S.; WU, W.; QU, L. Encapsulation efficiency and controlled release of Ganoderma lucidum polysaccharide microcapsules by spray drying using different combinations of wall materials. **International Journal of Biological Macromolecules**, v. 125, p. 962–969, 2019.

SHEN, Q.; QUEK, S. Y. Microencapsulation of astaxanthin with blends of milk protein and fiber by spray drying. **Journal of Food Engineering**, v. 123, p. 165–171, 2014.

SHEN, Z.; AUGUSTIN, M. A.; SANGUANSRI, L.; CHENG, L. J. Oxidative stability of microencapsulated fish oil powders stabilized by blends of chitosan, modified starch, and glucose. **Journal of Agricultural and Food Chemistry**, v. 58, n. 7, p. 4487–4493, 2010.

SHIBAMOTO, T. Volatile Chemicals from Thermal Degradation of Less Volatile Coffee Components. In: PREEDY, V. R. (Ed.). . **Coffee in Health and Disease Prevention**. London: Elsevier, 2015. p. 129–136.

SILVA, E. K.; GOMES, M. T. M. S.; HUBINGER, M. D.; CUNHA, R. L.; MEIRELES, M. A. A. Ultrasound-assisted formation of annatto seed oil emulsions stabilized by biopolymers. **Food Hydrocolloids**, v. 47, p. 1–13, 2015.

SILVA, E. K.; AZEVEDO, V. M.; CUNHA, R. L.; HUBINGER, M. D.; MEIRELES, M. A. A. Ultrasound-assisted encapsulation of annatto seed oil: Whey protein isolate versus modified starch. **Food Hydrocolloids**, v. 56, p. 71–83, 2016.

SILVIS, I. C. J.; LUNING, P. A.; KLOSE, N.; JANSEN, M.; RUTH, M. J. A. M. Similarities and differences of the volatile profiles of six spices explored by Proton Transfer Reaction Mass Spectrometry. **Food Chemistry**, v. 271, p. 318–327, 2019.

SOBEL, R.; VERSIC, R.; GAONKAR, A. G. **Introduction to Microencapsulation and**

Controlled Delivery in Foods. [s.l.] Elsevier Inc., 2014.

SOOTTITANTAWAT, A.; TAKAYAMA, K.; OKAMURA, K.; MURANAKA, D.; YOSHII, H.; FURUTA, T.; OHKAWARA, M.; LINKO, P. Microencapsulation of l-menthol by spray drying and its release characteristics. **Innovative Food Science and Emerging Technologies**, v. 6, n. 2, p. 163–170, 2005a.

SOOTTITANTAWAT, A.; BIGEARD, F.; YOSHII, H.; FURUTA, T.; OHKAWARA, M.; LINKO, P. Influence of emulsion and powder size on the stability of encapsulated D-limonene by spray drying. **Innovative Food Science and Emerging Technologies**, v. 6, n. 1, p. 107–114, 2005b.

SUN, X.; CAMERON, R. G.; BAI, J. Microencapsulation and antimicrobial activity of carvacrol in a pectin-alginate matrix. **Food Hydrocolloids**, v. 92, p. 69–73, 2019.

SUNARHARUM, W. B.; WILLIAMS, D. J.; SMYTH, H. E. Complexity of coffee flavor: A compositional and sensory perspective. **Food Research International**, v. 62, p. 315–325, 2014.

TAYLOR, A. J.; LINFORTH, R. S. T. Understanding flavour release : the key to better food flavour ? **Nutrition & Food Science**, v. 98, n. 4, p. 202–206, 1998.

THIES, C. Microencapsulation of Flavors by Complex Coacervation. In: LAKKIS, J. M. (Ed.). **Encapsulation and Controlled Release: Technologies in Food Systems**. 1. ed. [s.l.] Blackwell Publishing, 2007. p. 149–170.

THIJSSEN, H. A. C.; RULKENS, W. H. Retention of Aromas in Drying Food Liquids. **De l'ingenieur Chemical Technology**, v. 5, p. 45–47, 1968.

TOURNIER, C.; SULMONT-ROSSE, C.; GUICHARD, E. Flavour perception: aroma, taste and texture interactions. **Food**, v. 1, n. 2, p. 246–257, 2007.

TRUJILLO-CAYADO, L. A.; ALFARO, M. C.; SANTOS, J.; CALERO, N.; MUÑOZ, J. Influence of primary homogenization step on microfluidized emulsions formulated with thyme oil and Appyclean 6548. **Journal of Industrial and Engineering Chemistry**, v. 66, p. 203–208, 2018.

UBBINK, J.; KRÜGER, J. Physical approaches for the delivery of active ingredients in foods. **Trends in Food Science and Technology**, v. 17, n. 5, p. 244–254, 2006.

UHLEMANN, J.; SCHLEIFENBAUM, B.; BERTRAM, H. J. Flavor encapsulation technologies: An overview including recent developments. **Perfumer and Flavorist**, v. 27, n. 5, p. 52–61, 2002.

VAIDYA, S.; BHOSALE, R.; SINGHAL, R. S. Microencapsulation of Cinnamon Oleoresin by Spray Drying Using Different Wall Materials. **Drying Technology**, v. 24, n. 8, p. 983–992, 2006.

VICENTE, J.; PINTO, J.; MENEZES, J.; GASPAR, F. Fundamental analysis of particle formation in spray drying. **Powder Technology**, v. 247, p. 1–7, 2013.

VOILLEY, A.; ETIÉVANT, P. **Flavour in food**. 1. ed. [s.l.] Woodhead Publishing, 2006.

WALSTRA, P. Formation of Emulsions and Foams. In: FENNEMA, O. et al. (Eds.). . **Physical Chemistry of Foods**. New York: Marcel Dekker, 2003. p. 397–436.

WANG, M.; YANG, J.; LI, M.; WANG, Y.; WU, H.; XIONG, L.; SUN, Q. Enhanced viability of layer-by-layer encapsulated Lactobacillus pentosus using chitosan and sodium phytate. **Food Chemistry**, v. 285, p. 260–265, 2019.

WOO, M. W.; DAUD, W. R. W.; TASIRIN, S. M.; TALIB, M. Z. M. Controlling food powder deposition in spray dryers: Wall surface energy manipulation as an alternative. **Journal of Food Engineering**, v. 94, n. 2, p. 192–198, 2009.

YE, Q.; GEORGES, N.; SELOMULYA, C. Microencapsulation of active ingredients in functional foods: From research stage to commercial food products. **Trends in Food Science and Technology**, v. 78, n. May, p. 167–179, 2018.

YEO, Y.; BELLAS, E.; FIRESTONE, W.; LANGER, R.; KOHANE, D. S. Complex coacervates for thermally sensitivity controlled release of flavor compounds. **Journal of Agricultural and Food Chemistry**, v. 53, p. 7518–7525, 2005.

YERETZIAN, C.; JORDAN, A.; BADOUD, R.; LINDINGER, W. From the green bean to the cup of coffee : investigating coffee roasting by on-line monitoring of volatiles. **European Food Research and Technology**, v. 214, p. 92–104, 2002.

YERETZIAN, C.; JORDAN, A.; LINDINGER, W. Analysing the headspace of coffee by proton-transfer-reaction mass-spectrometry. **International Journal of Mass Spectrometry**, v. 223–224, p. 115–139, 2003.

ZELLER, B.; GAONKAR, A.; CERIALI, S.; WRAGG, A. Novel Microencapsulation System to Improve Controlled Delivery of Cup Aroma During Preparation of Hot Instant Coffee Beverages. In: GAONKAR, A. G. et al. (Eds.). **Microencapsulation in the Food Industry**. London: Elsevier, 2014. p. 455–468.

CAI, X.; DU, X.; CUI, D.; WANG, X.; YANG, Z.; ZHU, G. Improvement of stability of blueberry anthocyanins by carboxymethyl starch/xanthan gum combinations microencapsulation. **Food Hydrocolloids**, v. 91, p. 238–245, 2019.

ZUIDAM, N. J.; HEINRICH, E. Encapsulation of Aroma. In: ZUIDAM, N. J.; NEDOVIC, V. A. (Eds.). . **Encapsulation Technologies for Active Food Ingredients and Food Processing**. [s.l.] Springer, 2010. p. 127–160.

ZUIDAM, N. J.; SHIMONI, E. Cap. 2: Overview of microencapsulation for use in food products or process and methods to make them. **Encapsulation Technologies for active food ingredients and food processing**, p. 3–30, 2010.

CAPÍTULO 2 – HOW ULTRASOUND-ASSISTED EMULSIFICATION POWER AND EMULSION TEMPERATURE AFFECT ROASTED COFFEE OIL-IN-WATER EMULSION AND MICROPARTICLES CHARACTERISTICS

1 INTRODUCTION

Roasted coffee oil contains a high concentration of the flavor compounds that are responsible for the pleasant aroma of roasted coffee. It has potential use as a flavoring to improve the sensory properties of coffee products since the aroma is one of the main sensory attributes that affects purchase decision. However, the presence of unsaturated fatty acids and labile compounds make it susceptible to considerable losses during product storage (CALLIGARIS et al., 2009).

Microencapsulation is a process which entraps one substance (active agent or core material) into a wall material, and this technology has been used on food to protect bioactive materials from degradation by reducing their reactivity to environmental conditions (e.g., heat, moisture, air, and light). It also controls the release of the core materials and prevents that food ingredients reacting with each other within a mixture (BAKRY et al., 2016; BHANDARI et al. 1992; RÉ, 1998). Specifically, for oils and flavors, this technique has been used to increase their shelf life by protecting them against lipid oxidation as well as providing better retention of the volatile constituents (FRASCARELI et al., 2012; PELLICER et al., 2018).

Among the many techniques for encapsulation, spray drying is the most common procedure on the basis of the availability of equipment, low process cost, a wide choice of carrier solids, good retention of volatiles, and good stability of the products (BAKRY et al., 2016; REINECCIUS, 2004). In addition to the spray-drying process parameters (inlet and outlet temperature, atomizing pressure, feed flow rate) and equipment design, the microparticles are directly affected by the characteristics of the infeed emulsions (JAFARI et al., 2008a; REINECCIUS, 2004).

Emulsions are colloidal systems that consist of two immiscible liquids, with one of the liquids dispersed as small spherical droplets in the other. The formation of an emulsion involves homogenization, which converts these immiscible liquids into an emulsion (JAFARI; HE; BHANDARI, 2006; MCCLEMENTS, 2004a, 2004b).

In the last years, ultrasound-assisted emulsification has gained popularity among food processors based on its energy-efficiency, low production cost and ease of use. This process involves the production of high intensity acoustic waves that break the disperse phase into a continuous phase, followed by acoustic cavitation, which results in the formation of micro bubbles under reduced pressure (ABBAS et al., 2013; ASHOKKUMAR, 2015; CHANDRAPALA et al., 2012; MCCLEMENTS, 2004b).

Since it represents a high-intensity method, emulsification via sonication is usually associated with a significant rise in the temperature of the emulsions. Several studies have discussed the effect of temperature on the droplet size during sonication, but the extent of thermal effects (CANSELIER et al., 2002; JAFARI et al., 2006; NAZARZADEH; SAJJADI, 2013), and how that would affect the microparticle characteristics are still not clear.

The goal of this work was to study the effect of the ultrasound power and emulsion temperature on the properties of a roasted coffee oil-in-water emulsion and how these parameters affect the microparticles of coffee oil produced by spray drying.

2 MATERIAL AND METHODS

2.1 MATERIAL

Roasted coffee oil obtained from *Coffea arabica* was kindly supplied by Café Iguaçu (Cornélio Procópio, Brazil) and Capsul® starch (octenyl succinic anhydride starch derived from waxy maize) (OSA-starch) was provided by Ingredion (São Paulo, Brazil).

2.2 PRODUCTION OF ROASTED COFFEE OIL EMULSIONS

The OSA-starch solutions were prepared by dissolving modified starch at 27% w/w in deionized water (Millipore®) and mixing overnight to ensure the complete hydration of the molecules. The roasted coffee oil concentration was maintained at 10% with respect to total solids. The emulsions were prepared by incorporating the roasted coffee oil into the OSA-starch solution, and a pre-emulsion was prepared by homogenization at 3000 rpm for 90 s in a rotor-stator type homogenizer (TE-102, Tecnal, Brazil) (SILVA et al., 2015). The pre-emulsion was emulsified using a sonicator Q700 (QSonica, Newtown, USA) with a maximum power output of 700 W. A titanium probe with 12.7 mm diameter was used at a frequency of 20 kHz for 5

min. The emulsion temperature was kept constant using a thermostatically controlled water bath (TE-2005, Tecnal, Piracicaba, Brazil) coupled to a double jacket. To permit adequate temperature control, the device was set for 20 s active sonication intervals followed by a 3 s pause (NAZARZADEH; SAJJADI, 2013).

2.3 EXPERIMENTAL DESIGN

The effects of power and temperature on the emulsion characteristics were investigated using a 2^2 Central Composite Rotational Design (CCRD) including 10 treatments with 4 factorial points, 4 axial points and 2 replicated center points. The independent variables, their levels, and real values are presented in Table 1.

Table 1. Central Composite Rotational Designs (CCRD) 2^2 for ultrasound-assisted emulsification.

Experiment	**Coded variable levels**		**Uncoded varible levels**	
	Temperature (°C)	**Power (W)**	**Temperature (°C)**	**Power (W)**
1	-1	-1	20	210
2	1	-1	40	210
3	-1	1	20	560
4	1	1	40	560
5	-1,41	0	15	385
6	+1,41	0	45	385
7	0	-1,41	30	140
8	0	+1,41	30	630
9	0	0	30	385
10	0	0	30	385

The quadratic equation (Equation 1) was used to model the effect of the processing conditions on the responses (dependent variable).

$$y = \beta_0 + \sum_{i=1}^{k} \beta_i X_i + \sum_{i=1}^{k} \beta_{ii} X_i^2 + \sum_{i=1}^{k-1} \sum_{j=i+1}^{k} \beta_{ij} X_i X_j + e \quad (1)$$

Where: y is the dependent variable, β_0 is the constant of the model, β_i and β_{ij} are model coefficients, X_i and X_j are the coded independent variables (temperature and power, respectively), and e is the experimental error.

2.4 CHARACTERIZATION OF THE EMULSIONS

Immediately after their preparation, the roasted coffee oil-in-water emulsions were evaluated with respect to stability by creaming index, droplet size, and rheological behavior.

2.4.1 Creaming stability

Approximately 10 mL of the emulsion was transferred to 25 mL graduated tubes (internal diameter of 1.8 cm and height of 16.5 cm), and then sealed and stored at 25 °C for 72 h (YE; SINGH, 2006) to evaluate phase separation.

2.4.2 Emulsion droplet size

The droplet size distribution was determined by the acoustic attenuation spectroscopy technique (Zeta-APS, Matec Applied Sciences, Massachusetts, USA). The average diameter was calculated based on the average diameter of a sphere of a similar area (Sauter mean diameter, D_{32}).

2.4.3 Rheology properties

The rheological behavior and viscosity of the emulsions were evaluated using a Brookfield rotational rheometer (Brookfield R/S+, Massachusetts, USA) with a plate-plate geometry (50 mm) with 1.0 mm gap. The measurements were carried out at the same sonication temperatures (Table 1) to evaluate the effect of viscosity on the ultrasound process. After introduction into the rheometer, the samples were left to rest for 2 min to reach the target temperature, and the shear rate was varied between 100 and 300 s^{-1}.

2.5 SPRAY-DRYING PROCESS

All emulsions were dried in a laboratorial scale spray-dryer (LabPlant, SD 05, Huddersfield, England). The emulsion was fed into the main chamber (0.5 m × 0.215 m) through a peristaltic pump at 25 °C under the following conditions: 0.7 mm spray nozzle, air

flow rate at 73 $m^3 h^{-1}$, air pressure at 4 bar, compressed air flow rate at 1.1 $m^3 h^{-1}$, feed rate at 6 mL min^{-1}, inlet temperature at 180 °C ± 4 °C, outlet air temperature at 100 °C ± 5 °C (FRASCARELI et al., 2012).

2.6 PARTICLE CHARACTERIZATION

2.6.1 Encapsulation efficiency and surface oil

Encapsulation efficiency (EE) is defined as the ratio between the oil inside the encapsulating matrix (covered) and total oil (TO) (covered + surface oil (SO)) in the microparticles (Equation 2):

$$EE = \frac{(TO - SO)}{TO} \times 100 \quad (2)$$

The amount of total oil was determined gravimetrically using hexane:isopropanol (3:1 v/v) extraction after solubilizing the wall material using deionized water (adapted from GETACHEW; CHUN (2016)). The total oil content was calculated as the ratio between the masses of the extracted oil and the microparticles used. The percentage of SO of the microparticles was calculated based on the ratio of the extracted surface oil (g) and the initial mass of the microparticles (g) (SILVA et al., 2016).

2.6.2 Particle size distribution

The particle size distribution and average diameter of the microparticles were determined by the light scattering technique using laser diffraction (Mastersizer 2000, Malvern Instruments Ltd, UK). The mean diameter was determined based on the average diameter of a sphere of the same volume (D_{43}). The dispersant used was 99.5% ethanol.

2.6.3 Scanning electron microscopy (SEM)

The microparticles on the metallic stub were observed using a Scanning Electron Microscope Quanta 200 (FEI-Philips, Hillsboro, USA). The powders were covered with gold using a sputter coater SCD 050 (Bal-Tec, Germany). The micrographs were obtained using an accelerating voltage of 15 kV and a 101 pA emission current.

2.6.4 Moisture content, water activity, and bulk density

The moisture content of the roasted coffee oil microparticles was determined gravimetrically in a forced circulation oven to a constant weight at 105 °C (AOAC, 1997).

The water activity (a_w) was obtained using a digital hygrometer Aqualab 4TEV (Meter, USA). The bulk density was obtained by dividing the mass of the powder (approximately 2 g) by the volume occupied in a 25 mL graduated cylinder.

2.7 STATISTICAL ANALYSIS

Statistica 10® software (StatSoft, Tulsa, USA) was used to calculate the effects of ultrasound power and emulsification temperature on the emulsion and microparticles characteristics.

3. RESULTS AND DISCUSSION

3.1 ULTRASOUND-ASSISTED EMULSION

3.1.1 Creaming stability

The roasted coffee oil emulsions showed high stability with no phase separation within 72 h for all of the ultrasound-assisted emulsification conditions.

The use of OSA-starch as wall material was efficient as indicated by its effective emulsification properties, which stabilize the droplets against coalescence (SILVA et al., 2015; WANG; YUAN; YUE, 2015). The stabilization mechanism of biopolymers is predominantly steric; when dissolved in water, the hydrophilic carboxyl groups extend into the water phase, whereas the lipophilic octenyl chains are oriented towards the oil phase. The macromolecular structure of OSA-starch leads to the formation of a strong thick film that is resistant to rupture, thus providing to the emulsions resistance to agglomeration and a considerable emulsification effectiveness. The film on the oil surface act as a barrier between oil droplets to decelerate the possible coalescence (SWEEDMAN et al., 2013; WANG et al., 2015). In addition, the stability of the emulsion can be attributed to the micro size oil droplets produced by ultrasound emulsification (Table 2). As stated by Stokes's law, the velocity at which a droplet moves is

proportional to the square of its radius, and thus a microemulsion may be considered to be stable with no creaming instability (ASHOKKUMAR, 2015; CHANDRAPALA et al., 2012).

3.1.2 Droplet size and size distribution

The contour plots (Fig. 1) show the effects of applied ultrasound power and emulsion temperature on the oil droplet mean size (D_{32}) and viscosity, and the respective models and coefficient of determination (R^2) of the roasted coffee oil emulsions.

High power and high temperature increased the D_{32} values, probably due to the recoalescence of the droplets (JAFARI et al., 2008b), which was not observed at low power. At higher temperatures, the sonication was not efficient in reducing the droplet size due to the damping effect caused by the increasing vapor pressure inside the bubble, which reduces the pressure reached to break up droplets during the ultrasound process (CANSELIER et al., 2002). Lower power and temperatures also resulted in larger oil droplets, probably because the energy supplied was not sufficient to break up the oil phase to smaller droplets (CANSELIER et al., 2002; JAFARI et al., 2008b).

Figure 1. Contour plots showing the effects of applied power and temperature on the (a) oil droplet mean size D_{32} and (b) viscosity, and their respective models and coefficient of determination R^2 of roasted coffee oil emulsions stabilized by OSA-starch. y = dependent variable, x_1 = coded temperature, x_2 = coded power and n = number of experimental data.

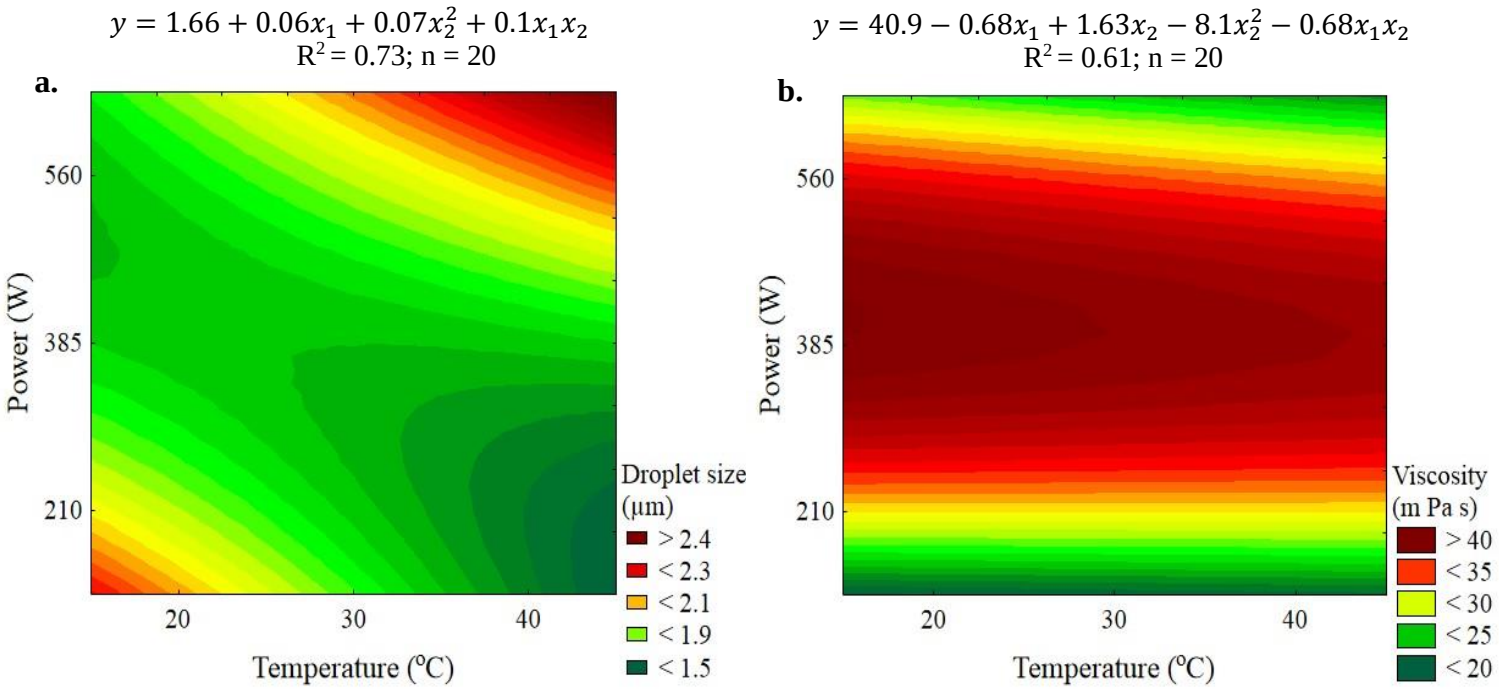

Fig. 2 shows the droplet sizes distribution of emulsion produced under the CCRD conditions (Table 1).

Figure 2. Droplet size distribution of emulsions produced under the CCRD conditions.

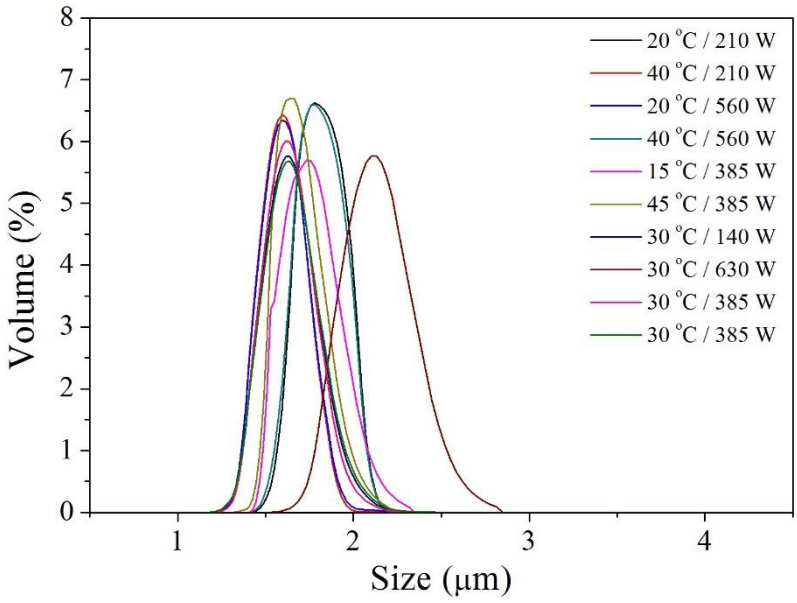

As expected for ultrasound-assisted emulsification, the droplet size distribution showed a narrow unimodal distribution (Fig. 2), which means the droplets are homogenous. These results reflected the high emulsion stability as observed by the creaming index results (DICKINSON; RADFORD; GOLDING, 2003; SILVA et al., 2016).

3.1.3 Rheological behavior

All roasted coffee oil emulsions exhibited Newtonian behavior (n ~ 1). Although the viscosity measurement for each emulsion was made at the same temperature at which the emulsion was produced (Table 1), the temperature had low effect on the emulsion viscosity as indicated by the mathematical model obtained by the CCRD (Fig. 1b). It is well known that the cavitation that occurs at the microscale bubble interface increases the overall temperature of the liquid over time, which results in a reduction of the viscosities of the dispersed and continuous phases of emulsion (ABBAS et al., 2013; MCCLEMENTS, 2004b). In this work, the range of temperatures used did not result in a significant effect on the emulsion viscosity.

The contour curve and the model for emulsion viscosity are shown in Fig. 1b. Because the coefficient of determination was low ($R^2 = 0.61$), the model was not considered to

be predictive but does indicate the behavior of temperature and power on the emulsion viscosity. Since the composition of all of the emulsions was the same, the viscosity variation was attributed to the droplet size – D_{32} (Fig. 1a), once smaller emulsion droplets tends to increase the viscosity. That behavior is attributed to the greater tendency of emulsion droplets to flocculate since smaller droplets demonstrated increased surface area and collision frequencies. In addition, the droplets flocculation increase the emulsion viscosity due to the increase in the effective volume fraction of the dispersed phase compared to the sum of the volume fractions of the individual droplets (PAL, 1996; MCCLEMENTS, 2004c).

The emulsions demonstrated low viscosities (Table 2) mainly because OSA-starch is soluble in cold water and maintains a relatively low viscosity even at a high concentration in solution (DOMIAN et al., 2015; WANG et al., 2015). The viscosity is important on emulsion study since it affects the encapsulation efficiency, which in turn improves the oil retention. High viscosities reduce the migration of internal oil droplets to the particle surface during the spray drying. However, if the viscosity increases excessively, oil retention decreases due to slower droplet formation and longer exposure during atomization (JAFARI et al., 2008a).

3.2 MICROPARTICLES

3.2.1 Encapsulation efficiency

The encapsulation efficiencies obtained under several ultrasound-assisted emulsification conditions are shown in Table 2.

Table 2. Central Composite Rotational Designs – CCRD results from emulsion and microparticles characterization.

Experiment	Variable levels		Emulsion properties		Microparticles properties				
	Temperature (°C)	Power (W)	D_{32} (μm)	Viscosity (m Pa s)	Encapsulation efficiency (%)	D_{43} (μm)	Moisture (g 100 g^{-1} d.b)	Water activity	Bulk density (g cm^{-3})
1	20	210	1.82 ± 0.04	35.08 ± 1.8	96.3 ± 3.3	29.7 ± 0.3	2.20 ± 0.13	0.153 ± 0.017	0.380 ± 0.008
2	40	210	1.61 ± 0.05	24.14 ± 2.7	95.7 ± 2.0	32.2 ± 0.2	3.80 ± 0.41	0.139 ± 0.014	0.344 ± 0.007
3	20	560	1.61 ± 0.02	41.24 ± 6.3	92.7 ± 0.1	29.3 ± 0.8	3.29 ± 0.04	0.209 ± 0.015	0.356 ± 0.027
4	40	560	1.81 ± 0.01	27.58 ± 7.6	67.3 ± 3.6	27.1 ± 0.1	1.37 ± 0.14	0.195 ± 0.014	0.342 ± 0.010
5	15	385	1.70 ± 0.05	35.44 ± 2.5	91.2 ± 1.8	28.0 ± 0.8	1.88 ± 0.08	0.182 ± 0.005	0.350 ± 0.017
6	45	385	1.69 ± 0.04	48.96 ± 1.6	70.1 ± 3.1	30.0 ± 0.4	3.25 ± 0.08	0.185 ± 0.014	0.346 ± 0.000
7	30	140	1.65 ± 0.02	24.30 ± 1.8	90.5 ± 1.5	35.9 ± 0.2	4.21 ± 0.48	0.178 ± 0.006	0.373 ± 0.018
8	30	630	2.00 ± 0.02	26.72 ± 3.5	94.8 ± 1.5	33.0 ± 0.3	2.15 ± 0.16	0.162 ± 0.008	0.333 ± 0.005
9	30	385	1.64 ± 0.01	39.44 ± 2.6	95.1 ± 4.0	27.2 ± 0.2	4.04 ± 0.06	0.152 ± 0.016	0.341 ± 0.006
10	30	385	1.66 ± 0.02	41.37 ± 5.6	95.6 ± 1.1	27.2 ± 1.4	3.39 ± 0.48	0.203 ± 0.012	0.348 ± 0.003

The results are presented as the mean ± standard deviation. D_{32} is the mean oil droplet size and D_{43} is the mean particle size.

In general, high encapsulation efficiency value (> 90%) were observed. High oil encapsulation efficiencies have also been previously reported for spray-dried microparticles with OSA-starch as wall material (RAMAKRISHNAN et al., 2018; DOMIAN et al., 2015; CARNEIRO et al., 2012). It is worth highlighting that the value of ultrasound during the emulsion preparation in obtaining higher encapsulation efficiency than in other works that obtained emulsion by rotor-stator homogenizer (PELLICER et al., 2018; SHAO et al., 2019; SUN; CAMERON; BAI, 2019). This improvement in encapsulation efficiency was due to the formation of more stable emulsions by a smaller droplet diameter through the use of ultrasound-assisted emulsification.

The contour plots for encapsulation efficiency and mean particle size are shown in Fig. 3.

Figure 3. Contour plots of the (a) encapsulation efficiency and (b) mean particle size D_{43} of microparticles as a function of the applied power and temperature during ultrasound-assisted emulsification, and their respective models and coefficient of determination R^2. y = dependent variable, x_1 = coded temperature, x_2 = coded power and n = number of experimental data.

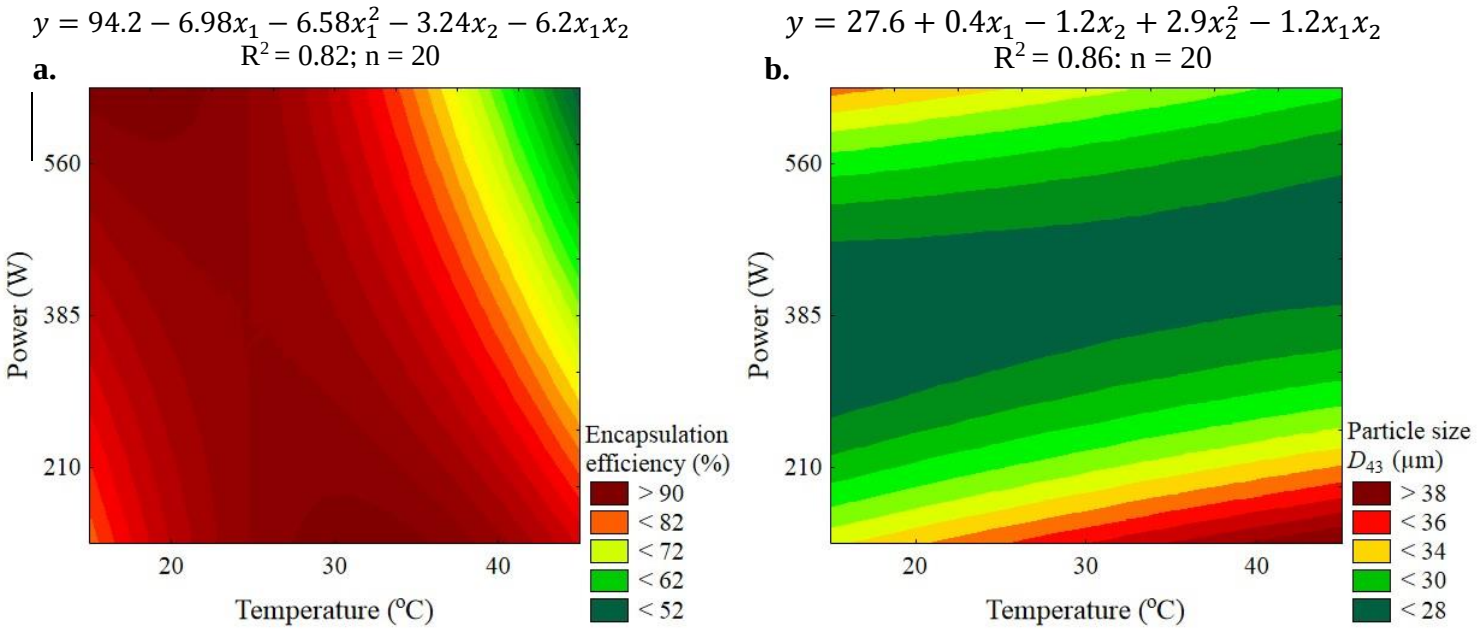

The contour plot of the EE (Fig. 3a) agrees with emulsion droplet size since it is related to encapsulation efficiency because, as previously discussed, smaller emulsion droplets are associated with an increase in the stability due to the reduced droplet velocity into the solution (Stokes's law), which results in greater retention of the core material. On the other hand, the formation of larger emulsion droplets reduces the EE due to a breakdown of the droplets through a shearing effect during spray drying atomization (SOOTTITANTAWAT et

al., 2003; CARNEIRO et al., 2012; RÉ, 1998; SILVA et al., 2016; WANG et al., 2015; MCCLEMENTS, 2004d).

For an ideal microencapsulation process, the core material must be within the wall; otherwise, the core material on the surface of the matrix is subject to evaporation and oxidation (RÉ, 1998). The higher encapsulation efficiency (Table 2) was due to the high emulsion stability during drying, and the thick film formed by OSA-starch acted as a barrier between oil droplets, which resulted in considerable emulsification effectiveness. As a consequence, the spray-dried microparticles presented less surface oil, which improve the retention of the volatile flavor constituents and retention and oxidative stability of the core material (WANG et al., 2015; CARNEIRO et al., 2012; SILVA et al., 2016; RÉ, 1998; MCCLEMENTS, 2004d).

3.2.2 Particle size distribution and morphology

The contour plot, the model, and coefficient of determination are shown in Fig. 3b. Particle size is highly influenced by the spray drying parameters and emulsion physical properties (viscosity and solids concentration) since affect the size of the atomized droplets into the spray dryer chamber. In general, high viscosity emulsions result in lager microparticles because the droplets atomized into the spray dryer chamber are larger (REINECCIUS, 2004; GHARSALLAOUI et al., 2007; MADENE et al., 2006; REINECCIUS; Yan, 2016).

In contrast to other studies (CARNEIRO et al., 2012; TONON et al., 2008), the D_{43} was not affected by viscosity probably due to the narrow range of temperature and power used to evaluate the emulsion viscosity behavior. Furthermore, the OSA-starch used as the wall material exhibits a low viscosity even at a high solid concentration (VERDALET-GUZMÁN, 2013; WANG et al., 2015).

Fig. 4 shows the particle size distribution of powders produced with different emulsification conditions.

Figure 4. Particle size distribution of microparticles obtained from emulsions produced according to CCRD.

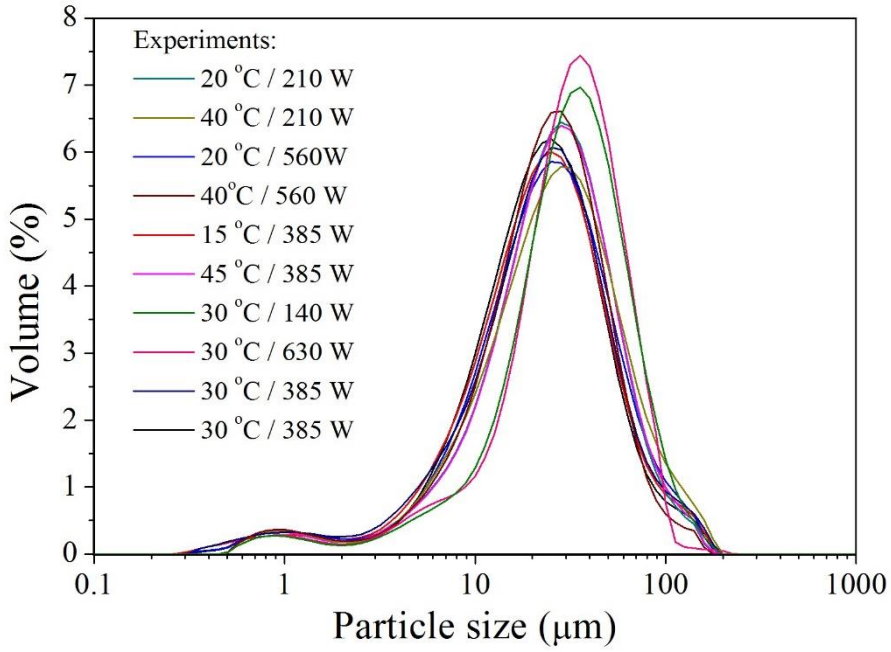

The particle sizes showed monomodal distributions with only one distinct peak. Although all the formulations had similar particle size distributions, the microparticles from experiments 7 and 8 (140 and 630 W, respectively, at 30 °C) showed a narrower distribution, which indicated that these particles were more homogeneous. The particle size distribution is important from a practical point of view since it influences the appearance, flowability, and dispersibility of a powder (REINECCIUS, 2004).

Fig. 5 presents the SEM micrographs of the spray-dried microparticles.

Figure 5. SEM image of the roasted coffee oil microparticles produced by spray drying. Emulsification conditions: ultrasound power: 560 W and temperature: 37 °C.

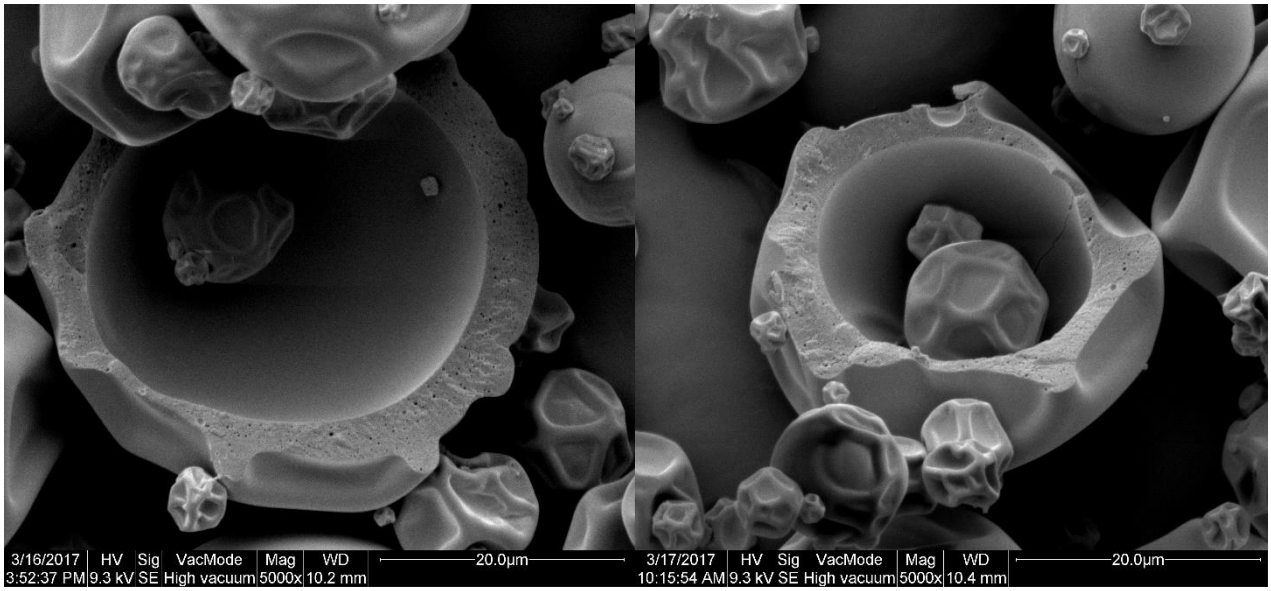

As shown in Fig. 5, the particles presented large voids that were formed due to the expansion during the latter stages of the drying process. Moreover, small droplets of roasted coffee oil were uniformly distributed through the wall matrix. The presence of numerous pores containing coffee oil may be associated with the high values of encapsulation efficiencies (Table 2). Furthermore, the spray-drying process led to the formation of microparticles with the appearance of shriveled spheres, and some of them exhibited apparent fissures, which are typical of powdered products obtained by spray drying. These features are related to the breakdown of the atomized droplets during the first stage of drying (FRASCARELI et al., 2012; RÉ, 1998; REINECCIUS, 2004; SILVA et al., 2016). Additionally, there is a correlation between particle morphology and powder flowability, since irregular shriveled particles do not flow freely due to bonding through mechanical interlocking (GARCÍA-CRUZ et al., 2013; WALTON; MUMFORD, 1999).

3.2.3 Moisture content, water activity, and bulk density

The model of moisture content (MC) is represented by the following equation:

$$y = 3.7 + 0.2x_1 - 0.63x_1^2 - 0.53x_2 - 0.32x_2^2 - 0.88x_1x_2 \qquad R^2 = 0.86.$$

The CCRD model of water activity (a_w) did not explain the aw behavior as a function of temperature and power ($R^2 < 0.26$).

Both parameters influence the stability of encapsulated materials once they are directly related to the glass transition temperatures. Since there is a rapid formation of a dense skin at the beginning of the drying process, the low MC and a_w of biopolymers indicates low molecular mobility and thus, oxygen permeability, which reduce the lipid oxidation (GHARSALLAOUI et al., 2007; ROCCIA et al., 2014). In the same way, at higher MC and a_w values the aroma compounds are easily released because the wall is destroyed (MADENE et al., 2006; GHARSALLAOUI et al., 2007; REINECCIUS; YAN, 2016).

There is evidence that emulsion viscosity, inlet temperature, and pump rate influence moisture content and water activity (BHANDARI et al., 1992; REINECCIUS; YAN, 2016; ROCCIA et al., 2014; TONON et al., 2008). In the present study, the inlet temperature, atomization air flow rate and pump rate were the same for all experiments, thus the emulsion viscosity directly affected the final MC of the powders once the skin is formed rapidly during drying and water is hindered from achieving the surface (BHANDARI et al., 1992; FRASCARELI et al., 2012).

The microparticles showed a significant variation in bulk density with a range of 0.333 to 0.380 g cm^{-3} as a function of the emulsification conditions. The model is presented below:

$$y = 0.34 - 0.004x_1 + 0.003x_1^2 - 0.01x_2 + 0.006x_2^2 + 0.006x_1x_2$$

$R^2 = 0.93$; number of experimental data = 20

The model indicates that higher bulk density is achieved when lower emulsification power and temperatures were applied. That result agreed with the model for emulsion viscosity, which was also lower when lower emulsification power and temperatures are applied. The bulk density depends on the emulsion viscosity, which influences water movement inside the capsule: low emulsion viscosity favors the removal of water during drying and, as a result, the volume of the microcapsule is reduced due to contraction (BHANDARI et al., 1992). Microparticles presenting high bulk density have some advantages that include storage of high amount of product in smaller compartments and a lower oxidation susceptibility since there is less air inside of the microparticles (CARNEIRO et al., 2012).

4. CONCLUSIONS

The effects of the ultrasound power and emulsion temperature on droplet size and viscosity during ultrasound-assisted emulsification were evaluated. Smaller emulsion

droplet size was closely related to high encapsulation efficiency, and both parameters demonstrated high interaction power × temperature effect. Surprisingly, particle size and emulsion viscosity showed an unexpected relationship in which high viscosity emulsions resulted in smaller particle sizes. Ultrasound was found to be effective in producing submicron emulsions successfully stabilized by OSA-starch, narrow droplet size distributions, and no phase separation up to 72 h after preparation. The microparticles presented the typical shape of spray-dried microparticles and showed high encapsulation efficiency (> 90%). The Central Composite Rotational Design effectively modeled the effects of ultrasound power and emulsion temperature on the emulsion properties.

REFERENCES

AOAC. (1997). In Association of Official Analytical Chemistse AOAC. Official ofanalysis (16th ed.) (Washington).

ABBAS, S.; HAYAT, K.; KARANGWA, E.; BASHARI, M.; ZHANG, X.. An Overview of Ultrasound-Assisted Food-Grade Nanoemulsions. **Food Engineering Reviews**, v. 5, n. 3, p. 139–157, 2013.

ASHOKKUMAR, M. Applications of ultrasound in food and bioprocessing. **Ultrasonics Sonochemistry**, v. 25, n. 1, p. 17–23, 2015.

BAKRY, A. M.; ABBAS, S.; ALI, B.; MAJEED, H.; ABOUELWAFA, M. Y.; MOUSA, A.; LIANG, L. Microencapsulation of Oils: A Comprehensive Review of Benefits, Techniques, and Applications. **Comprehensive Reviews in Food Science and Food Safety**, v. 15, n. 1, p. 143–182, 2016.

BHANDARI, B. R.; DUMOULIN, E. D.; RICHARD, H. M. J.; NOLEAU, I.; LEBERT, A. M. Flavor Encapsulation by Spray Drying: Application to Citral and Linalyl Acetate. **Journal of Food Sc**, v. 57, n. 1, p. 217–221, 1992.

CALLIGARIS, S.; MUNARI, M.; ARRIGHETTI, G.; BARBA, L. Insights into the physicochemical properties of coffee oil. **European Journal of Lipid Science and Technology**, v. 111, n. 12, p. 1270–1277, 2009.

CANSELIER, J. P.; DELMAS, H.; WILHELM, A. M.; ABISMAIL, B. Ultrasound Emulsification—An Overview. **Journal of Dispersion Science and Technology**, v. 23, n. 1–3, p. 333–349, 2002.

CARNEIRO, H. C. F.; TONON, R. V.; GROSSO, C. R. F.; HUBINGER, M. D. Encapsulation efficiency and oxidative stability of flaxseed oil microencapsulated by spray drying using different combinations of wall materials. **Journal of Food Engineering**, v. 115, p. 443–451, 2013.

CHANDRAPALA, J.; OLIVER, C.; KENTISH, S.; ASHOKKUMAR, M. Ultrasonics in food

processing. **Ultrasonics Sonochemistry**, v. 19, n. 5, p. 975–983, 2012.

DICKINSON, E.; RADFORD, S. J.; GOLDING, M. Stability and rheology of emulsions containing sodium caseinate: Combined effects of ionic calcium and non-ionic surfactant. **Food Hydrocolloids**, v. 17, n. 2, p. 211–220, 2003.

DOMIAN, E.; BRYNDA-KOPYTOWASKA, A.; CENKIER, J.; SWIRYDOW, E. Selected properties of microencapsulated oil powders with commercial preparations of maize OSA starch and trehalose. **Journal of Food Engineering**, v. 152, p. 72–84, 2015.

FRASCARELI, E. C.; SILVA, V. M.; TONON, R. V.; HUBINGER, M. D. Effect of process conditions on the microencapsulation of coffee oil by spray drying. **Food and Bioproducts Processing**, v. 90, n. 3, p. 413–424, 2012.

GARCÍA-CRUZ, E. E.; RODRÍGUEZ-RAMÍREZ, J.; LAGUNAS, L. L. M.; MEDINA-TORRES, L. Rheological and physical properties of spray-dried mucilage obtained from Hylocereus undatus cladodes. **Carbohydrate Polymers**, v. 91, n. 1, p. 394–402, 2013.

GETACHEW, A. T.; CHUN, B. S. Optimization of coffee oil flavor encapsulation using response surface methodology. **LWT - Food Science and Technology**, v. 70, p. 126–134, 2016.

GHARSALLAOUI, A.; ROUDAUT, G.; CHAMBIN, O.; VOILLEY, A.; SAUREL, R. Applications of spray-drying in microencapsulation of food ingredients: An overview. **Food Research International**, v. 40, n. 9, p. 1107–1121, 2007.

JAFARI, S. M.; ASSADPOOR, E.; HE, Y.; BHANDARI, B. Encapsulation Efficiency of Food Flavours and Oils during Spray Drying. **Drying Technology**, v. 26, n. 7, p. 816–835, 2008a.

JAFARI, S. M.; ASSADPOOR, E.; HE, Y.; BHANDARI, B. Re-coalescence of emulsion droplets during high-energy emulsification. **Food Hydrocolloids**, v. 22, n. 7, p. 1191–1202, 2008b.

JAFARI, S. M.; HE, Y.; BHANDARI, B. Production of sub-micron emulsions by ultrasound and microfluidization techniques. **Journal of Food Engineering**, v. 82, n. 4, p. 478–488, 2007.

JAFARI, S.M.; HE, Y.; BHANDARI, B. Nano-emulsion production by sonication and microfluidization - A comparison. **International Journal of Food Properties**, v. 9, n. 3, p. 475–485, 2006.

MADENE, A.; JACQUOT, M.; SCHER, J.; DESEBRY. Flavour encapsulation and controlled release - A review. **International Journal of Food Science and Technology**, v. 41, n. 1, p. 1–21, 2006.

MCCLEMENTS, D. J. **Food Emulsions**. [s.l.] CRC Press LLC, 1999.

MCCLEMENTS, D. J. Context and background. In: MCCLEMENTS, D. J. (Ed.). . **Food Emulsions: Principle, Practices, and Techniques**. Second edi ed. [s.l.] CRC Press LLC,

2004a. p. 1–26.

MCCLEMENTS, D. J. Emulsion formation. In: MCCLEMENTS, D. J. (Ed.). . **Food Emulsions: Principle, Practices, and Techniques**. [s.l.] CRC Press LLC, 2004b. p. 233–267.

NAZARZADEH, E.; SAJJADI, S. Thermal effects in nanoemulsification by ultrasound. **Industrial and Engineering Chemistry Research**, v. 52, n. 28, p. 9683–9689, 2013.

PAL, R. Effect of Droplet Size on the Rheology of Emulsions. **AIChE Journal**, v. 42, n.11, p. 3181–3190, 1996.

PELLICER, J. A.; FORTEA, M. I.; TRABAL, J.; RODRÍGUEZ-LÓPEZ, M. I.; CARAZO-DÍAZ, C.; GABALDÓN, J. A.; NÚÑEZ-DELICADO, E. Optimization of the microencapsulation of synthetic strawberry flavour with different blends of encapsulating agents using spray drying. **Powder Technology**, v. 338, p. 591–598, 2018.

RAMAKRISHNAN, Y.; ADZAHAN, N. M.; YUSOF, Y. A.; MUHAMMAD, K. Effect of wall materials on the spray drying efficiency, powder properties and stability of bioactive compounds in tamarillo juice microencapsulation. **Powder Technology**, v. 328, p. 406–414, 2018.

RÉ, M. I. Microencapsulation by spray drying. **Drying Technology**, v. 16, n. 6, p. 1195–1236, 1998.

REINECCIUS, G. A. The spray drying of food flavors. **Drying Technology**, v. 22, n. 6, p. 1289–1324, 2004.

REINECCIUS, G. A.; YAN, C. Factors controlling the deterioration of spray dried flavourings and unsaturated lipids. **Flavour and Fragrance Journal**, v. 31, n. 1, p. 5–21, 2016.

ROCCIA, P.; MARTÍNEZ, M. L.; LLABOT, J. M.; RIBOTTA, P. D. Influence of spray-drying operating conditions on sunflower oil powder qualities. **Powder Technology**, v. 254, p. 307–313, 2014.

SHAO, P.; XUAN, S.; WU, W.; QU, L. Encapsulation efficiency and controlled release of Ganoderma lucidum polysaccharide microcapsules by spray drying using different combinations of wall materials. **International Journal of Biological Macromolecules**, v. 125, p. 962–969, 2019.

SILVA, E. K.; GOMES, M. T. M. S.; HUBINGER, M. D.; CUNHA, R. L.; MEIRELES, M. A. A. Ultrasound-assisted formation of annatto seed oil emulsions stabilized by biopolymers. **Food Hydrocolloids**, v. 47, p. 1–13, 2015.

SILVA, E. K.; AZEVEDO, V. M.; CUNHA, R. L.; HUBINGER, M. D.; MEIRELES, M. A. A. Ultrasound-assisted encapsulation of annatto seed oil: Whey protein isolate versus modified starch. **Food Hydrocolloids**, v. 56, p. 71–83, 2016.

SOOTTITANTAWAT, A.; YOSHII, H.; FURUTA, T.; OHKAWARA, M.; LINKO, P.

Microencapsulation by Spray Drying : Influence of Emulsion Size on the retention of volatile compounds. **Food Engineering and Physical Properties**, v. 68, n. 7, p. 2256–2262, 2003.

SUN, X.; CAMERON, R. G.; BAI, J. Microencapsulation and antimicrobial activity of carvacrol in a pectin-alginate matrix. **Food Hydrocolloids**, v. 92, p. 69–73, 2019.

SWEEDMAN, M. C.; TIZZOTI, M. J.; SCHÄFER, C.; GILBERT, R. G. Structure and physicochemical properties of octenyl succinic anhydride modified starches: A review. **Carbohydrate Polymers**, v. 92, n. 1, p. 905–920, 2013.

TONON, R. V.; BRABET, C.; HUBINGER, M. D. Influence of process conditions on the physicochemical properties of açai (Euterpe oleraceae Mart.) powder produced by spray drying. **Journal of Food Engineering**, v. 88, n. 3, p. 411–418, 2008.

VERDALET-GUZMÁN, I. Characterization of new sources of derivative starches as wall materials of essential oil by spray drying. **Food Science and technologie**, v. 33, n. 4, p. 757–764, 2013.

WALTON, D. E.; MUMFORD, C. J. Spray dried products-Characterization of particle morphology. **Institution of Chemical Engineers**, v. 77, p. 21–38, 1999.

WANG, X.; YUAN, Y.; YUE, T. The application of starch-based ingredients in flavor encapsulation. **Starch/Staerke**, v. 67, n. 3–4, p. 225–236, 2015.

YE, A.; SINGH, H. Heat stability of oil-in-water emulsions formed with intact or hydrolysed whey proteins : influence of polysaccharides. **Food Hydrocolloids**, v. 20, p. 269–276, 2006.

CAPÍTULO 3 – NOVEL EXPERIMENTAL APPROACH TO STUDY AROMA RELEASE UPON RECONSTITUTION OF INSTANT COFFEE PRODUCTS

1. INTRODUCTION

The aroma of foods and beverages is central to food science and technology, not only from a sensory perspective and related to consumer's acceptance and preferences, but also owing to its relation to food safety and ripeness degree for vegetables and fruits. Since aroma perception is the outcome of interactions of aroma active volatile organic compounds (VOC) with our olfactory receptors in the nose, understanding how and when these compounds are released during food and beverage preparation or consumption (SÁNCHEZ-LÓPEZ et al., 2016) becomes central for our understanding of our sensory perception and for food and beverage acceptance (ELLIS, MAYHEW, 2014a).

The most commonly used technique for identification and quantification of VOC is gas chromatography coupled to mass spectrometry (GC-MS), capable of detecting very small quantities of VOCs, a few parts per billion (ppb) (BLAKE; MONKS; ELLIS, 2009). Although GC-MS is a sensitive and accurate technique when it comes to the identification of compounds, it is not well suited to monitor time-concentration changes of VOC for fast processed (temporal resolution). In addition, VOC analysis by GC-MS requires time for sample collection and preparation and in some instances for pre-concentration prior to injection. Another drawback of GC-MS is related to the fact that there is no suitable capillary column for all compounds, requiring different columns for specific applications (BLAKE et al., 2009; BIASIOLI et al., 2011; MESTDAGH et al., 2014).

New analytical methodologies, capable of monitoring volatile compounds in real time have been described, including electronic systems (GUTIÉRREZ; HORRILLO, 2014) and direct-injection mass spectrometry (BIASIOLI et al., 2011). In this context, PTR-MS (Proton Transfer Reaction Mass Spectrometry) has been highlighted as a particularly powerful technique. While some of the basic concepts were developed in the 1960s by Ferguson, Fehsenfeld; Schmeltkopf (1969), the PTR-MS technology was later established and implemented by Lindinger; Hansel; Jordan (1998). PTR-MS, in particular if equipped with a Time-of-Flight (ToF) mass detector, opened the door for a rapid monitoring of complex mixtures of VOCs with high sensitivity and selectivity. No sample preparation was required,

unlike traditional chromatographic methods. In PTR-MS, an analyte (VOC) is ionized to form a VOC-H^+ (protonated compound) as shown in the reaction R1 (BLAKE et al., 2009):

$$R_{(g)} + H_3O^+_{(g)} \rightarrow RH^+_{(g)} + H_2O \qquad R1$$

The technique uses H_3O^+ as proton donor because most VOCs have larger proton affinity than $H_3O^+_{(g)}$. This results in essentially a quantitative transfer of a proton from the primary ionization agent H_3O^+ to most VOCs, within the drift tube. Proton transfer tends to be a soft ionization process (forming protonated molecular ions), which impart little residual energy onto the subject molecule and, as a consequence, there is little or no fragmentation. This fact is relevant when analyzing complex gas mixtures, where intense fragmentation may cause misidentification (ELLIS & MAYHEW, 2014b). In addition to the possibility for online monitoring (LINDINGER et al., 1998), PTR-MS gives information about dynamic VOC formation, detecting rapid changes in the concentration of VOC and in vivo release (BIASIOLI et al., 2011; ELLIS & MAYHEW, 2014b; GLÖESS et al., 2014; YERETZIAN et al., 2002).

PTR-MS has been applied to the analysis of VOCs in diverse areas of food science, such as for flavour and volatile release from tomatoes (FARNETI et al., 2013), for characterizing chocolates (ACIERNO et al., 2016), differentiating of wines (CAMPBELL-SILLS et al., 2016), determining VOC composition in milk (LIU et al., 2018), and evaluating the impact of fruits texture on aroma release and perception (BONNEAU et al., 2018).

While over a thousand of VOCs have been identified in coffee, only about 30 of them represent potent odorants (FLAMENT, 2002; SUNARHARUM et al., 2014; YERETZIAN et al., 2019; YERETZIAN, 2017). The complexity of the flavour compounds formed during coffee roasting as well as their release during preparation and consumption of coffee beverages stimulated investigations about flavour formation during coffee roasting (GLÖESS et al., 2014), characterization of coffee from different origins (YENER et al., 2014), dynamic extraction of VOC during espresso coffee preparation (SÁNCHEZ-LÓPEZ, ZIMMERMANN, YERETZIAN, 2014), effect of roasting degree on coffee flavour formation and flavour perception (CHARLES et al., 2015), effect of water temperature and pressure on the extraction kinetics of VOC in espresso coffee (LÓPEZ et al., 2016), nose-space analysis (SÁNCHEZ-LÓPEZ et al., 2016; GERMAN, YERETZIAN, TOLSTOGUZOV, 2007; YERETZIAN et al., 2004) or the use of PTR-ToF-MS as a tool to discriminate coffee species (COLZI et al., 2017).

The use of the PTR-ToF-MS technique, that provides results in real time, is crucial to elucidate the mechanism of VOC release during beverage preparation. Since the

temporal evolution and intensity of the aroma released and perceived during reconstitution of instant coffee products is an important olfactory impression and quality feature of instant products, it is important to have analytical tools that allow documenting such information. This will allow better understanding current instant products and develop next generation products with improved aroma quality and consumer acceptance (YERETZIAN et al., 2004; BLAKE et al., 2009; MESTDAGH et al., 2014; LINDINGER et al., 2008).

Despite the growing number of dynamic studies applied in coffee science, no information is available on aroma release from instant coffee and related products such as instant cappuccino. Because such products are quickly prepared the assays need to be carried out in a closed system that allows targeting VOCs released directly into headspace (HS), inside the measurement/sampling setup. For this reason, a new setup for rapid measurement of dynamic aroma release during preparation of instant coffee and instant cappuccino is proposed in the current work. The use of this new experimental setup coupled to PTR-ToF-MS has the potential of being an efficient tool for reproducible studies of the dynamic aroma release upon reconstitution of instant coffee products.

2. MATERIAL AND METHODS

2.1. SAMPLING SETUP

Instant coffee and instant cappuccino samples were provided by Café Iguaçu (Cornélio Procópio, Paraná, Brazil). The dynamics of VOC release were monitored on-line during the brew preparation using the schematic experimental setup shown in Figure 1.

Figure 1. Setup used for online monitoring of VOCs during coffee preparation.

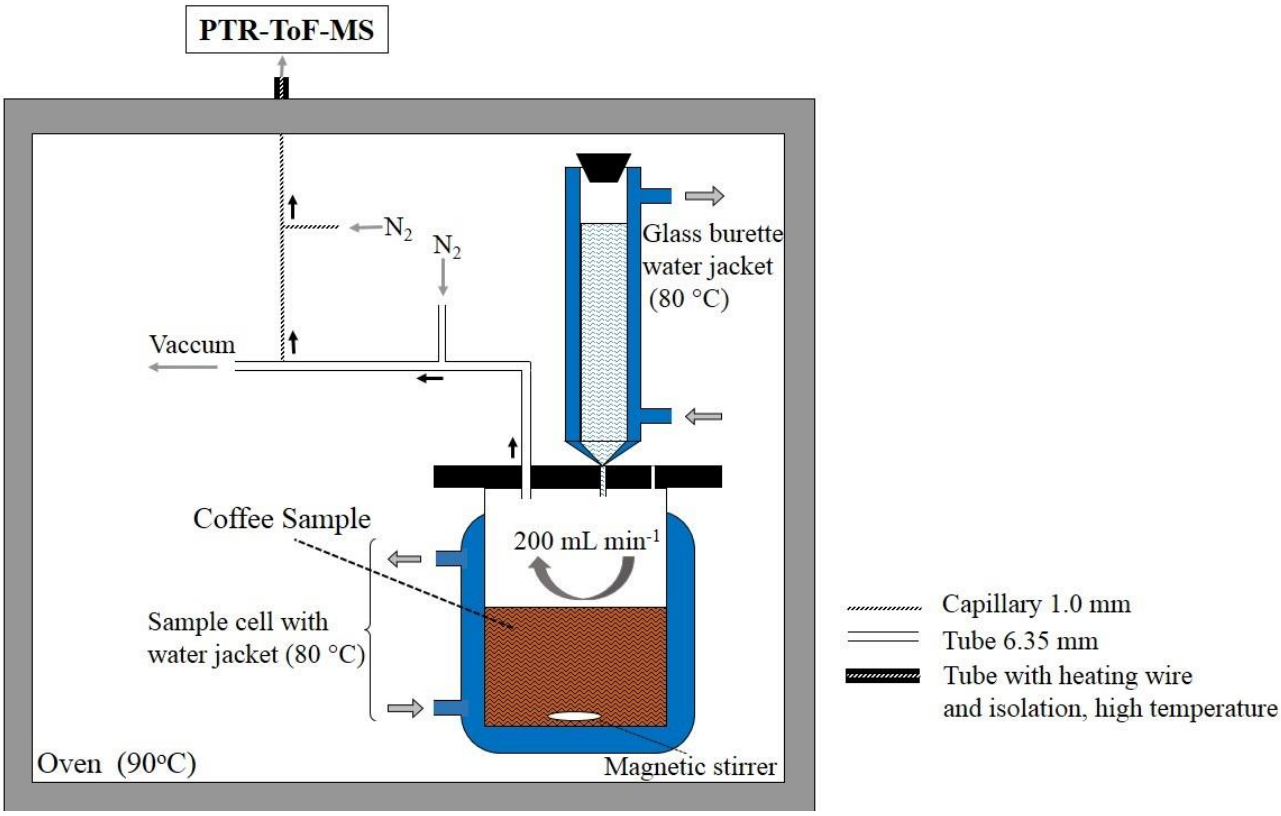

N_2 flow of the first dilution (tube): 1500 mL min^{-1}; N_2 flow of the second dilution (capillary): 300 mL min^{-1}; vacuum pump flow: 1640 mL min^{-1}; PTR-MS FC inlet flow rate: 360 mL min^{-1}.

For the analysis of dynamic release of VOC during preparation of instant coffee beverages, 4.0 g of instant coffee or instant cappuccino were inserted in a 150 mL double-jacketed glass vessel, temperature controlled by a water bath at 80 °C with external thermostat (Haake F6, USA). A 110 mL double-jacketed glass burette was also temperature stabilized to 80 °C and was used to pre-heat the water to be used for preparation of coffee beverage. The sampling setup was installed inside an oven (Thermo Scientific UT6420, Germany) that allowed maintaining the temperature of the whole setup at 90 °C ± 0.5 °C (Figure 1).

The 4.0 g of instant coffee powder was dissolved in 100 mL of water at 80 °C, which was inserted in the vessel at an average rate of 12.5 mL s^{-1}; hence it took 8 s to add the full 100 mL of water. The sample cell was connected to the fix-mounted top cover to be disconnected and filled with the coffee sample. In the first 10 seconds of brew preparation, the samples were stirred by a magnetic stirrer to simulate an instant coffee preparation procedure.

During the analysis, which took 5 min, the HS of the cell sample was purged continuously with 200 mL min^{-1} of N_2 through pre-heated tubes (90 °C). The flow from the sampling cell was diluted in a two-step dilution setup as shown in Figure 1. The dilution is

needed to avoid interference of water vapor in the PTR (prevent formation of water clusters) and to avoid water and VOC condensation in the sampling lines. A vacuum pump was used to pump the gas flow (set at 1640 mL min^{-1}) through the cell and N_2 flow was added accordingly to yield a differential flow of 200 mL min-1 through the sampling cell. The PTR-MS inlet actively sampled gas from the vacuum pump flow as shown in Figure 1. The PTR-MS flow was diluted in an additional step by N_2 gas, to yield a total dilution factor of the gas from the sampling cell of 37.5-fold. All gas flows in the sampling and dilution lines were controlled by mass flow controllers (Bronkhorst, Ruurlo, Netherlands) and verified using a bubble flowmeter.

The preparation of beverages was carried out quickly to avoid temperature changes of the sample, oven, and HS vessel. Twelve replicates for each coffee product were analyzed to verify the repeatability and of the method uncertainty of the results.

2.2. PTR-TOF-MS

A PTR-ToF-MS 8000 instrument (Ionicon Analytik GmbH, Innsbruck, Austria) was used for all measurements. The diluted sample was introduced via a heated sampling line (at 50 mL min^{-1} flow rate) into the drift tube operated at 2.3 mbar, 90 °C and 600 V drift tube voltage, resulting in an E/N value (electric field strength/gas number density) of 140 Townsend (Td, 1 Td = 10−17 cm^2/Vs). PTR-ToF-MS data were recorded by TOFDAQ v.183 data acquisition software (Tofwerk AG, Thun, Switzerland). Mass spectra were recorded in the mass-to-charge (m/z) range of 0–300 with one mass-spectrum recorded every 1 second. Mass axis calibration was performed on mass peaks $[H_3{}^{18}O]^+$, $[H_2O\ H_3{}^{18}O]^+$, and $[C_3H_7O]^+$. Data was further processed by using PTR-ToF Data Analyzer, the intensity normalized by primary ion concentration and ion count corrected for Poisson distribution (MÜLLER et al., 2013). Means of two data points were used for further data analysis (2 second time resolution).

2.3. STATISTICAL ANALYSIS

The time–intensity profiles of previously selected m/z were normalized to their maximum intensity and subjected to Hierarchical Cluster Analysis (HCA) using Ward's minimum variance method and half-squared Euclidean distances to identify compounds with similar time–intensity profile. All analyses were performed by using the software Statistica 10 (StatSoft, Tulsa, USA).

3. RESULTS AND DISCUSSION

The PTR-ToF-MS analysis detected 176 signals of VOCs released upon reconstitution of instant coffee samples and 88 for instant cappuccino samples. Based on their reported aroma impact (LÓPEZ et al., 2016; MESTDAGH et al., 2014; FLAMENT, 2002; SUNARHARUM; WILLIAMS; SMYTH, 2014) and their signal intensity, 15 VOCs for instant coffee and 11 VOCs for instant cappuccino were selected to be studied in detail in this work (Tables 1 and 2).

These compounds were tentatively identified based on their mass peaks and grouped into families using Hierarchical Cluster Analysis (HCA) (Tables 1 and 2). Their main physico-chemical properties, boiling point, vapor pressure, octanol-water partition coefficient (log K_{ow}) (LÓPEZ et at., 2016) and Henry's Law constant (HLC) (SANDER, 2015; WESCHENFELDER et al., 2015; WIELAND et al., 2015) are presented in Tables 1 and 2 for instant coffee and instant cappuccino, respectively.

Table 1. Compounds of soluble coffee tentatively identified by their mass peaks, assigned sum formula and physico-chemical properties. Compounds were grouped into families using Hierarchical Cluster Analysis (HCA).

	m/z measured	*m/z* theoretical	Tentative identification	CAS [1]	Sum formula	Boiling point (°C)	Vapor pressure (kPa) at 25°C	Water solubility (g L^{-1})	log K_{ow}	HLC (mol (m^3 Pa)$^{-1}$) [4]	Sensorial effect [2,3]	Odor description [3,5]
Family A												
	73.064	73.065	Butanone	78-93-3	$C_4H_9O^+$	80	12.10	223	0.29	1.8×10^{-1}	Negative	Ethereal
	83.048	83.049	Methylfuran	534-22-5	$C_5H_7O^+$	65	20.80	3	1.85	1.5×10^{-3}	Positive	Chocolate
	87.079	87.080	Methylbutanal	590-86-3	$C_5H_{11}O^+$	94	1.39	10	1.23	2.4×10^{-2}	Positive	Malty
Family B												
	75.044	75.044	Methylacetate	79-20-9	$C_3H_7O_2^+$	57	28.80	Miscible	0.18	8.1×10^{-2}	Negative	Ethereal
	80.049	80.049	Pyridine	110-86-1	$C_5H_6N^+$	115	2.77	Miscible	0.65	1.1	Positive	Fishy
	87.043	87.044	Butanedione	431-03-8	$C_4H_7O_2^+$	88	7.57	200	-1.34	2.6	Positive	Buttery
	97.026	97.028	Furfural	98-01-1	$C_5H_5O_2^+$	162	0.295	77	0.41	0.38	Negative	Bready
	101.058	101.060	Pentanedione	600-14-6	$C_5H_9O_2^+$	138	0.495	166	0.40	Not available	Positive	Sweet, caramel
	123.089	123.092	Trimethylpyrazine	14667-55-1	$C_7H_{11}N_2^+$	171	0.193	15.2	0.95	Not available	Negative	Cooked/sulfurous
Family C												
	61.028	61.028	Acetic acid	64-19-7	$C_2H_5O_2^+$	118	2.09	Miscible	-0.17	40	Negative	Chemical
	99.042	99.044	2-furanmethanol	98-00-0	$C_5H_7O_2^+$	171	0.081	Miscible	0.28	1.2×10^{2}	Positive	Burned
	109.07	109.076	Dimethylpyrazine	123-32-0	$C_6H_9N_2^+$	156	0.365	38.2	0.54	7.1	Positive	Nutty
	111.042	111.044	Methylfurfural	620-02-0	$C_6H_7O_2^+$	187	0.091	29.1	0.67	Not available	Positive	Spicy, caramel
	125.056	125.060	Guaiacol	90-05-1	$C_7H_9O_2^+$	205	0.014	18.7	1.32	5.4	Negative	Chemical
Family D												
	127.036	127.039	Maltol	118-71-8	$C_6H_7O_3^+$	93	0.4×10^{-4}	12	0.09	Not available	Positive	Sweet, caramel

[1]Chemical Abstracts Service; [2]Bassoli, 2006; [3]Kalschne et al., 2018; [4]Henry's Law constant: defined by the partial pressure of the chemical by its aqueous-phase concentration; [5]Flament, 2002.

Table 2. Compounds of instant cappuccino tentatively identified by their mass peaks, assigned sum formula and physic-chemical properties. Compounds were grouped into families using Hierarchical Cluster Analysis (HCA).

	m/z measured	*m/z* theoretical	Tentative identification	CAS [1]	Sum formula	Boiling point (°C)	Vapor pressure (kPa) at 25°C	Water solubility (g L^{-1})	log K_{ow}	HLC (mol (m^3 Pa)$^{-1}$) [4]	Sensorial effect [2,3]	Odor description [3,5]
Family A												
	45.034	45.033	Acetaldehyde	75-07-0	$C_2H_5O^+$	20	120	Miscible	-0.34	1.7×10^{-1}	Negative	Ethereal
	61.028	61.028	Acetic acid	64-19-7	$C_2H_5O_2^+$	118	2.1	Miscible	-0.17	40	Negative	Chemical
	69.033	69.033	Furan	110-00-9	$C_4H_5O^+$	31	80	10	1.34	1.8×10^{-3}	Not available	Not available
	73.064	73.065	Butanone	78-93-3	$C_4H_9O^+$	80	12.1	223	0.29	1.8×10^{1}	Negative	Ethereal
	87.043	87.044	Butanedione	431-03-8	$C_4H_7O_2^+$	88	7.6	200	-1.34	7.3×10^{-1}	Positive	Buttery
	89.058	89.060	Methyl propanoate	554-12-1	$C_4H_9O_2^+$	80	11.2	62.4	0.84	5.7×10^{-2}	Not available	Not available
Family B												
	97.027	97.028	Furfural	98-01-1	$C_5H_5O_2^+$	162	0.3	77	0.41	2.6	Negative	Bready
	97.059	97.065	Dimethylfuran	625-86-5	$C_6H_9O^+$	200	11.5	> 1	2.24	Not available	Negative	Ethereal
Family C												
	83.049	83.049	Methylfuran	534-22-5	$C_5H_7O^+$	65	20.8	3	1.85	1.46×10^{-3}	Positive	Chocolate
	101.058	101.060	Pentanedione	600-14-6	$C_5H_9O_2^+$	138	0.5	166	0.40	Not available	Positive	Caramel
Family D												
	111.041	111.044	Methylfurfural	620-02-0	$C_6H_7O_2^+$	187	0.09	29.1	0.67	Not available	Positive	Spicy, caramel

[1]Chemical Abstracts Service; [2]Bassoli, 2006; [3]Kalschne et al., 2018; [4]Henry's Law constant: K_H defined by the partial pressure of the chemical by its aqueous-phase concentration; [5]Flament, 2002.

The current study investigates the kinetics of fast release of VOC upon reconstitution of instant coffee and instant cappuccino. Figure 2 shows the time-intensity profiles of three selected compounds monitored in both instant products: butanone, furfural and methylfuran. Overall, the intensities observed in instant cappuccino were approximately 10-times lower than in instant coffee. As indicated by the standard deviations from 12 repetitions, the technique showed high reproducibility. Furthermore, the setup allowed measuring fast changes in the release dynamics of VOC, similar to previously reported studies (BIASIOLI et al., 2011; BLAKE et al., 2009; LINDINGER et al., 1998). For a few compounds, such as the highly volatile methylfuran (Figure 2B), a background signal was observed already prior to reconstitution, which likely stems from the release of such VOC form the solid instant cappuccino powder.

Figure 2. Time-intensity profile of the three selected compounds in both soluble coffee (A) and instant cappuccino (B) and the confidence interval at the level of 10% during 100 seconds of analyze.

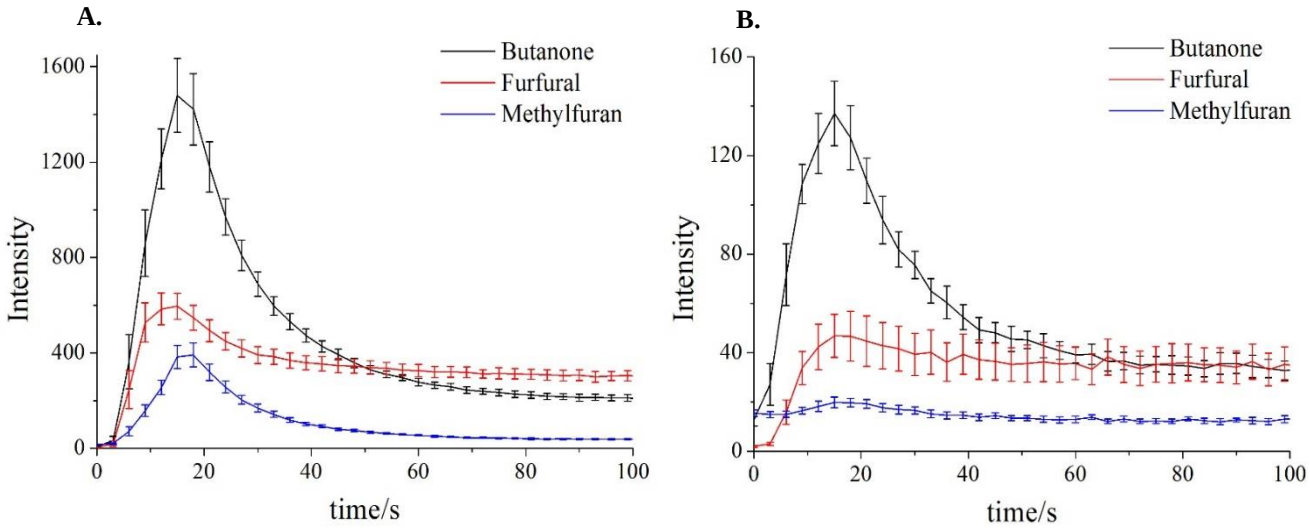

3.1 INSTANT COFFEE

According to the normalized time–intensity profiles in Figures 3A and 3B, the 15 compounds released from instant coffee presented similar release behavior, with the exception of maltol (Family D). A proper interpretation of the measured release curves ideally requires modelling the processes involved in the dissolution of the powder, diffusion and volatilization of VOCs. While, the focus here is on the establishment of an instrumental methodology to monitor, at high time-resolution and sensitivity, the temporal release of VOCs upon reconstitution, we provide here a tentative and qualitative interpretation of the observed

time-intensity release curves. Roughly, we divide released curves of VOC into three phases: burst, transition and liquid-air partitioning.

Upon reconstitution a burst of VOC was observed that reached a maximum at around 18 s (Figure 3). The initial peak of aroma release is tentatively explained as a burst of gas, trapped and/or adsorbed inside the porous structure of the instant coffee powder. Upon addition of water to the dry powder, VOC are directly released into the HS without being dissolved into the water, generating an aroma burst (DE ROOS, 2003; FLORES; KONG, 2017). The burst is followed by a gradual decrease, transitioning into a third phase characterized by a linear decrease (after 1 minute) indicative of a liquid-gas partitioning (Henry-Law Constant; HLC) of aroma compounds dissolved in the brew. In this later phase of the release curve, all instant powder has dissolved in the hot water and the concentrations of VOCs in the brew are constant. The transition between both release regimes – the burst on the short-time side and linear regime at longer times - reflects a phase where the powder is fully surrounded by liquid but not fully dissolved. During dissolution it is believed that the gas trapped in the instant coffee matrix is released, forming bubbles and facilitates the release of VOCs already dissolved in the brew. While the concentration continues to increase until full dissolution of the powder, the driving out of volatiles from released gases gradually declines until full dissolution. The observed release curves can be summarized as a succession of three phases, each characterized (although not exclusively) by one release mode: First phase – burst (0 to approx. 20 s): direct release of VOC into the gas phase while the instant powder is being wetted, opening its porous structure and releasing VOC. While it takes about 8 seconds to add all 100 mL hot water, the dissolution will extend beyond this first phase. Second phase – full dissolution (30 - 60 s): This phase is essentially characterized by the completion of the dissolution of instant power, leading to a gradual increase of the concentration of the brew. It is believed that during dissolution, some gas is being released as well, driving out dissolved VOC. This effect decreases gradually during the second phase as dissolution is completed. Phase three – partitioning: All powder is dissolved and the measured concentration is governed for each compound by the air-liquid partition function at 80 °C (WIELAND et al. 2015; POLLIEN et al., 2003).

While the proposed three-phase model allows roughly explaining the overall time-intensity behavior of VOC release, further studies and in particular a physical modelling of the reconstitution dynamics and VOC release are needed, in order to better understand the release of VOC from instant coffee, upon reconstitution.

Figure 3. Graph A presents normalized time–intensity profiles of the 15 individual compounds in soluble coffee while the graph B presents the normalized time–intensity profiles for the four families (average of all compounds within each family), during the first 125 seconds upon start of reconstitution (water addition).

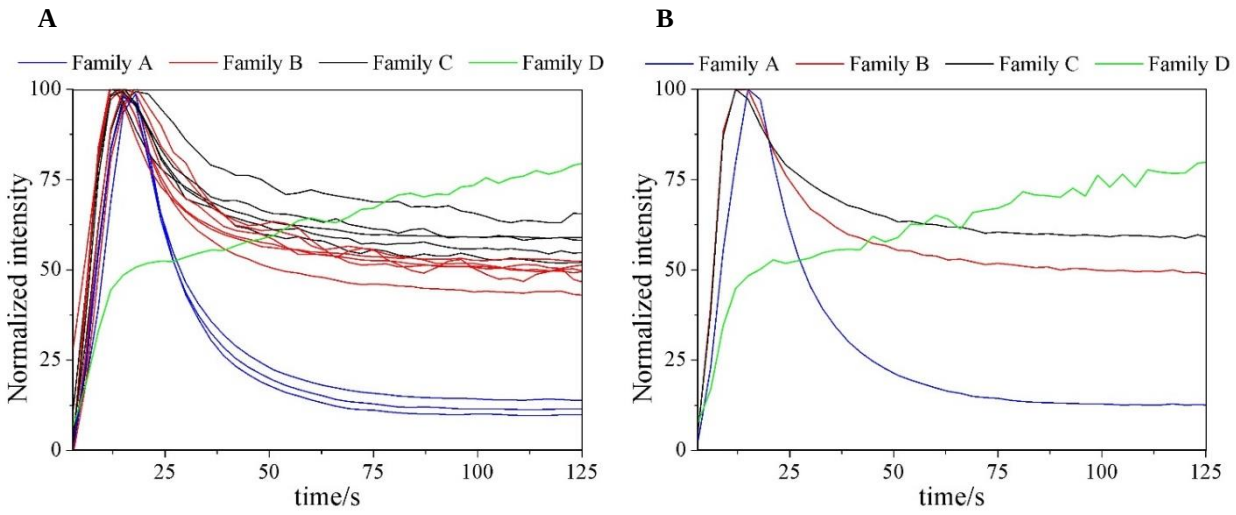

Hierarchical Clustering Analysis (HCA) was applied to the normalized time–intensity profiles of the individual VOC, clustering the 15 compounds into four distinct families, based on similarities of their time–intensity profiles (Table 1 and Fig. 3B). Maltol showed a singular time–intensity profile that was not observed for any other compound; for this reason it was classified into a distinct family (Family D).

Family A (3 VOC): VOCs classified into family one were released rapidly, within the first 20 seconds of reconstitution, and their concentration in the HS decreased strongly after an initial burst. After two minutes, their HS intensities reached an intensity of only 15%, relative to the maximum of the burst. These compounds mainly contribute to a burst of aroma within the first minute of reconstitution but have a limited impact at longer times. Hence they will mostly impact the aroma profile during preparation of the cup but will hardly contribute later during consumption. This family of compounds may therefore be grouped to produce a "burst" of aroma.

Family B (6 VOC): Their intensities increased to reach a maximum at around 15 s, but then continue to be released at relative high concentrations into the HS. Two minutes after reconstitution, their intensities were still above 50% of the maximum of the burst. Hence, these compounds contribute on the one hand to the burst, but most notable remain at relatively high concentrations in the HS over several minutes, while the coffee is being consumed. They hence form the "core" of the aroma.

Family C (5 VOC): The intensity also increased quickly at the beginning, but their released extended over slightly longer times. Together with Family B, these compounds contribute to the aroma quality at longer times, once the burst is over. Both family together form the core of the reconstituted instant coffee. But the differences in the decline between family B and C with time leads to a gradual change in the aroma profile, where compounds in family C will increasingly dominate the aroma profile above the cup. The interplay of the compounds form these two families will lead to temporal change of the HS aroma profile, which we call here the "melody" of the cup.

Family D (1 VOC): Maltol – was the least volatile compound. The intensity also increased relatively quickly at the beginning, within the first 20 seconds, albeit relatively slower than the three first families. This may be indicative of a direct release into the gas phase (some burst). In contrary, the release of maltol extended over longer times, without ever reaching a maximum in released intensity, over the 5-minute time window examined here. Such compounds will eventually dominate the aroma profile at longer time which we may call the "mature" phase of the cup.

Hence, on a molecular level and based on HCA, the individual VOCs can be classified into distinct families. Each family can be attributed some particular (dominant) role to the overall aroma profile above the cup. Some are mainly responsible for the burst. Other contribute to the core while differences in their time-intensity behavior will lead to a temporal evolution of the aroma profile above the cup – we termed this the melody of the coffee. Finally, the HS intensity of some aroma compounds may increase to dominate the profile at longer time and transitioning into the mature phase of the cup.

Referring to Tables 1 and 2, can the classification of aroma compounds classified into different families be rationalzed based on physical properties? The polarity (as expressed through the water solubility and log K_{ow} - partition coefficient between octanol and water) was found to be the main molecular property that drives extraction and release during the preparation of espresso coffee. More polar compounds (higher water solubility and lower log K_{ow}) were shown to be extracted and released faster than less polar ones (lower water solubility and higher log K_{ow}) (LÓPEZ et al., 2016; MESTDAGH et al., 2014). However, in this current study, the brews were prepared from instant coffee powder, where no extraction occurs. The release rate from the solid is only limited by the dissolution of the instant powder and no diffusion/extraction through the solid coffee matrix occurs. The release dynamics from the solid phase of instant coffee are fast, compared to espresso extraction. Hence, the polarity of VOCs

did not have a strong influence on the initial release profile of the compounds (burst effect). Acetaldehyde, acetic acid, furan, butanone, butanedione, methyl propanoate, for example, which belong to family A, are less polar (water solubility between 3 and 223 g L^{-1} and log K_{ow} between 0.29 and 1.85) and showed a faster release profile than compounds that belong to family B and C (solubility higher than 15.2 g L^{-1} and log K_{ow} between -1.34 and 1.32) that are on average less polar.

Compounds of family A were released rapidly, with the signal reaching the maximum intensity and then reducing by half in less than 30 seconds after the preparation of the brew (Figure 3B). This behavior may be attributed to the high volatility of the compounds of this family as expressed by their vapor pressure (1.39 - 20.8 kPa) and HLC (1.5×10^{-3} - 1.8×10^{-1} mol $(m^3\ Pa)^{-1}$), favouring their release to the gas phase. As stated by Roberts, Pollien, Antille, Lindinger, & Yeretzian (2003), volatility in water solutions was the main property that correlated with the release of flavour compound. On the other hand, release behavior of maltol could also be explained by its very low vapor pressure (0.4×10^{-4} kPa) because, despite having a low water solubility, maltol had a greater tendency to remain in the aqueous phase at the beginning of brew preparation but will be released to the HS in higher intensity, later during reconstitution. Overall, the vapor pressure and HLC appear to the two main factors that differentiate VOC classified into different families.

3.2 INSTANT CAPPUCCINO

Figure 4A shows the release profile of 11 compounds from instant cappuccino until 300 seconds of analysis. All compounds monitored during the instant cappuccino preparation reached their maximum intensity in the HS within 20 seconds, after which their concentration decreased (Figure 4A). In general, intensities were approximately one order of magnitude lower, as compared to Instant coffee. This reduction can be attributed to two factors. First, components present in the formulation, such as milk, sugar, fat, and emulsifier, reduce the coffee fraction amount in the product (lower concentration of VOCs from coffee). Second, a higher retention by the components in the brew will further reduce their HS concentration. Hence, the reduction of the aroma can be related to lower initial amounts of aroma compounds in the instant cappuccino matrix and to modified Henry's law constants due to the presence of additional components in the matrix. Even at these low overall amounts of released VOCs, the

PTR-ToF-MS could successfully detect the dynamics of aroma release during instant cappuccino preparation (Figure 2B).

Figure 4. Graph A presents normalized time–intensity profile of the 11 individual compounds in instant cappuccino while the graph B presents normalized time-intensity profiles for the four families (average of all compounds within each family), during the first 300 seconds upon start of reconstitution (water addition).

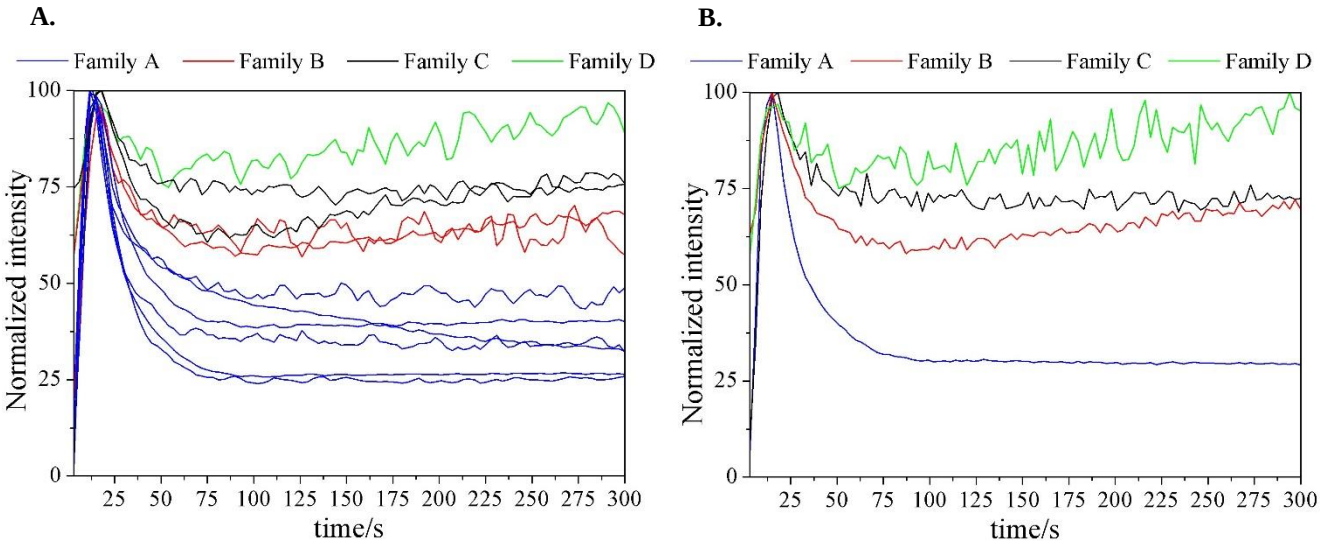

Similar to the results on instant coffee, the compounds detected in cappuccino were grouped into families according to similarities of their time–intensity profiles, using Hierarchical Clustering Analysis. Thus, the 11 compounds monitored were grouped into four families (Table 2 and Fig. 4). Figure 4B shows the release features of the families during instant cappuccino preparation.

Family A (6 VOC): Compounds are released over a relatively short period of time, with a reduction to approximately 30% relative to the maximum of the burst, within 90 seconds. Hence, these compounds may be responsible for the intense aroma burst from instant cappuccino during the first minute upon reconstitution.

Family B (2 VOC): The intensity also increased rapidly at the beginning of the reconstitution process but remained high until the end of the analysis (72% after 5 minutes, relative to the maximum of the burst).

Family C (2 VOC): These VOC presented a similar profile to those in family B but were already being released from the powder, prior to reconstitution. These compounds showed an increase in concentration after water addition and a marked reduction shortly after the maximum peak. In analogy to instant coffee, compounds in Family B and C collectively may

be considered the core of the aroma (after the initial burst), while family C compounds additionally contribute to the aroma of the powder, as well.

Family D (1 VOC): These VOC presented similar characteristic to family C, but after the peak of intensity and later reduction, the intensity seemed to increases slightly again, at longer times, although this increase is not significant compared to the detection limit (3 × noise on base-line).

In the same way, as for instant coffee, the volatility (vapor pressure and HLC) had a strong influence on the release profile of the aroma compounds in instant cappuccino and hence their classification into families. For example, the rapid increase and subsequent reduction in the release behavior of family A (Figure 4B) is attributed to higher vapor pressure and higher HLC (ROBERTS et al., 2003). On the other hand, the release of methylfurfural (Family D), which presents lower vapor pressure and lower HLC, lasted longer (Table 2). Moreover, unlike instant coffee, in instant cappuccino, the polarity (water solubility and K_{ow}) affected the aroma release, as one might expect, since the instant cappuccino formulation contains lipids (SOUKOULIS et al., 2012). In this way, compounds that have greater water solubility and lower Kow (polar compounds), e.g. butanedione in Family A, are favoured for their release to the HS when compared to less polar compounds such as methylfuran (Family C).

The lipids present in the cappuccino composition play an important role in the release of volatile compounds (MESTDAGH et al., 2014). The multicomponent characteristic of the instant cappuccino causes a reduction of the intensity of the less polar compounds that partially dissolve in the milk fat and decreases their release rate into the HS (ROBERTS; POLLIEN; WATZKE, 2003; ROBERTS et al., 2003). The reduction of the intensity of the more polar compounds is due to their interactions with the protein present on fat droplets membrane layer and also with the fat-protein complex itself that acts as a barrier to the release of hydrophilic compounds (SOUKOULIS et al., 2012).

4. CONCLUSIONS

The online analysis of volatile organic compounds (VOC) using the reconstitution setup coupled to PTR-ToF-MS is a powerful approach for studying the kinetics of coffee aroma release. It allows for a reproducible reconstitution of instant powder, the release of VOC into the HS and the accurate monitoring of the time-intensity release curves for individual compounds by PTR-ToF-MS. This approach has shown to provide accurate data on

the aroma release upon reconstitution and insight into the impact of the matrix on such release, as applied to instant coffee and instant cappuccino.

The main objective of this work was to establish such a robust and sensitive methodology to measure the time-intensity release of volatile aroma compounds upon reconstitution of instant coffee products (and other instant products as well). Furthermore, a tentative interpretation of the observed time-intensity profiles was proposed.

On a macroscopic level, we have tentatively divided the process of dissolution and release into three phases: *burst (0 to 30 s)* - essentially characterized by compounds that are directly released into to the gas phase, upon dissolution of the porous instant coffee matrix; *transition (up to ~ 90 s)* - instant powder continues to gradually dissolve into the water, increasing the concentration of dissolved aroma compounds; and *partitioning (from ~90 s on)* - once all compounds are dissolved, the release becomes mainly governed by the liquid-air partitioning volatility.

On a molecular level, individual volatile aroma compounds were divided into families with different time-intensity profiles. One family was showing a strong first burst in HS concentration, with a maximum at around 20 s, and rapidly decreasing thereafter to less than 30% (instant cappuccino) or even below 15% after only 90 s, relative to the maximum of the burst. These compounds are characterized as being of rather high volatility and are released directly into the gas phase without getting dissolved. They are important to the "burst" upon reconstitution. A second set of compounds were showing as well some initial burst but then remained at relatively high HS concentrations. They were collectively defining the "core" of the aroma of reconstituted instant coffee. Finally, for maltol, the HS intensity increased over the entire 5 minutes. It is speculated that such compound will contribute mainly to the aroma at longer time, a phase that was term as *"mature"*. Some compounds being characteristic for the burst, some for the core and finally a third group for the maturate phase.

It appears that the volatility (vapor pressure and Henry's Law constant) is the main driving force for VOC release from instant coffee while polarity did not have an influence on the release profile. On the other hand, for instant cappuccino, both volatility and polarity affected the VOC release.

While this molecular interpretation and classification is still based on a small number of compounds, it allows for some working hypotheses upon which to modulate the time-intensity profile upon reconstitution of instant coffee either by the aromatic composition or the matrix.

The methodology developed here will next be applied to investigate the release of aroma from instant coffee products with different aroma encapsulation techniques as a mean to modulate the aroma release from instant coffee. Furthermore, we will attempt to model the observed release curves based on underlying physical models, towards a better interpretation of the data. Ultimately, such work will permit to predict the evolution of consumers' perception over time, from product preparation to consumption for instants products in general.

REFERENCES

ACIERNO, V.; YENER, S.; ALEWIJN, M.; BIASIOLI, F.; VAN RUTH, S. Factors contributing to the variation in the volatile composition of chocolate: Botanical and geographical origins of the cocoa beans, and brand-related formulation and processing. **Food Research International**, v. 84, p. 86–95, 2016.

BASSOLI, D. G. **Impacto Aromático Dos Componentes Voláteis Do Café Solúvel : Impacto Aromático Dos Componentes Voláteis Do Café Solúvel :** [s.l.] Universidade Estadual de Londrina, 2006.

BIASIOLI, F. YERETZIAN, C.; GASPERI, F.; MÄRK, T. D. PTR-MS monitoring of VOCs and BVOCs in food science and technology. **TrAC - Trends in Analytical Chemistry**, v. 30, n. 7, p. 968–977, 2011.

BLAKE, R. S.; MONKS, P. S.; ELLIS, A. M. Proton-Transfer Reaction Mass Spectrometry. **Chemical Reviews**, v. 44, p. 861–896, 2009.

BONNEAU, A.; BOULANGER, R.; LEBRUN, M.; MARAVAL, I.; VALETTE, J.; GUICHARD, E.; GUNATA, Z. Impact of fruit texture on the release and perception of aroma compounds during in vivo consumption using fresh and processed mango fruits. **Food Chemistry**, v. 239, p. 806–815, 2018.

CAMPBELL-SILLS, H.; CAPOZZI, V.; ROMANO, A.; CAPPELLIN, L.; SPANO, G.; BRENIAUX, M.; LUCAS, P.; BIASIOLI, F. Advances in wine analysis by PTR-ToF-MS: Optimization of the method and discrimination of wines from different geographical origins and fermented with different malolactic starters. **International Journal of Mass Spectrometry**, v. 397–398, p. 42–51, 2016.

CHARLES, M.; ROMANO, A.; YENER, S.; BARNABÀ, M.; NAVARINI, L.; MÄRK, T. D., BIASIOLI, F.; GASPERI, F. Understanding flavour perception of espresso coffee by the combination of a dynamic sensory method and in-vivo nosespace analysis. **Food Research International**, v. 69, p. 9–20. 2015.

COLZI, I.; TAITI, C.; MARONE, E.; MAGNELLI, S.; GONNELLI, C.; MANCUSO, S. Covering the different steps of the coffee processing : Can headspace VOC emissions be exploited to successfully distinguish between Arabica and Robusta? **Food Chemistry**, v. 237, p. 257–263, 2017.

DE ROOS, K. B. Effect of texture and microstructure on flavour retention and release. **International Dairy Journal**, v. 13, n. 8, p. 593–605, 2003.

ELLIS, A. M.; MAYHEW, C. A. Background. In: **Proton Transfer Reaction Mass Spectrometry. Principles and Applications**. [s.l: s.n.]. p. 2–23a.

ELLIS, A. M.; MAYHEW, C. A. PTR-MS in the Food Sciences. In: **Proton Transfer Reaction Mass Spectrometry. Principles and Applications**. [s.l: s.n.]. p. 221–265.

FARNETI, B.; ALGARRA, ALARCÓN, A. A.; CRISTESCU, S. M.; COSTA, G.; HARREN, F. J. M.; HOLTHUYSEN, N. T. E.; WOLTERING, E. J. Aroma volatile release kinetics of tomato genotypes measured by PTR-MS following artificial chewing. **Food Research International**, v. 54, n. 2, p. 1579–1588, 2013.

FERGUSON, E. E.; FEHSENFELD, F.; SCHMELTKOPF, A. L. Flowing afterglow measurements of ion-neutral reactions. **Advances in Atomic and Molecular Physics**, v. 5, p. 1–56, 1969.

FLAMENT, I. From the raw bean to the roast coffee. In: FLAMENT, I. (Ed.). . **Coffee Flavour Chemistry**. Chichester: John Wiley & Sons, 2002. p. 37–52.

FLORES, F. P.; KONG, F. In Vitro Release Kinetics of Microencapsulated Materials and the Effect of the Food Matrix. **Annual Review of Food Science and Technology**, v. 8, p. 237–259, 2017.

GERMAN, J. B.; YERETZIAN, C.; TOLSTOGUZOV; V. B. Olfaction, where Nutrition, Memory and Immunity Intersect. In R.G. Berger (Ed.), *Flavours: Chemistry, Technology and Resources* (pp. 25-41). Berlin: Springer, 2007.

GLÖESS, A. N.; VIETRI, A.; WIELAND, F.; SMRKE, S.; SCHÖNBÄCHLER, B.; LÓPEZ, J. A. S.; PETROZZI, S.; BONGERS, S.; KOZIOROWSKI, T.; YERETZIAN, C. Evidence of different flavour formation dynamics by roasting coffee from different origins: On-line analysis with PTR-ToF-MS. **International Journal of Mass Spectrometry**, v. 365–366, p. 324–337, 2014.

GUTIÉRREZ, J.; HORRILLO, M. C. Advances in artificial olfaction: Sensors and applications. **Talanta**, v. 124, p. 95–105, 2014.

KALSCHNE, D. L.; VIEGAS; M. C., DE CONTI; A. J., CORSO; M. P., BENASSI, M. T. Steam pressure treatment of defective Coffea canephora beans improves the volatile profile and sensory acceptance of roasted coffee blends. **Food Research International**, v. 105, 393–402, 2018.

LINDINGER, C.; LABBE, D.; POLLIEN, P.; RYTZ, A.; JUILLERAT, M. A.; YERETZIAN, C.; BLANK, I. When Machine Tastes Coffee: Instrumental Approach to Predict Sensory Profile of Espresso Coffee. **Analytical Chemistry**, v. 80, n. 5, p. 1574–1581, 2008.

LINDINGER, W.; HANSEL, A.; JORDAN, A. On-line monitoring of volatile organic compounds at pptv levels by means of proton-transfer-reaction mass spectrometry (PTR-MS)

medical applications, food control and environmental research. **International Journal of Mass Spectrometry and Ion Processes**, v. 173, n. 3, p. 191–241, 1998.

LIU, N.; KOOT, A.; HETTINGA, K.; JONG, J.; RUTH, S. M. Portraying and tracing the impact of different production systems on the volatile organic compound composition of milk by PTR-(Quad)MS and PTR-(ToF)MS. **Food Chemistry**, v. 239, p. 201–207, 2018.

LÓPEZ, J. A. S.; WELLINGER, M.; GLOESS, A. N.; ZIMMERMANN, R.; YERETZIAN, C. Extraction kinetics of coffee aroma compounds using a semi-automatic machine: On-line analysis by PTR-ToF-MS. **International Journal of Mass Spectrometry**, v. 401, p. 22–30, 2016.

MESTDAGH, F.; DAVIDEK, T.; CHAUMONTEUIL, M.; FOLMER, B.; BLANK, I. The kinetics of coffee aroma extraction. **Food Research International**, v. 63, p. 271–274, 2014.

MÜLLER, M.; MIKOVINY, T.; JUD, W.; D'ANNA, B.; WISTHALER, A. A new software tool for the analysis of high resolution PTR-TOF mass spectra. **Chemometrics and Intelligent Laboratory Systems**, v. 127, p. 158–165, 2013.

POLLIEN, P.; JORDAN, A.; LINDINGER, W.; YERETZIAN, C. Liquid-air partitioning of volatile compounds in coffee: dynamic measurements using proton-transfer-reaction mass spectrometry, **International Journal of Mass Spectrometry**, v. 228, p. 69-80, 2003.

ROBERTS, D. D., POLLIEN, P., ANTILLE, N., LINDINGER, C., YERETZIAN, C. Comparison of Nosespace , Headspace , and Sensory Intensity Ratings for the Evaluation of Flavor Absorption by Fat. **Journal of Agricultural and Food Chemistry**, v. 51, p. 3636–3642, 2003.

ROBERTS, D. D., POLLIEN, P., WATZKE, B. Experimental and Modeling Studies Showing the Effect of Lipid Type and Level on Flavor Release from Milk-Based Liquid Emulsions. **Journal of Agricultural and Food Chemistry**, v. 51, 189–195, 2003.

SÁNCHEZ-LÓPEZ, J. A.; ZIMMERMANN, R.; YERETZIAN, C. Insight into the time-resolved extraction of aroma compounds during espresso coffee preparation: Online monitoring by PTR-ToF-MS. **Analytical Chemistry**, v. 86, n. 23, p. 11696–11704, 2014.

SANDER, R. Compilation of Henry's law constants (version 4.0) for water as solvent. **Atmospheric Chemistry and Physics**, v. 15, n. 8, p. 4399–4981, 2015.

SOUKOULIS, C., BIASIOLI, F., APREA, E., SCHUHFRIED, E., CAPPELLIN, L., MÄRK, T. D., GASPERI, F. PTR-TOF-MS Analysis for Influence of Milk Base Supplementation on Texture and Headspace Concentration of Endogenous Volatile Compounds in Yogurt. **Food and Bioprocess Technology**, v. 5, n. 6, p. 2085–2097, 2012.

SUNARHARUM, W. B.; WILLIAMS, D. J.; SMYTH, H. E. Complexity of coffee flavor: A compositional and sensory perspective. **Food Research International**, v. 62, p. 315–325, 2014.

WESCHENFELDER, T. A.; LANTIN, P.; VIEGAS, M. C.; DE CASTILHOS, F.; SCHEER, A. D. P. Concentration of aroma compounds from an industrial solution of soluble coffee by

pervaporation process. **Journal of Food Engineering**, v. 159, p. 57–65, 2015.

WIELAND, F.; NEFF, A.; GLÖESS, A. N.; POISSON, L.; ATLAN, S.; LARRAIN, D.; PRÊTRE, D.; BLANK, I.; YERETZIAN, C. Temperature dependence of Henry's law constants: An automated, high-throughput gas stripping cell design coupled to PTR-ToF-MS. **International Journal of Mass Spectrometry**, v. 387, p. 69–77, 2015.

YENER, S.; ROMANO, A.; CAPPELLIN, L.; MÄRK, T. D.; SÁNCHEZ, J.; GASPERI, F. PTR-ToF-MS characterisation of roasted coffees (C . arabica) from different geographic origins. **Journal of Massa Spectrometry**, v. 49, p. 929–935, 2014.

YERETZIAN, C.; JORDAN, A.; BADOUD, R.; LINDINGER, W. From the green bean to the cup of coffee : investigating coffee roasting by on-line monitoring of volatiles. **European Food Research and Technology**, v. 214, p. 92–104, 2002.

YERETZIAN, C.; OPITZ, S.E.W; SMRKE, S., WELLINGER, M. Coffee volatile and aroma compounds: from the green bean to the cup. In A. Farah (Ed.), *Coffee: production, quality and chemistry* (pp. 726-770). London: Royal Society of Chemistry, 2019.

YERETZIAN, C. Special Food Aroma: Coffee. The Aroma of Coffee – Status and Trends, In A. Buettner (Ed.), *Springer Handbook of Odour* (pp. 107-127). Cham: Springer, 2017.

YERETZIAN, C.; POLLIEN, P.; LINDINGER, C.; ALI, S. Individualization of Flavor Preferences: Toward a Consumer-centric and Individualized Aroma Science. **Comprehensive Reviews in Food Science and Food Safety**, v. 3, p. 152-159, 2004.

CAPÍTULO 4 - COFFEE AROMA PROFILE OF ROASTED COFFEE OIL EMULSION AND SPRAY DRIED MICROPARTICLES - INFLUENCE OF PROCESSING PARAMETERS AND THE EFFECTS OVER AROMA RELEASE PROFILE

1. INTRODUCTION

Coffee aroma comprehends thousands of substances that arise from degradation of lipids, carbohydrates, proteins and sugars, Maillard reaction, and transformation of less volatile constituents, upon roasting process (BUFFO; CARDELLI-FREIRE, 2004; SHIBAMOTO, 2015; SUNARHARUM; WILLIAMS; SMYTH, 2014). The pleasant coffee aroma depends on the balance of these compounds but only a small fraction of them, including hydrocarbons, aldehydes, alcohols, ketones, carboxylic acids, esters, pyrazines, pyridines, furans, phenols among others are described as key aroma compounds. (BUFFO; CARDELLI-FREIRE, 2004; SUNARHARUM; WILLIAMS; SMYTH, 2014). Roasted coffee oil is the fraction that contains most part of coffee aroma however, these volatile aroma compounds are easily lost (BUFFO; CARDELLI-FREIRE, 2004; CALLIGARIS et al., 2009; HURTADO-BENAVIDES; DORADO; SÁNCHEZ-CAMARGO, 2016).

As alternative for preventing such losses, the microencapsulation is a technique in which a core (bioactive or labile compounds) is protected by a wall. It is used to prevent losses during storage, besides that it may also be used to control release (BAKRY et al., 2016; SHAO et al., 2019; YE; GEORGES; SELOMULYA, 2018). Among many ways, spray drying is the most common techniques to obtain microparticles in which emulsification is used as sample preparation. The formation of a fine and stable emulsion provides a protective matrix to aroma compounds that can reduce losses during the encapsulation process (FANG et al., 2019; SAIFULLAH et al., 2019; SOOTTITANTAWAT et al., 2005; RÉ, 1998).

Emulsification process is the primary step to microencapsulate by spray drying and can also play a significant role in aroma retention once emulsion stability and composition affect its retention (DE SOUZA et al., 2016; SAIFULLAH et al., 2019; SILVA et al., 2016). Among the several methods to produce emulsions, the ultrasound-assisted stands out to form stable emulsions with smaller droplet size and narrow size distribution. Moreover, it is an energy-efficient process in which the apparatus has low cost and it is easy to operate (CHANDRAPALA et al., 2012; MCCLEMENTS, 2004; SAIFULLAH et al., 2019).

It is known that aroma release and perception is changing over time due to different physicochemical properties (PIGGOTT, 2000; BUETTNER; BEAUCHAMP, 2010; ZANIN, 2019). The development of rapid and direct mass spectrometric techniques has obtained an increasing interest in flavor analysis due to their potential for studying aroma release processes (BIASIOLI et al., 2011; ZANIN, 2019). Therefore, direct on-line aroma analysis might give an insight into the dynamics of coffee aroma release during food preparation and thus their perception in relation to food characteristics (REGUEIRO et al., 2017; ZANIN, 2019).

These reports revealed the complexity of the microencapsulation process and how it depends on several variables; therefore, there is still the need to generate more systematic data, particularly focused on the effects of ultrasound-assisted emulsification and spray drying processes about the changes in a multi-component matrix, such coffee aroma, that possess different properties of each volatile aroma compounds. In addition, it is important to highlight the relevance of aroma release monitoring during coffee preparation to better understand the dynamic aroma release upon microparticle solubilization and instant coffee reconstitution. Such information could expand the existing knowledge and fill gaps still present in the applications of roasted coffee aroma.

The main goal of this study was to assess the changes in the composition of roasted coffee aroma taking place during ultrasound-assisted emulsification and spray drying microencapsulation process, and the effect of microparticles of roasted coffee oil on increasing aroma intensity in instant coffee products.

2. MATERIAL AND METHODS

2.1 MATERIAL

Roasted coffee oil from *Coffea arabica*, instant coffee products (soluble coffee and instant cappuccino) were supplied by Café Iguaçu (Cornélio Procópio, Paraná, Brazil). n-octenyl succinic anhydride waxy maize starch – (OSA-starch) (Capsul®) was provided by Ingredion (São Paulo, São Paulo, Brazil).

2.2 PRODUCTION OF ROASTED COFFEE OIL EMULSIONS

The solutions of coating material (27% w/w) were prepared by dispersing the OSA-starch in deionized water (Millipore®), and then it was mixed overnight to enhance hydration. Roasted coffee oil (10% w/w of wall material) was first pre-emulsified into the hydrated wall material by a rotor-stator type homogenizer (TE-102, Tecnal, Brazil) operating at 3000 rpm for 90 s, followed by sonication (sonicator Q700, QSONICA, USA), using a ultrasonic probe with diameter of 12.7 mm, 20 kHz for 5 min (SILVA et al., 2015). The conditions of ultrasound-assisted emulsification are presented in Table 1. The temperature of each assay was kept constant by a thermostatically-controlled water bath (TE-2005, Tecnal, Brazil) coupled to a double jacket.

Table 1. Screening design of ultrasound-assisted emulsification of roasted coffee oil.

Experiment	Temperature (°C)	Power (W)
1	20	210
2	40	210
3	20	560
4	40	560
5	15	385
6	45	385
7	30	140
8	30	630
9	30	385
10	30	385

2.3 MICROPARTICLES PREPARATION

Emulsions were spray-dried in a laboratorial spray dryer LabPlant SD 05 (LabPlant SD 05, Huddersfield, England) using a double-fluid atomizer nozzle with a 0.7 mm diameter orifice. The process parameters were: inlet temperature: 180°C ± 4 °C; outlet air temperature: 100 ± 5 °C; air flow rate: 73 $m^3 h^{-1}$; compressed air flow rate: 1.1 $m^3 h^{-1}$; feed flow rate: 6 mL min^{-1}; and air pressure: 4 bar. The dried microparticles were stored in plastic bags at 4 °C for further analysis.

2.4 EXTRACTION AND DETERMINATION OF AROMA PROFILE

The aroma profiles were determined for the non-encapsulated roasted coffee oil, all emulsions, and the surface and interior volatiles compounds of microparticles.

2.4.1. Extraction of volatile compounds

The aroma profile of roasted coffee oil non-encapsulated was determined by weighing 1.0 g of roasted coffee oil in 20 mL vials sealed with a silicone septum (Supelco, Bellenfont, PA, USA), equilibrated at 70 °C. The system was submitted to SPME (solid-phase micro extraction) exposed to the headspace for 30 minutes (VIEGAS; BASSOLI, 2007, with modifications).

Volatile compounds were extracted from roasted coffee oil emulsions according to Tian et al. (2013). An aliquot of 5 mL of emulsion was inserted into a 20 mL headspace vial (Agilent, California, USA) and sealed with a silicone septum. The vials were equilibrated under stirring for 10 min and the sampling time were 40 min at 50 °C.

The extraction of aroma compounds from the surface and interior of particles were carried out according to Adamiec, Kalemba (2006) and Ruíz-García, Pino, Lami, Martínez-Pérez (2015) with modifications. For surface volatile compounds, 2.0 g of microparticles were inserted into 10 mL vials, while for total aroma compounds, 0.1 g of powder, 2.0 g of NaCl and 8 mL of deionized water were placed into a 15 mL glass vial, with constant magnetic stirring (200 min^{-1}). The SPME fiber was exposed to the vial headspace for 30 min at 60 °C. Then the fiber was transferred to the injection port of the GC (gas chromatograph) system. The interior aroma profile was calculated by the difference between total and surface aroma.

2.4.2. Chromatography analysis

The profile of coffee aroma of non-encapsulated roasted coffee oil, emulsion, and microparticles (total and surface aroma compounds) were performed using headspace-solid phase microextraction (HS-SPME) followed by quantification using an Agilent 6890 N gas chromatograph (California, USA) equipped with an Agilent 5975B mass spectrometric detector and MSD Chemstation software.

The following standards (Sigma Aldrich, St. Louis, USA) were used: 2-3-dimethylpyrazine, 2-ethyl-3-methylpyrazine, pyrazine, 4-methylthiazole, 2-isobutyl-3-methylpyrazine, 2,3-butanedione, 2,3-pentanedione, acetoin, benzyl alcohol, maltol, furaneol, benzaldehyde, furfuryl acetate, limonene, 3-methylbutanal, 2,4-dimethyl-3-pentanone, 2,5-dimethylpyrazine, pyridine, 2,6-dimethylpyrazine, 4,5-dimethylthiazole, 2-furfurylthiol, 5-methylfurfural, 2-acetylpyridine, vanillin, phenylethyl alcohol, 4-ethylguaiacol, 4-vinylguaiacol, cis-isoeugenol, isovaleric acid, methanethiol, dimethyldisulfide, acetic acid, 2,3,5-trimethylpyrazine, propanoic acid, acetaldehyde, guaiacol, methional, 2,3-diethyl-5-methylpyrazine, furfural, linalool, 5-hydroxymethylfurfural, 2-methoxy-3-methylpyrazine, 2,3,5,6-tetramethylpyrazine, 2-isobutyl-3-methoxypyrazine and 2-acetyl-3,5-dimethylpyrazine.

After the extraction, the fiber Divinylbenzene/Carboxen/Polydimethylsiloxane (film thickness of 50/30 μm, desorption temperature of 230–270 °C) (Sigma Aldrich, St. Louis, USA) was inserted immediately into the injection port of GC for thermal desorption for 10 min and transferred to an Innowax column (60 m × 0.32 mm × 0.25 μm) (Agilent, California, USA).

The chromatography condition was followed as described by Kalschne et al. (2018): flow rate of gas helium at 1.3 mL min^{-1} and injector temperature at 250 °C. The heating profile started at 40 °C (5 min), up to 60 °C at 4 °C min^{-1} and then maintained at 60°C for 5 min, and up to 250 °C at 8 °C min^{-1}, held at 250 °C for 3 min. The mass spectrometer operated at 280 °C interface temperature, ion source temperature of 230 °C, quadrupole temperature of 150 °C to scan a range m/z of 35–400 amu.

2.5 Coffee aroma release profile

The release profile of coffee aroma compounds from the microparticles incorporated in a coffee beverage matrix was monitored according to Zanin et al. (2019). 100 mL of water at 80 °C was added in 4.0 grams of coffee sample (90/10 w/w instant coffee and microparticles) and stirred during the first 10 s. The total time of analysis of the release of aroma compounds was 5 min. All samples were analyzed eight times.

The diluted sample was introduced in a commercial PTR-ToF-MS (Proton Transfer Reaction Time-of-flight Mass Spectrometry) 8000 instrument (Ionicon Analytik GmbH, Innsbruck, Austria) via a heated sampling line into the drift tube operated at 2.3 mbar, 90 °C and 600 V drift tube voltage, resulting in an E/N value (electric field strength/gas number

density) (E/N) value of 140 Townsend (Td, 1 Td = 10−17 cm^2/V.s). PTR-ToF-MS data were recorded by TOFDAQ v.183 data acquisition software (Tofwerk AG, Thun, Switzerland). Mass spectra were recorded in the mass-to-charge (m/z) range of 0–300 with one mass-spectrum recorded every 1 s. Mass axis calibration was performed on $[H_3{}^{18}O]^+$, $[H_2O{\bullet}H_3{}^{18}O]^+$, and $[C_3H_7O]^+$.

3. RESULTS AND DISCUSSION

3.1 CLASS OF SUBSTANCES

Forty one compounds were identified in roasted coffee oil non-encapsulated, which were grouped into their chemical classes (Table 2).

Table 2. Class of substances, odor description, sensorial effect of volatile compounds in crude roasted coffee oil non-encapsulated identified by HS-SPME-GC–MS.

Class	Substance	Odor description[1,2,3]	Sensorial effect[1,2,3]
Ketones	2,3-butanodione	Sweet, caramel	+[†]
	2,3-pentanodione	Sweet, caramel	+
	Acetoin	Sweet, caramel	+
	2,4-Dimethyl-3-pentanone	Fruity	+
Alcohols	Benzyl alcohol	Sweet, caramel	+
	Maltol	Sweet, caramel	+
	Furaneol	Sweet, caramel	+
	Phenylethyl alcohol	Smoked, phenolic	-[§]
Aldehydes	Benzaldehyde	Floral	+
	3-Methylbutanal	Fruity	+
	Acetaldehyde (ethanal)	Pungent, putrid	-
	Methional	Spicy, cooked, sulfur	-
	Vanillina	Vanila, sweet	+
Furans	Furfuryl acetate	Floral	+
	2-Furfurylthiol	Burned, toasted, cereal	+
	5-Methylfurfural	Burned, toasted, cereal	+
	Furfural	Vegetable, herbaceous	-
	5-Hydroxymethylfurfural	Chemical	-
Terpenes	Limonene	Floral	+
	Linalool	Vegetable, herbaceous	-
Pyrazines	2,5-Dimethylpyrazine	Nuts	+
	2,3-Dimethylpyrazine	Nuts	+
	2,6-Dimethylpyrazine	Burned, toasted, cereal	+

	2-Ethyl-3-methylpyrazine	Fruity, burned, toasted, cereal	+
	2,3,5-Trimethylpyrazine	Spicy, cooked, sulfur	-
	2,3-Diethyl-5-methylpyrazine	Spicy, cooked, sulfur	-
	2-Methoxy-3-methylpyrazine	Not available	Not available
	2,3,5,6-Tetramethylpyrazine	Not available	Not available
	2-Isobutyl-3-methylpyrazine	Not available	Not available
	2-Isobutyl-3-methoxypyrazine	Not available	Not available
	2-Acetyl-3,5-dimethylpyrazine	Sweet	+
	Pyrazine	Moldy, earth	-
Pyridines	Pyridine	Burned, toasted, cerel	+
	2-Acetylpyridine	Burned, toasted, cerel	+
Phenolics	4-Ethylguaiacol	Smoked, phenolic	-
	4-Vinylguaiacol	Smoked, phenolic	-
	Cis-isoeugenol	Smoked, phenolic	-
	Guaiacol	Chemical, etheral	-
Acids	Propanoic acid	Vegetable, herbaceous	-
	Isovaleric acid	Fermented, sour	-
	Acetic acid	Chemical, etheral	-

† Positive effect.
§ Negative effect.
[1] Kalschne et al., 2018.
[2] Bassoli, 2006.
[3] Flament, 2002.

Furans, pyrazines, alcohols, aldehydes, acids, pyridines, and others were the main chemical classes identified in coffee aroma (FLAMENT, 2002; BLANK, SEN, GROSCH, 1992; BUFFO; CARDELLI-FREIRE, 2004; SUNARHARUM et al., 2014) (Table 2). Among these aroma classes, furans and pyrazines compose the main classes of coffee aroma compounds. Furans are formed during the roasting process through degradation of carbohydrates, ascorbic acid or unsaturated fatty acids, and their sensorial effect includes floral, toasted and chemical flavors (AKIYAMA et al., 2007; CREWS; CASTLE, 2007). Pyrazines are well-known as Maillard reaction products and recognized as one of the key aromas of coffee with a low sensory threshold. This class is thought to be responsible for the nut, burned and sweet flavor of roasted coffee (BLANK; SEN; GROSCH, 1992; CZERNY; MAYER; GROSCH, 1999; SEMMELROCH; GROSCH, 1996).

Both alcohols and aldehydes presented on coffee aroma come from lipid oxidation, the alcohols identified are sensory described as positive sweet and caramel, and negative smoked and phenolic notes (MOREIRA, TRUGO, DE MARIA, 2000; FLAMENT, 2002; KALSCHNE et al., 2018). The length of the carbon chain of aldehydes determines their sensorial characteristics, i.e. short chain aldehydes have undesirable spicy, sulfur and pungent

flavors, and long chain aldehydes typically exhibit pleasant flavor of fruits and vanilla (FLAMENT, 2002; KALSCHNE et al., 2018).

Phenolic and pyridines arise from thermal degradation of chlorogenic acids under heat treatment, and from the Maillard reaction between an amino acid and sugar (MOON; SHIBAMOTO, 2009). All phenolic identified in this current work is recognized as presenting negative sensorial effect which has a smoked and chemical flavor (BICHO et al., 2011; BLANK; SEN; GROSCH, 1992; SEMMELROCH; GROSCH, 1996), and pyridines are responsible for roasted coffee flavor (burned, toasted and cereal notes) (FLAMENT, 2002; SHIBAMOTO, 2015).

Ketones are related with sugar degradation products and all ketones identified present positive sensorial effect (sweet, caramel and fruity) (AKIYAMA et al., 2007; BUFFO; CARDELLI-FREIRE, 2004; SHIBAMOTO, 2015). Propanoic, isovaleric and acetic acid exhibit unpleasant flavor of vegetable, fermented and chemical, and represent volatile acids that are formed during roasting by the degradation of glycerides (KALSCHNE et al., 2018; MOREIRA; TRUGO; DE MARIA, 2000).

The terpenic compounds, linalool, and limonene come from different ways. Linalool is produced through carotenoid degradation during the roasting and present vegetable negative effect. Another one, limonene, has a positive floral effect and formed by lipid degradation during roasting (MOREIRA; TRUGO; DE MARIA, 2000; SHIBAMOTO, 2015).

3.2 AROMA PROFILE

The percentage of the chemical classes in the roasted coffee oil, emulsion, and interior and surface of microparticles are shown in Table 3.

Table 3. Percentage of classes of substances characteristics of roasted coffee aroma.

Sample*	Component	Class of substance (% relative to all classes)								
		Ketones	Alcohol	Aldehydes	Furans	Terpenes	Pyrazines	Pyridines	Phenolics	Carboxylic acids
Roasted coffee oil non-encapsulated		0.6	4.2	6.5	63.0	0.1	3.6	2.5	6.5	13.1
1	Emulsion	1.2	0.1	5.9	83.1	0.0	2.5	0.1	5.8	1.4
	Interior†	0.0	0.5	98.6	1.6	0.0	0.0	0.0	0.0	0.0
	Surface	3.3	0.0	0.0	58.2	0.0	0.0	0.0	38.5	0.0
2	Emulsion	1.0	0.0	5.6	84.5	0.0	2.3	0.1	5.4	1.0
	Interior	0.0	0.0	53.8	24.6	0.0	0.0	0.0	0.0	21.9
	Surface	1.9	0.0	81.7	2.8	0.0	0.0	0.0	13.6	0.0
3	Emulsion	1.8	0.0	18.6	65.7	0.3	1.3	0.0	11.8	0.4
	Interior	0.0	0.0	57.7	4.4	0.0	0.0	0.0	0.0	38.1
	Surface	0.6	0.0	0.0	85.2	0.0	1.3	0.0	12.5	0.4
4	Emulsion	0.6	0.1	0.7	89.0	0.0	1.4	0.2	7.5	0.5
	Interior	0.0	1.0	90.1	0.9	0.0	0.0	0.0	0.0	8.3
	Surface	21.7	0.0	11.2	32.9	0.0	0.0	0.0	24.3	9.9
5	Emulsion	0.6	0.1	4.8	84.6	0.0	2.6	0.1	6.5	0.7
	Interior	0.0	0.0	89.6	0.0	0.0	0.0	0.0	0.0	11.1
	Surface	0.0	1.7	0.0	14.9	0.0	0.0	0.0	83.5	0.0
6	Emulsion	0.9	0.1	5.9	84.1	0.0	2.3	0.1	6.0	0.5
	Interior	0.0	0.0	86.9	0.0	0.0	0.0	0.0	0.0	14.3
	Surface	3.6	0.0	67.3	11.2	0.0	2.9	0.0	14.9	0.0
7	Emulsion	1.2	0.1	5.4	82.1	0.0	4.6	0.1	5.4	1.1
	Interior	0.0	0.0	46.7	32.2	0.0	0.0	0.0	0.0	21.7
	Surface	12.4	0.0	0.0	7.2	0.0	2.1	0.0	75.6	0.0

8	Emulsion	0.4	0.2	0.5	85.9	0.0	3.5	0.1	8.4	0.8
	Interior	0.0	0.1	87.8	0.7	0.0	0.0	0.0	0.0	11.8
	Surface	0.0	0.0	0.0	48.6	0.0	2.4	0.0	49.0	0.0
9	Emulsion	0.4	0.1	0.7	89.2	0.0	2.0	0.1	6.8	0.6
	Interior	0.0	0.7	33.7	39.5	0.0	0.1	0.1	0.8	25.2
	Surface	19.2	3.6	0.5	5.4	0.0	5.4	0.0	65.8	0.0
10	Emulsion	0.7	0.0	1.2	88.6	0.0	2.4	0.1	6.4	0.5
	Interior	0.0	0.4	41.1	26.6	0.0	0.0	0.1	0.0	32.3
	Surface	0.4	0.0	0.0	43.7	0.0	2.6	0.0	52.0	0.0

*Samples obtained at several combinations of temperature and ultrasound power for ultrasound-assisted emulsification of roasted coffee oil. Assay 1: 20°C/210 W; 2: 40°C/210W; 3: 20°C/560 W; 4: 40°C/560 W; 5: 15°C/385 W; 6: 45°C/385 W; 7: 30°C/140 W; 8: 30°C/630 W; 9 and 10: 30°C/385 W.

† Interior = total oil - surface oil.

The balance of aroma composition of non-encapsulated roasted coffee oil, in descending order of amount, was the following: furans (63.0%), carboxylic acids (13.1%), phenolics (6.5%), aldehydes (6.5%), alcohols (4.2%), pyrazines (3.6%), pyridines (2.5%), ketones (0.6%) and terpenes (0.1%) (Table 3). That result was used to compare the changes in coffee aroma profile during the emulsification and microencapsulation process.

3.2.1 Emulsion coffee aroma balance

Some changes could be noted on the coffee aroma composition balance when comparing roasted coffee oil non-encapsulated and emulsion (Table 3). Once the balance of each coffee aroma classes is calculated as relative percentage if the amount of some class is reduced the relative percentage of the others will increase. Furan class was the most representative fraction amount of coffee aroma due to its relative percentage (values above 80%) was increased probably by the losses of other compounds (BARANAUSKIENE et al., 2006). Phenolic compounds were present in a considerable amount as well as observed in the class of aldehydes, presenting great variability (118%) among all emulsion. Pyrazines group concentration was also representative ranging from 1 to 5%. On the other hand, the carboxylic acids content, corresponding to 13% in non-encapsulated roasted coffee oil, in the emulsion composed less than 2%. The other groups were present in minor quantities as detected in roasted coffee oil.

There was not a clear tendency of how ultrasound parameters studied (power and emulsion temperature) determined the change on the balance of aroma composition in the emulsion. Nevertheless, when high ultrasound power was applied, phenolic compounds were better retained while the retention of carboxylic acids and ketones were favorable at lower power.

There is evidence that high energy ultrasound-assisted emulsification affects the oil composition induced by cavitation that causes modification in oil by the formation of free radical species inducing lipid oxidation and consequently changing aroma composition. In addition, part of energy produced by the collapse of cavitation bubbles is dissipated as heat, as a result high volatility of aroma compounds might lead to a higher loss of aroma during ultrasound emulsification (CHEMAT et al., 2004; HALIM; THOO, 2018; HASHEMI; KHANEGHAH; AKBARIRAD, 2015; PINGRET; FABIANO-TIXIER; CHEMAT, 2013).

The efficiency in retaining core material during emulsification depends mainly on the ability of the matrix to form films at the interfaces between the emulsion phases (REINECCIUS, 2004). OSA-starch represents a good alternative to other wall material frequently applied to microencapsulation, once this modified starch presents good emulsifying and stabilizing properties, and it also displays a film-forming ability (SWEEDMAN et al., 2013; WANG, YUAN, YUE, 2015).

3.2.2 Microparticles coffee aroma balance

The encapsulation efficiency is one of the most important characteristics of the microencapsulation process; however it does not take into consideration the retention of volatiles that is quite important for a pleasant coffee aroma (BUFFO; CARDELLI-FREIRE, 2004; RÉ, 1998; REINECCIUS, 2004; SUNARHARUM; WILLIAMS; SMYTH, 2014).

Once the retention of volatile aroma compounds is complex and controlled by many factors, significant changes in the composition of coffee aroma in the interior of microparticles and emulsions were observed. Aldehydes (33.7% - 98.6%), furans (0.0% – 39.5%) and carboxylic acids (0.0% - 38.1%) (Table 3) were the best retained classes in the microparticles. Alcohols and pyridines were not detected or presented a very low percentage. Ketone, terpenes, phenolic, and pyrazine were totally lost during the spray-drying process or they were not detected by the method. Likewise, it could be detected an increasing of positive impact volatiles and also compounds presenting negative effect. This result did not indicate a reduction of coffee flavor quality, because, as verified by Kalschne et al. (2018), the balance of positive and negative effect compounds determines the global coffee flavor quality.

The relative percentage of volatile aroma on the particle surface is an important factor in microencapsulation since they are not protected by the wall, being susceptible to volatilization and lost during powder storage (BARANAUSKIENÉ et al., 2007). Furans, aldehydes and phenolic compounds were the main classes on the surface of microparticles, while terpenes and pyridines were not detected. The coffee aroma balance on the surface of microparticles presented higher variability among samples compared to emulsion and interior of microparticles.

The volatile and non-volatile coffee flavor composition comprises thousands of compounds with different physicochemical properties, for example, volatility and water solubility, that are directly related to their release (BUFFO; CARDELLI-FREIRE, 2004;

FREIBERGER et al., 2015; SUNARHARUM; WILLIAMS; SMYTH, 2014, ZANIN, 2019). Even though spray drying is the main technique for microencapsulation of aroma (REINECCIUS, 2004), volatile compounds may be lost during microencapsulation procedure due to the high air drying temperature (> 150 °C). In addition, water soluble compounds, for example, terpenes that were not detected either inside or on the surface of microparticles, might be lost during spray drying when they are solubilized into the water phase and then vaporized during drying (REINECCIUS, 2004; FREIBERGER et al., 2015).

It should be pointed out that the volatile aroma on the particle surface might be due to the diffusion mechanism, in which a substance is released from a matrix by permeation from its interior to the surrounding medium. Mainly two mechanisms control the rate of aroma diffusion from microparticles: physicochemical properties of compounds, such as vapor pressure, polarity and molecular weight; and resistance to mass transport through the polymer matrix determined by its properties such as thickness, particle size, shape and state (amorphous or glassy) also influence the volatile aroma diffusion (GOUBET et al., 1998; HUANG; BRAZEL, 2001; SAIFULLAH et al., 2019).

3.3 COFFEE AROMA RELEASE PROFILE

Since instant coffee products are rapidly consumed after their preparation, the flavor above the cup must be quickly released. This is important because the aroma is the first sensorial impression felt by consumers (YERETZIAN et al., 2004; KAUR et al., 2018). To study the effect of the addition of microparticles containing roasted coffee oil in two coffee beverages (soluble coffee and instant cappuccino) on the release profile of some aroma compounds, real time on-line analyze was applied. The time-intensity profiles of spray dried samples added in soluble coffee and instant cappuccino are presented in Figures 1 and 2, respectively.

Figure 1. Time intensity profile during 300 s of (A and B) two positive effect compounds and (C and D) two negative effect compounds from soluble coffee preparation containing microparticles. Samples 1 to 10 correspond to the experiments of Table 1.

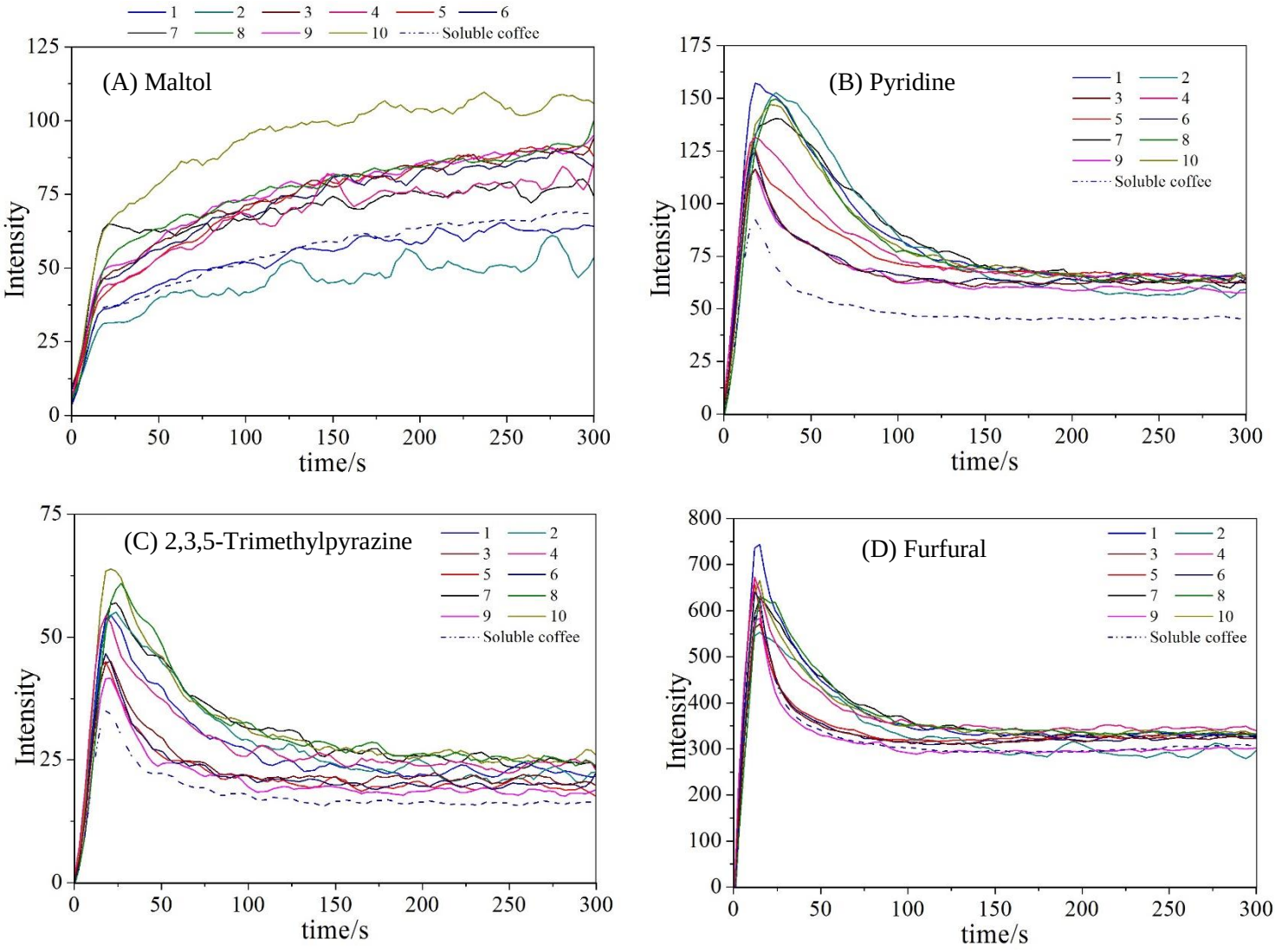

During coffee dissolution, the water comes into contact with the coffee brew containing microparticles, in which they are dissolved and the volatile compounds are released into the headspace (SARAGONI; AGUILERA; BOUCHON, 2007; UBBINK; KRÜGER, 2006). With the exception of maltol that presents lower volatility (vapor pressure at 25 °C: 0.4 x 10^{-4} kPa) and was released over the longest time with its intensity continuously increasing during the time, other compounds showed a rapid increase when water was added to product followed by a decrease in their release rate (Figure 1). This behavior is known as burst, in which

there is a fast release of volatile compounds at the beginning of microparticles dissolution and then, the intensity is reduced (FLORES; KONG, 2017; YE; KIM; PARK, 2010).

Figure 2. Time intensity profile during 300 s of (A and B) two positive effect compounds and (C and D) two negative effect compounds from instant cappuccino preparation containing microparticles. Samples 1 to 10 correspond to the experiments of Table 1.

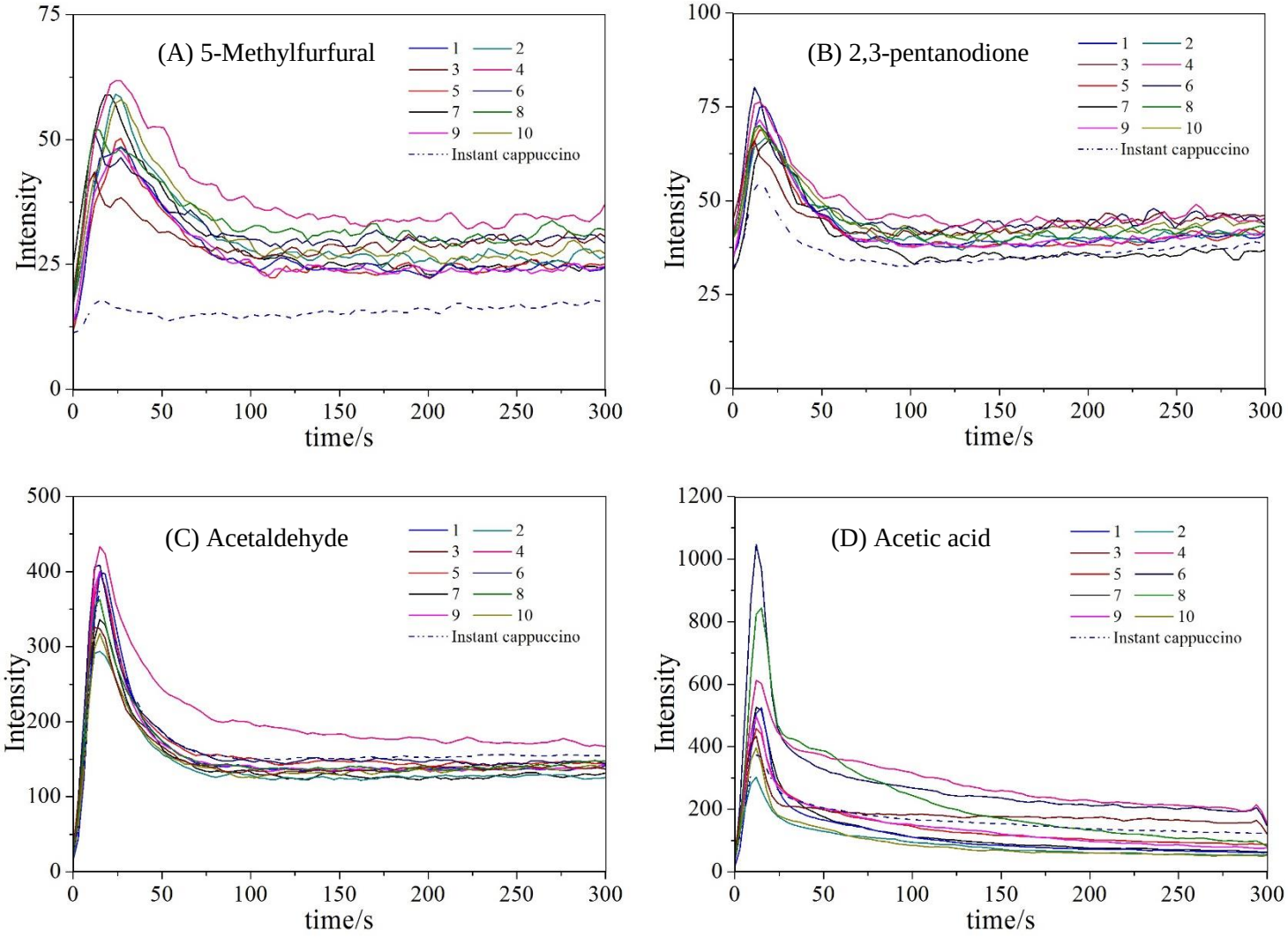

The addition of microparticles was relevant in improving coffee aroma since most of microparticles were favorable for aroma intensity comparing to only soluble coffee and instant cappuccino (Figure 1 and 2). It is worth to highlight that instant cappuccino is a multi-component product that, besides coffee, contains other components, consequently, less coffee aroma compounds. As a result, the addition of microparticles was even more efficient for enhancing coffee aroma. On the other hand for those microparticles that did not significantly increase coffee aroma intensity probably lost volatile aroma during processing because of the

temperatures used in spray drying microencapsulation or by diffusion mechanism, as previously discussed (FREIBERGER et al., 2015; REINECCIUS, 2004).

The release behavior of aroma compounds depends on their physicochemical properties, solubility, volatility or hydrophobicity. Therefore, the composition of coffee brew can affect the release profile of aroma compounds from microparticles. As stated before, instant cappuccino is composed by several ingredients, for instance, sugar, milk, fat and powder chocolate, which influences release profile by the interactions of ingredients and coffee aroma compounds (ZANIN et al., 2019).

Likewise, there was an increase in coffee aroma with positive sensory effect, the intensity of coffee aroma with a negative sensory effect was also increased (Figure 1 and 2). Even though both classes of compounds (positive and negative) were increased by the presence of microparticles, as previously discussed the sensorial acceptance of coffee aroma depends on the balance of volatile compounds (KALSCHNE et al., 2018; BUFFO; CARDELLI-FREIRE, 2004; SUNARHARUM; WILLIAMS; SMYTH, 2014).

4. CONCLUSIONS

Relevant changes could be identified on coffee aroma composition during ultrasound-assisted emulsification and spray drying microencapsulation process. The results showed about the changes on the balance of classes of aroma compounds in the roasted coffee oil non-encapsulated, emulsion and microparticles provided useful information to obtain more comprehensive explanations of how emulsification process and spray drying may affect the aroma composition during microencapsulation. The use of real-time online analysis was a powerful tool for a better understanding of the evolution of aroma release.

REFERENCES

ADAMIEC, J.; KALEMBA, D. Analysis of Microencapsulation Ability of Essential Oils during Spray Drying. **Drying Technology**, v. 24, n. 9, p. 1127–1132, 2006.

AKIYAMA, M.; MURAKAMI, K.; IKEDA, M.; IWATSUKI, K.; WADA, A.; TOKUNO, K.; ONISHI, M.; IWABUCHI, H. Analysis of the headspace volatiles of freshly brewed arabica coffee using solid-phase microextraction. **Journal of Food Science**, v. 72, n. 7, 2007.

BAKRY, A. M.; ABBAS, S.; ALI, B.; MAJEED, H.; ABOUELWAFA, M. Y.; MOUSA, A.; LIANG, L. Microencapsulation of Oils: A Comprehensive Review of Benefits, Techniques, and Applications. **Comprehensive Reviews in Food Science and Food Safety**, v. 15, n. 1, p.

143–182, 2016.

BARANAUSKIENE, R.; VENSKUTONIS, P. R.; DEWETTINCK, K.; VERHÉ, R. Properties of oregano (Origanum vulgare L.), citronella (Cymbopogon nardus G.) and marjoram (Majorana hortensis L.) flavors encapsulated into milk protein-based matrices. **Food Research International**, v. 39, n. 4, p. 413–425, 2006.

BARANAUSKIENÉ, R.; BYLAITÉ, E.; ZUKAUSKAITÉ, J.; VENSKUTONIS, R. Flavor retention of peppermint (*Mentha piperita L.*) essential oil spray-dried in modified starches during encapsulation and storage. **Journal of Agricultural and Food Chemistry**, v. 55, n. 8, p. 3027–3036, 2007.

BASSOLI, D. G. **Impacto Aromático Dos Componentes Voláteis Do Café Solúvel : Impacto Aromático Dos Componentes Voláteis Do Café Solúvel :** [s.l.] Universidade Estadual de Londrina, 2006.

BICHO, N. C.; LEITÃO, A. E.; RAMALHO, J. C.; LIDON, F. C. Identification of chemical clusters discriminators of the roast degree in Arabica and Robusta coffee beans. **European Food Research and Technology**, v. 233, p. 303–311, 2011.

BLANK, I.; SEN, A.; GROSCH, W. Potent odorants of the roasted powder and brew of Arabica coffee. **Zeitschrift für Lebensmittel-Untersuchung und -Forschung**, v. 195, n. 3, p. 239–245, 1992.

BRINGAS-LANTIGUA, M.; EXPÓSITO-MOLINA, I.; REINECCIUS, G. A.; LÓPEZ-HERNANDEZ, O.; PINO, J. A. Influence of Spray-Dryer Air Temperatures on Encapsulated Mandarin Oil. **Drying Technology**, v. 29, p. 520–526, 2011.

BRINGAS-LANTIGUA, M.; VALDÉS, D.; PINO, J. A. Influence of spray-dryer air temperatures on encapsulated lime essential oil. **International Journal of Food Science and Technology**, v. 47, n. 7, p. 1511–1517, 2012.

BUFFO, R. A.; CARDELLI-FREIRE, C. Coffee flavour: An overview. **Flavour and Fragrance Journal**, v. 19, n. 2, p. 99–104, 2004.

CALLIGARIS, S.; MUNARI, M.; ARRIGHETTI, G.; BARBA, L. Insights into the physicochemical properties of coffee oil. **European Journal of Lipid Science and Technology**, v. 111, n. 12, p. 1270–1277, 2009.

CHANDRAPALA, J.; OLIVER, C.; KENTISH, S.; ASHOKKUMAR, M. Ultrasonics in food processing. **Ultrasonics Sonochemistry**, v. 19, n. 5, p. 975–983, 2012.

CHEMAT, F.; ZILL-E-HUMA; KHAN, M. K. Applications of ultrasound in food technology: Processing, preservation and extraction. **Ultrasonics Sonochemistry**, v. 18, n. 4, p. 813–835, 2011.

CZERNY, M.; MAYER, F.; GROSCH, W. Sensory study on the character impact odorants of roasted Arabica coffee. **Journal of Agricultural and Food Chemistry**, v. 47, n. 2, p. 695–699, 1999.

FANG, S.; ZHAO, X.; LIU, Y.; LIANG, X.; YANG, Y. Fabricating multilayer emulsions by using OSA starch and chitosan suitable for spray drying: Application in the encapsulation of β-carotene. **Food Hydrocolloids**, v. 93, p. 102-110, 2019.

FERNANDES, R. V. B.; BORGES, S. V.; SILVA, E. K.; SILVA, Y. F.; SOUZA, H. J. B.; CARMO, E. L.; OLIVEIRA, C. R.; YOSHIDA, M. I.; BOTREL, D. A. Study of ultrasound-assisted emulsions on microencapsulation of ginger essential oil by spray drying. **Industrial Crops and Products**, v. 94, p. 413–423, 2016.

FLAMENT, I. From the raw bean to the roast coffee. In: FLAMENT, I. (Ed.). . **Coffee Flavour Chemistry**. Chichester: John Wiley & Sons, 2002. p. 37–52.

FLORES, F. P.; KONG, F. In Vitro Release Kinetics of Microencapsulated Materials and the Effect of the Food Matrix. **Annual Review of Food Science and Technology**, v. 8, p. 237–259, 2017.

FRASCARELI, E. C.; SILVA, V. M.; TONON, R. V.; HUBINGER, M. D. Effect of process conditions on the microencapsulation of coffee oil by spray drying. **Food and Bioproducts Processing**, v. 90, n. 3, p. 413–424, 2012.

FREIBERGER, E. B.; KAUFMANN, K. C.; BONA, E.; ARAÚJO, P. H. H.; SAYER, C.; LEIMANN, F. V.; GONÇALVES, O. H. Encapsulation of roasted coffee oil in biocompatible nanoparticles. **LWT - Food Science and Technology**, v. 64, n. 1, p. 381–389, 2015.

GOUBET, I.; LE QUERE, J.; VOILLEY, A. J. Retention of Aroma Compounds by Carbohydrates: Influence of Their Physicochemical Characteristics and of Their Physical State. A Review. **Journal of Agricultural and Food Chemistry**, v. 46, p. 1981–1990, 1998.

HUANG, X.; BRAZEL, C. S. On the importance and mechanism of burst release in matrix controlled drug delivery systems. **Journal of Controlled Release**, v. 73, p. 121–136, 2001.

HURTADO-BENAVIDES, A.; DORADO, D. A.; SÁNCHEZ-CAMARGO, A. D. P. Study of the fatty acid profile and the aroma composition of oil obtained from roasted Colombian coffee beans by supercritical fluid extraction. **Journal of Supercritical Fluids**, v. 113, p. 44–52, 2016.

JAFARI, S. M.; ASSADPOOR, E.; HE, Y.; BHANDARI, B. Encapsulation Efficiency of Food Flavours and Oils during Spray Drying. **Drying Technology**, v. 26, n. 7, p. 816–835, 2008.

KALSCHNE, D. L.; VIEGAS; M. C., DE CONTI; A. J., CORSO; M. P., BENASSI, M. T. Steam pressure treatment of defective Coffea canephora beans improves the volatile profile and sensory acceptance of roasted coffee blends. **Food Research International**, v. 105, 393–402, 2018.

KAUR, R.; KUKKAR, D.; BHARDWAJ, S. K.; KIM, K. H.; DEEP, A. Potential use of polymers and their complexes as media for storage and delivery of fragrances. **Journal of Controlled Release**, v. 285, p. 81–95, 2018.

LAOKULDILOK, N.; THAKEOW, P.; KOPERMSUB, P.; UTAMA-ANG, N. Optimisation

of microencapsulation of turmeric extract for masking flavour. **Food Chemistry**, v. 194, p. 695–704, 2015.

MCCLEMENTS, D. J. Emulsion formation. In: MCCLEMENTS, D. J. (Ed.). . **Food Emulsions: Principle, Practices, and Techniques**. [s.l.] CRC Press LLC, 2004. p. 233–267.

MOREIRA, R. F. A.; TRUGO, L. C.; DE MARIA, C. A. B. Componentes voláteis do café torrado. Parte II. Compostos alifáticos, alicíclicos e aromáticos. **Química Nova**, v. 23, n. 2, p. 195–203, 2000.

PINGRET, D.; FABIANO-TIXIER, A. S.; CHEMAT, F. Degradation during application of ultrasound in food processing: A review. **Food Control**, v. 31, n. 2, p. 593–606, 2013.

RÉ, M. Microencapsulation By Spray Drying. **Drying Technology**, v. 16, n. 6, p. 1195–1236, 1998.

REINECCIUS, G. A. The spray drying of food flavors. **Drying Technology**, v. 22, n. 6, p. 1289–1324, 2004.

RUÍZ-GARCÍA, Y.; PINO, J. A.; LAMI L.; MARTÍNEZ-PÉREZ, Y. Development and Validation of a Solid-Phase Microextraction Method for the Determination of Total Flavouring Content in Encapsulated Flavouring. **Food Analytical Methods**, v. 8, n. 9, p. 2228–2234, 2015.

SAIFULLAH, M.; SHISHIR, M. R. I.; FERDOWSI, R.; RAHMAN, M. R. T.; VUONG, Q. V. Micro and nano encapsulation, retention and controlled release of flavor and aroma compounds: A critical review. **Trends in Food Science and Technology**, v. 86, p. 230–251, 2019.

SARAGONI, P.; AGUILERA, J. M.; BOUCHON, P. Changes in particles of coffee powder and extensions to caking. **Food Chemistry**, v. 104, n. 1, p. 122–126, 2007.

SEMMELROCH, P.; GROSCH, W. Studies on character impact odorants of coffee brews. **Journal of Agricultural and Food Chemistry**, v. 44, n. 2, p. 537–543, 1996.

SHAO, P.; XUAN, S.; WU, W.; QU, L. Encapsulation efficiency and controlled release of Ganoderma lucidum polysaccharide microcapsules by spray drying using different combinations of wall materials. **International Journal of Biological Macromolecules**, v. 125, p. 962–969, 2019.

SHIBAMOTO, T. Volatile Chemicals from Thermal Degradation of Less Volatile Coffee Components. In: PREEDY, V. R. (Ed.). . **Coffee in Health and Disease Prevention**. London: Elsevier, 2015. p. 129–136.

SILVA, E. K.; GOMES, M. T. M. S.; HUBINGER, M. D.; CUNHA, R. L.; MEIRELES, M. A. A. Ultrasound-assisted formation of annatto seed oil emulsions stabilized by biopolymers. **Food Hydrocolloids**, v. 47, p. 1–13, 2015.

SILVA, E. K.; AZEVEDO, V. M.; CUNHA, R. L.; HUBINGER, M. D.; MEIRELES, M. A. A. Ultrasound-assisted encapsulation of annatto seed oil: Whey protein isolate versus

modified starch. **Food Hydrocolloids**, v. 56, p. 71–83, 2016.

SOOTTITANTAWAT, A.; BIGEARD, F.; YOSHII, H.; FURUTA, T.; OHKAWARA, M.; LINKO, P. Influence of emulsion and powder size on the stability of encapsulated D-limonene by spray drying. **Innovative Food Science and Emerging Technologies**, v. 6, n. 1, p. 107–114, 2005.

SUNARHARUM, W. B.; WILLIAMS, D. J.; SMYTH, H. E. Complexity of coffee flavor: A compositional and sensory perspective. **Food Research International**, v. 62, p. 315–325, 2014.

SWEEDMAN, M. C.; TIZZOTTI, M. J.; SCHÄFER, C.; GILBERT, R. G. Structure and physicochemical properties of octenyl succinic anhydride modified starches: A review. **Carbohydrate Polymers**, v. 92, n. 1, p. 905–920, 2013.

TIAN, H.; YANG, X.; HO, C. T.; HUANG, Q.; SONG, S. Development of a solid phase microextraction protocol for the GC-MS determination of volatile off-flavour compounds from citral degradation in oil-in-water emulsions. **Food Chemistry**, v. 141, n. 1, p. 131–138, 2013.

TONON, R. V; GROSSO, C. R. F.; HUBINGER, M. D. Influence of emulsion composition and inlet air temperature on the microencapsulation of flaxseed oil by spray drying. **Food Research International**, v. 44, n. 1, p. 282–289, 2011.

UBBINK, J.; KRÜGER, J. Physical approaches for the delivery of active ingredients in foods. **Trends in Food Science and Technology**, v. 17, n. 5, p. 244–254, 2006.

WANG, X.; YUAN, Y.; YUE, T. The application of starch-based ingredients in flavor encapsulation. **Starch/Staerke**, v. 67, n. 3–4, p. 225–236, 2015.

YE, M.; KIM, S.; PARK, K. Issues in long-term protein delivery using biodegradable microparticles. **Journal of Controlled Release**, v. 146, n. 2, p. 241–260, 2010.

YE, Q.; GEORGES, N.; SELOMULYA, C. Microencapsulation of active ingredients in functional foods: From research stage to commercial food products. **Trends in Food Science and Technology**, v. 78, p. 167–179, 2018.

YERETZIAN, C.; POLLIEN, P.; LINDINGER, C.; ALI, S. Individualization of Flavor Preferences: Toward a Consumer-centric and Individualized Aroma Science. **Comprehensive Reviews in Food Science and Food Safety**, v. 3, n. 4, p. 152-159, 2004.

CAPÍTULO 5 - IMPACT OF MICROPARTICLES OF ROASTED COFFEE OIL ON AROMA INTENSITY OF INSTANT COFFEE PRODUCTS BY PTR-ToF-MS

1. INTRODUCTION

Coffee is one of the most appreciated beverages worldwide and a major economic and social factor for producing and consuming countries alike. While coffee comes in many different formats and preparation modes, the most commercially significant product categories are roasted coffee – whole and ground, soluble coffee, single serve pods, capsules, liquid, ready to drink and coffee concentrate (ICO, 2018, CECAFE, 2019).

The main sensory characteristic of coffee is its aroma that comprises a large range of compounds formed during the roasting process (FLAMENT, 2002; BUFFO, CARDELLI-FREIRE, 2004; GLÖESS et al., 2014). Its composition depends on the cultivar, climate conditions and soil, post-harvest processing and also coffee extraction methods (BHUMIRATANA, ADHIKARI, & IV, 2011; LÓPEZ et al., 2016). Among these methods, coffee brews prepared from roasted and ground coffee (either bulk or single serve) are the most appreciated due to its flavor characteristics (SANZ et al., 2002; ZELLER et al., 2014).

On the other hand, from the perspective of convenience (easy to transport and prepare) instant coffee products, such as soluble coffee and instant cappuccino, represent a good practical offering. However, instant coffee products face the drawback that reconstituted coffee beverage lacks significantly on flavor and freshness characteristics, due to aromatic losses that occur during their processing transformations (FLAMENT, 2002; SANZ et al., 2002; ZELLER et al., 2014).

For this reason, researches have been conducting to figure out technologies for aroma recovery and aroma reconstitution in order to improve the flavor quality and promote soluble coffee based products (ZELLER et al., 2014; WESCHENFELDER et al., 2015). An example is the incorporation of recovered aroma into coffee oil and further addition to soluble coffee at the end of the drying process (DORDEVIC et al., 2014).

Roasted coffee oil is an important carrier of roasted coffee aroma that contains a significant amount of the compounds responsible for the pleasant aroma of roasted coffee, such as pyridines, pyrazines, furans, ketones, etc; therefore, it could be considered an interesting matrix for use as a flavouring ingredient (BUFFO et al., 2004; CALLIGARIS et al., 2009). Nevertheless, roasted coffee oil presents polyunsaturated fatty acids which makes it susceptible

to oxidative degradation. In addition, many of these aroma compounds present high volatility, being easily lost during storage (CALLIGARIS et al., 2009; HURTADO-BENAVIDES, DORADO, SÁNCHEZ-CAMARGO, 2016).

A promising technique used to protect the coffee oil against adverse storage conditions is the microencapsulation process (FRASCARELI et al., 2012; GETACHEW, CHUN, 2016; FREIBERGER et al., 2015). In this process, the core material is surrounded by a coating wall to form the microparticles, reducing its susceptibility for oxidation and formation of unpleasant tastes and odours, and interaction with other food ingredients (FRASCARELLI et al., 2012; DORDEVIC et al., 2014; SOBEL, VERSIC, GAONKAR, 2014; GETACHEW et al., 2016; FREIBERGER et al., 2015). In addition, the microencapsulation process can be used for controlled release of bioactive components such as essential oils, flavors, and antioxidants, and to avoid losses of aroma compounds by volatilization during storage (BAKRY et al., 2016).

The core material may be released from the microparticles by two main ways: it is gradually released to the medium, in which concentration of the core material increases during longer time; or there is a rapid release of core material into the medium with an initial large concentration, followed by a slow and gradual release. This last one, known as “burst effect”, is quite important for instant products once the flavor must be quickly released when the product is consumed (FLORES, KONG, 2017; HUANG, BRAZEL, 2001; KAUR et al., 2018).

A proper understanding of the aroma release mechanism from the microparticles is important to determine the release profile of aroma compounds and to monitor how volatile emission changes as a function of time. Knowledge of this behavior leads to a better comprehension of the aroma impact on food products and their acceptability (ELLIS, MAYHEW, 2014; TAYLOR, LINFORTH, 1998). For this reason, real-time and high-time resolution analytical techniques, p. ex. Proton Transfer Reaction Time-of-Flight Mass Spectrometry (PTR-ToF-MS) are valuable for processing information and to explore events that happen relatively rapidly, such as flavor release during instant coffee reconstitution (BIASIOLI et al., 2011; ELLIS, MAYHEW, 2014; SÁNCHEZ-LÓPEZ, ZIMMERMANN, YERETZIAN, 2014).

Given the importance of aroma for food acceptance, the lack of knowledge about the impact of microparticles of roasted coffee oil on instant coffee aroma, and the future implications this research could bring out, the aims of this study are the evaluation of the effect of roasted coffee oil microencapsulated into the soluble coffee and instant cappuccino on

increasing coffee aroma intensity and the release profile of aroma compounds by PTR-ToF-MS during brew preparation.

2. MATERIAL AND METHODS

2.1 MATERIAL

Roasted coffee oil obtained from Coffea arabica, soluble coffee, and instant cappuccino were kindly supplied by Café Iguaçu (Cornélio Procópio, Paraná, Brazil). Capsul® starch, (modified food starch derived from waxy maize) (OSA-starch), was provided by Ingredion (São Paulo, São Paulo, Brazil).

2.2 SPRAY-DRYING MICROCAPSULES

Prior to the microencapsulation process, emulsions containing 27% of modified starch (w/w) and 10%, 20% and 30% (w/w) of roasted coffee oil in relation to total solids (oil + modified starch) were prepared. The OSA-starch was dissolved in deionized water (Millipore®) by mixing overnight at room temperature.

The roasted coffee oil was added into wall solution and first, a pre-emulsion was prepared by homogenization at 3000 RPM for 90 s in a rotor-stator type homogenizer (TE-102, Tecnal, Brazil). The emulsion was then obtained by sonication (sonicator Q700, QSONICA, USA), using an ultrasonic probe with a diameter of 12.7 mm, 20 kHz and nominal power of 385 W for 5 min (SILVA et al., 2015). The temperature was kept constant (30 °C) by a thermostatically-controlled water bath (TE-2005, Tecnal, Brazil) coupled to a double jacket. For the temperature control, the device was set for a 20 s active sonication interval followed by a 3 s pause (NAZARZADEH, SAJJADI, 2013).

The emulsion was immediately spray-dried in a laboratory spray-dryer (LabPlant SD 05, Huddersfield, England) equipped with chamber of 500 mm × 215 mm and double fluid atomizer nozzle with a 0.7 mm diameter orifice. Prior to drying, the dryer was fed with distilled water, until thermal equilibrium and steady-state conditions were reached. During spray drying, the emulsion was maintained under magnetic agitation and fed into the main chamber through a peristaltic pump under the following conditions: air flow rate of 73 $m^3\ h^{-1}$, air pressure of 4 bar, compressed air flow rate of 1.1 $m^3\ h^{-1}$, feed flow rate of 6 mL min^{-1}, inlet

temperature of 180 ± 4 °C (FRASCARELI et al., 2012), and outlet air temperature of 100 ± 5 °C.

2.3 COFFEE PREPARATION

Prior to the coffee beverage preparation, the microparticles were added to the soluble coffee (SC) and instant cappuccino (IC) in a proportion of 10% (w/w) (CHAHAN YERETZIAN, personal communication, July 1, 2017).

The brew preparation followed the same procedure described by Zanin et al. (2018). 100 mL of water was added in 4.0 grams of sample. During the first 10 s the samples were stirred to simulate the real preparation form. The total time of analysis of the release of aroma compounds was 5 min. The SC and IC samples without microparticles addition were analyzed 12 times and each sample of SC and IC containing 10, 20 or 30% of oil microencapsulated (SC-10, SC-20, SC-30, IC-10, IC-20, IC-30) were analyzed six times.

2.4 PTR-TOF-MS

A commercial PTR-ToF-MS 8000 instrument (Ionicon Analytik GmbH, Innsbruck, Austria) was used for all measurements. The diluted sample was introduced via a heated sampling line into the drift tube operated at 2.3 mbar, 90 °C and 600 V drift tube voltage, resulting in an E/N value (electric field strength/gas number density) of 140 Townsend (Td, 1 Td = 10−17 cm^2/V.s). PTR-ToF-MS data were recorded by TOFDAQ v.183 data acquisition software (Tofwerk AG, Thun, Switzerland). Mass spectra were recorded in the mass-to-charge (m/z) range of 0–300 with one mass-spectrum recorded every 1 s. Mass axis calibration was performed on $[H_3{}^{18}O]^+$, $[H_2O{\bullet}H_3{}^{18}O]^+$, and $[C_3H_7O]^+$.

2.5 STATISTICAL ANALYSIS

A completely randomized design was used and the results were submitted to analysis of variance (ANOVA), for the evaluation of the effect of the addition of the microcapsules in the two products, and one-way Tukey's test ($p \leq 0.10$) by using the software Statistica 10 (Statsoft, Tulsa, USA).

3. RESULTS AND DISCUSSIONS

The instant coffee products, soluble coffee and instant cappuccino, with and without microparticles were analyzed by PTR-ToF-MS (Table 1 and 2). Although it was detected 176 product ions (m/z) in soluble coffee and 88 m/z in instant cappuccino, we focused on the compounds that present coffee aroma impact and based on their time-intensity over time (FLAMENT, 2002; KALSCHNE et al., 2018; LÓPEZ et al., 2016; ROMANO et al., 2014).

The PTR-ToF-MS signal is proportional to the measured concentration (LINDINGER, HANSEL, JORDAN, 1998), it was possible to obtain a value proportional to the total amount of the compound on the headspace by integrating the whole area under of the curve of time intensity profiles. Once there is no previous studies regarding that approach, four parameters were obtained from the peaks to enable the comparison among the samples: (i) area under the curve (AUC) that corresponds to the intensity of compound on the headspace and it was calculated by integrating the total area of time intensity curve (0 - 300 s); (ii) area under the curve of the burst (AUC burst): it was calculated by integrating the area under the curve from the beginning of beverage preparation until the time when the intensity decreases and reach the plateau; (iii) maximum intensity: maximum intensity reached on the headspace and (iv) final intensity: average headspace intensity in the last 5 s of the analyze, respectively.

These parameters were determined since they characterize time-independent (AUC, maximum intensity and final intensity) and time-dependent (AUC burst) behaviors and might give information regarding the interaction between product and consumers by showing the temporal dominance of each compound during coffee preparation.

Table 1. Selected headspace mass peaks and corresponding parameters in soluble coffee with and without microcapsules of roasted coffee oil. Means and standard deviations are reported for each sample.

m/z Measured	*m/z* Theoretical	Sum formula	Tentative identification Sensorial effect (+/-)	Parameter	Sample			
					SC	SC-10 †	SC-20 ‡	SC-30 §
61.028	61.028	$C_2H_5O_2^+$	(-) Acetic acid	*AUC* *	222195.2 ± 36493.7^a	211515.8 ± 36255.8^a	213524.5 ± 37415.8^a	183903.2 ± 10187.7^a
				AUC Burst **	43832.3 ± 6914.3^a	52976.5 ± 18013.1^a	50761.5 ± 18042.9^a	51168.0 ± 15772.1^a
				Maximum Intensity	3946.4 ± 746.1^a	4478.8 ± 1380.6^a	4708.0 ± 852.5^a	3946.9 ± 937.1^a
				Final Intensity	2088.7 ± 326.7^a	1708.8 ± 129.8^b	1783.0 ± 214.1^{ab}	1643.6 ± 13.2^b
73.064	73.065	$C_4H_9O^+$	(-) Butanone	*AUC*	30773.4 ± 2774.6^a	25835.3 ± 3133.2^b	29940.4 ± 2568.5^{ab}	28238.2 ± 3171.6^{ab}
				AUC Burst	12138.6 ± 1922.7^a	10203.6 ± 1330.4^a	11457.3 ± 2189.5^a	11061.4 ± 1650.9^a
				Maximum Intensity	1535.3 ± 348.6^a	1149.5 ± 231.2^b	1361.2 ± 297.0^{ab}	1298.0 ± 209.4^{ab}
				Final Intensity	220.4 ± 16.4^a	184.1 ± 16.2^b	204.0 ± 4.8^{ab}	195.3 ± 14.7^b
75.044	75.044	$C_3H_7O_2^+$	(-) Methylacetate	*AUC*	38235.7 ± 6411.7^a	34216.1 ± 5224.9^a	36562.6 ± 4766.8^a	34221.0 ± 2721.3^a
				AUC Burst	7834.7 ± 1289.6^a	8776.2 ± 2646.6^a	8756.1 ± 2908.1^a	9232.5 ± 2541.0^a
				Maximum Intensity	758.8 ± 153.9^a	917.1 ± 360.3^a	848.8 ± 176.7^a	765.9 ± 181.0^a
				Final Intensity	357.6 ± 54.1^a	284.4 ± 26.3^b	317.0 ± 24.4^{ab}	304.8 ± 3.2^b
80.049	80.049	$C_5H_6N^+$	(+) Pyridine	*AUC*	5219.8 ± 288.4^a	6871.9 ± 536.5^b	10209.1 ± 393.4^c	13096.4 ± 696.7^d
				AUC Burst	1118.4 ± 146.1^a	1467.0 ± 294.2^b	2326.4 ± 209.0^c	3507.0 ± 441.9^d
				Maximum Intensity	101.2 ± 17.7^a	108.6 ± 19.2^a	192.7 ± 33.2^b	241.5 ± 29.5^c
				Final Intensity	45.7 ± 4.4^a	60.7 ± 5.0^b	84.6 ± 1.7^c	101.2 ± 3.0^d
83.048	83.049	$C_5H_7O^+$	(+) Methylfuran	*AUC*	6561.4 ± 361.3^a	6059.9 ± 673.9^a	8100.0 ± 317.5^b	8432.9 ± 722.3^b
				AUC Burst	3018.5 ± 447.4^a	2718.4 ± 339.2^a	3876.9 ± 466.2^b	4167.5 ± 526.5^b
				Maximum Intensity	420.6 ± 114.3^{ab}	328.0 ± 80.8^a	529.7 ± 91.7^{bc}	541.7 ± 84.7^c
				Final Intensity	41.0 ± 4.8^a	41.0 ± 2.3^a	45.5 ± 4.7^{ab}	49.6 ± 2.0^b
87.043	87.044	$C_4H_7O_2^+$	(+) Butanedione	*AUC*	35605.3 ± 5185.0^a	32843.0 ± 6114.8^a	35392.0 ± 3725.4^a	33100.7 ± 2188.2^a
				AUC Burst	8649.7 ± 684.2^a	7895.7 ± 1776.1^a	8787.9 ± 2149.8^a	8338.1 ± 1121.5^a
				Maximum Intensity	792.1 ± 167.0^a	757.6 ± 203.9^a	827.5 ± 101.8^a	790.9 ± 190.3^a
				Final Intensity	338.0 ± 34.9^a	274.9 ± 25.3^b	314.9 ± 18.8^{ab}	292.6 ± 2.3^b

87.079	87.080	$C_5H_{11}O^+$	(+) Methylbutanal	*AUC*	14082.4 ± 1067.1^{a}	11004.0 ± 2493.1^{b}	13814.0 ± 1426.0^{a}	13305.4 ± 1946.3^{ab}
				AUC Burst	5865.5 ± 1151.0^{a}	4828.7 ± 777.2^{a}	5901.4 ± 1196.8^{a}	5789.5 ± 992.0^{a}
				Maximum Intensity	779.1 ± 198.2^{a}	569.0 ± 158.4^{b}	722.1 ± 160.3^{ab}	706.9 ± 128.7^{ab}
				Final Intensity	89.9 ± 10.7^{a}	70.8 ± 17.6^{b}	84.7 ± 4.0^{ab}	85.8 ± 12.9^{ab}
97.026	97.028	$C_5H_5O_2^+$	(-) Furfural	*AUC*	31826.0 ± 4480.7^{a}	32516.4 ± 2222.7^{a}	35534.4 ± 1331.3^{b}	34754.2 ± 1159.4^{ab}
				AUC Burst	6973.8 ± 919.6^{a}	6684.4 ± 1255.6^{a}	7351.4 ± 741.2^{a}	7574.9 ± 621.4^{a}
				Maximum Intensity	657.6 ± 104.1^{ab}	545.4 ± 77.3^{a}	714.7 ± 140.3^{b}	610.0 ± 90.2^{ab}
				Final Intensity	312.5 ± 34.9^{a}	300.8 ± 35.3^{a}	348.9 ± 16.5^{b}	335.7 ± 7.8^{ab}
99.042	99.044	$C_5H_7O_2^+$	(+) 2-furanmethanol	*AUC*	8017.1 ± 1509.3^{a}	7708.2 ± 929.6^{a}	8786.8 ± 763.9^{a}	8771.3 ± 549.7^{a}
				AUC Burst	1677.2 ± 316.6^{a}	1682.1 ± 348.6^{ab}	1880.2 ± 369.9^{ab}	1998.4 ± 291.0^{b}
				Maximum Intensity	143.6 ± 31.2^{a}	148.9 ± 40.8^{a}	179.3 ± 46.1^{a}	158.3 ± 31.1^{a}
				Final Intensity	77.9 ± 16.6^{a}	73.1 ± 3.0^{a}	79.2 ± 7.6^{a}	78.7 ± 4.4^{a}
101.058	101.060	$C_5H_9O_2^+$	(+) Pentanedione	*AUC*	7129.5 ± 891.4^{a}	7284.0 ± 493.5^{ab}	8529.2 ± 838.7^{b}	8264.0 ± 218.6^{b}
				AUC Burst	1676.0 ± 100.7^{a}	1632.0 ± 189.7^{a}	1936.9 ± 165.0^{b}	2048.4 ± 125.6^{b}
				Maximum Intensity	141.8 ± 10.0^{ab}	131.7 ± 22.8^{a}	164.4 ± 17.5^{bc}	165.4 ± 16.8^{c}
				Final Intensity	70.3 ± 7.9^{a}	72.9 ± 5.5^{ab}	80.3 ± 7.5^{b}	78.1 ± 6.2^{ab}
107.047	107.049	$C_7H_7O^+$	(+) Benzaldehyde	*AUC*	1184.5 ± 88.7^{a}	1090.4 ± 60.5^{a}	1287.8 ± 99.1^{b}	1343.3 ± 54.9^{b}
				AUC Burst	221.0 ± 27.2^{a}	200.4 ± 23.0^{b}	244.4 ± 20.3^{ac}	277.2 ± 9.1^{c}
				Maximum Intensity	19.5 ± 2.5^{ab}	18.1 ± 2.4^{a}	21.0 ± 2.8^{ab}	21.9 ± 1.8^{b}
				Final Intensity	11.9 ± 1.1^{a}	9.7 ± 1.0^{b}	12.8 ± 1.6^{a}	12.3 ± 1.2^{a}
109.070	109.076	$C_6H_9N_2^+$	(+) Dimethylpyrazine	*AUC*	5425.4 ± 578.8^{a}	5657.3 ± 610.1^{a}	7020.4 ± 319.5^{b}	7817.1 ± 326.2^{c}
				AUC Burst	1181.6 ± 74.7^{a}	1237.0 ± 200.5^{a}	1635.5 ± 146.6^{b}	2013.2 ± 110.3^{c}
				Maximum Intensity	105.4 ± 13.3^{a}	104.9 ± 10.9^{a}	153.1 ± 23.4^{b}	171.9 ± 10.2^{b}
				Final Intensity	54.6 ± 5.8^{a}	54.8 ± 7.5^{a}	62.7 ± 2.0^{b}	64.1 ± 1.8^{b}
111.042	111.044	$C_6H_7O_2^+$	(+) Methylfurfural	*AUC*	8884.0 ± 601.5^{a}	8869.3 ± 873.0^{a}	10417.3 ± 1251.2^{b}	11378.3 ± 508.1^{b}
				AUC Burst	1856.4 ± 115.4^{a}	1800.5 ± 319.8^{a}	2081.5 ± 106.8^{a}	2559.5 ± 253.1^{b}
				Maximum Intensity	163.3 ± 12.5^{ac}	131.7 ± 18.1^{b}	180.7 ± 20.7^{cd}	188.3 ± 20.7^{d}
				Final Intensity	80.0 ± 15.2^{a}	86.6 ± 6.4^{a}	104.7 ± 8.7^{b}	105.4 ± 7.1^{b}
123.089	123.092	$C_7H_{11}N_2^+$	(-) Trimethylpyrazine	*AUC*	1813.3 ± 247.4^{a}	1949.3 ± 274.3^{a}	2706.2 ± 404.3^{b}	3558.6 ± 610.2^{c}

			AUC Burst	408.0 ± 61.2^{a}	475.0 ± 101.3^{a}	653.9 ± 82.7^{b}	921.3 ± 220.5^{c}
			Maximum Intensity	39.8 ± 7.6^{a}	43.8 ± 6.0^{a}	64.0 ± 13.6^{b}	77.3 ± 16.6^{b}
			Final Intensity	15.4 ± 2.5^{a}	18.5 ± 4.8^{ab}	22.5 ± 5.8^{bc}	26.3 ± 3.6^{c}
125.056	125.060	$C_7H_9O_2^+$	(-) Guaiacol	*AUC*	5236.8 ± 626.4^{a}	4853.0 ± 693.7^{a}	6194.4 ± 507.1^{b}	6577.2 ± 252.6^{b}
				AUC Burst	991.6 ± 182.7^{a}	971.0 ± 213.3^{a}	1176.4 ± 138.2^{ab}	1359.2 ± 101.2^{b}
				Maximum Intensity	82.8 ± 17.7^{ab}	71.8 ± 12.4^{a}	101.2 ± 20.0^{b}	99.5 ± 9.6^{b}
				Final Intensity	49.3 ± 7.6^{a}	49.4 ± 2.2^{a}	61.1 ± 7.2^{b}	59.8 ± 2.9^{b}
127.036	127.039	$C_6H_7O_3^+$	(+) Maltol	*AUC*	5541.3 ± 2334.9^{a}	7863.3 ± 578.3^{b}	6377.6 ± 1073.3^{ab}	7139.9 ± 1353.5^{ab}
				Final Intensity	68.2 ± 29.4^{a}	94.6 ± 12.7^{a}	78.9 ± 11.6^{a}	83.6 ± 17.1^{a}
141.061	141.055	$C_7H_9O_3^+$	(+) Furfurylacetate	*AUC*	400.5 ± 104.5^{a}	537.3 ± 130.0^{ab}	712.8 ± 160.0^{b}	987.8 ± 133.6^{c}
				AUC Burst	73.0 ± 13.7^{a}	146.3 ± 39.8^{b}	165.0 ± 45.0^{b}	259.2 ± 51.8^{c}
				Maximum Intensity	8.7 ± 2.8^{a}	13.2 ± 3.9^{b}	16.1 ± 4.37^{b}	22.3 ± 2.6^{c}
				Final Intensity	3.3 ± 1.5^{a}	4.3 ± 1.0^{ab}	5.8 ± 1.3^{bc}	6.8 ± 2.4^{c}

Superscript annotations are used to display differences between coffees (Tukey's HSD, $p < 0.10$).
SC: Soluble coffee.
† SC-10: Soluble coffee + microparticles with 10% (w/w) of roasted coffee oil in relation to total solids (oil + OSA-starch).
‡ SC-20: Soluble coffee + microparticles with 20% (w/w) of roasted coffee oil in relation to total solids (oil + OSA-starch).
§ SC-30: Soluble coffee + microparticles with 30% (w/w) of roasted coffee oil in relation to total solids (oil + OSA-starch).
* AUC: Area under the curve.
** AUC burst: Area under the curve of the burst.

Table 2. Selected headspace mass peaks and corresponding parameters in instant cappuccino with and without spray drying microcapsules of roasted coffee oil. Means and standard deviations are reported for each sample.

m/z Measured	*m/z* Theoretical	Sum formula	Tentative identification Sensorial effect (+/-)	Parameter	Sample			
					IC	IC-10 †	IC-20 ‡	IC-30 §
45.034	45.033	$C_2H_5O^+$	(-) Acetaldehyde	*AUC* *	17007.0 ± 3756.0^{ab}	15781.3 ± 1570.8^{a}	21210.4 ± 2379.4^{b}	19878.3 ± 1008.1^{b}
				AUC Burst **	3077.5 ± 647.8^{a}	3411.9 ± 456.7^{ab}	4089.6 ± 435.4^{b}	4238.8 ± 416.4^{b}
				Maximum Intensity	391.3 ± 100.4^{a}	411.5 ± 92.8^{ab}	453.0 ± 65.0^{ab}	538.6 ± 102.3^{b}
				Final Intensity	155.2 ± 33.7^{a}	143.1 ± 12.9^{a}	125.3 ± 5.4^{a}	162.0 ± 4.6^{a}
61.028	61.028	$C_2H_5O_2^+$	(-) Acetic acid	*AUC*	14747.8 ± 7846.4^{a}	13092.4 ± 2625.0^{a}	17518.8 ± 1932.8^{a}	16162.0 ± 3780.1^{a}
				AUC Burst	2843.0 ± 1464.3^{a}	3783.7 ± 843.2^{a}	5037.7 ± 600.1^{ab}	5912.4 ± 1777.6^{b}
				Maximum Intensity	300.8 ± 106.0^{a}	559.3 ± 223.2^{ab}	412.0 ± 117.0^{a}	913.0 ± 471.8^{b}
				Final Intensity	110.2 ± 50.5^{a}	77.3 ± 16.9^{a}	65.8 ± 14.4^{a}	80.6 ± 8.4^{a}
69.033	69.033	$C_4H_5O^+$	Furan	*AUC*	1214.4 ± 379.4^{a}	1665.8 ± 162.9^{a}	2596.1 ± 111.9^{b}	3645.0 ± 608.1^{c}
				AUC Burst	203.8 ± 57.7^{a}	351.6 ± 43.4^{a}	731.3 ± 43.3^{b}	929.6 ± 294.4^{b}
				Maximum Intensity	27.6 ± 8.9^{a}	40.2 ± 6.7^{a}	62.2 ± 2.1^{b}	102.1 ± 21.5^{c}
				Final Intensity	12.6 ± 4.3^{a}	13.4 ± 1.8^{a}	11.9 ± 1.5^{a}	22.2 ± 2.5^{b}
73.064	73.065	$C_4H_9O^+$	(-) Butanone	*AUC*	4204.7 ± 818.6^{a}	5112.9 ± 249.6^{b}	6519.7 ± 233.0^{c}	7783.8 ± 792.4^{d}
				AUC Burst	1095.7 ± 146.5^{a}	1605.3 ± 129.7^{b}	2470.8 ± 121.0^{c}	2558.7 ± 355.2^{c}
				Maximum Intensity	139.5 ± 28.1^{a}	196.9 ± 41.8^{b}	221.5 ± 16.2^{b}	332.2 ± 77.5^{c}
				Final Intensity	35.2 ± 8.7^{a}	34.3 ± 3.1^{a}	34.5 ± 2.6^{a}	46.5 ± 1.2^{b}
87.043	87.044	$C_4H_7O_2^+$	(+) Butanedione	*AUC*	65363.7 ± 9352.9^{a}	61247.6 ± 1641.0^{a}	66839.9 ± 4004.7^{a}	63253.8 ± 3473.1^{a}
				AUC Burst	15655.3 ± 601.7^{a}	15388.9 ± 789.9^{a}	19550.3 ± 767.9^{b}	14280.5 ± 1767.3^{a}
				Maximum Intensity	2090.6 ± 499.2^{a}	1922.2 ± 215.4^{a}	1871.9 ± 197.2^{a}	1897.9 ± 422.7^{a}
				Final Intensity	541.4 ± 74.5^{a}	485.7 ± 28.8^{a}	523.7 ± 20.2^{a}	516.2 ± 13.3^{a}
89.058	89.06	$C_4H_9O_2^+$	Methylpropanoate	*AUC*	2075.7 ± 322.0^{a}	2240.5 ± 240.0^{ab}	2362.9 ± 206.8^{ab}	2562.5 ± 252.5^{b}
				AUC Burst	425.7 ± 64.4^{a}	531.5 ± 44.1^{b}	542.0 ± 82.9^{abc}	655.5 ± 105.4^{c}
				Maximum Intensity	58.8 ± 11.5^{a}	82.6 ± 17.6^{ab}	58.7 ± 11.5^{a}	99.2 ± 35.6^{b}
				Final Intensity	16.4 ± 2.7^{a}	17.0 ± 3.5^{ab}	16.6 ± 0.5^{ab}	20.5 ± 0.4^{b}

97.027	97.028	$C_5H_5O_2^+$	(-) Furfural	*AUC*	3501.9 ± 1419.4[a]	7378.4 ± 289.4[b]	10196.2 ± 398.0[c]	11190.9 ± 1982.4[c]
				AUC Burst	435.2 ± 185.2[a]	1604.9 ± 485.4[b]	2650.5 ± 237.7[c]	2561.4 ± 897.0[c]
				Maximum Intensity	47.3 ± 18.1[a]	151.9 ± 8.6[b]	207.8 ± 16.8[c]	288.1 ± 68.4[c]
				Final Intensity	35.5 ± 15.6[a]	61.2 ± 3.9[b]	60.8 ± 3.1[b]	75.8 ± 9.2[b]
97.059	97.065	$C_6H_9O^+$	(-) Dimethylfuran	*AUC*	696.6 ± 287.1[a]	1253.6 ± 307.1[b]	1800.6 ± 57.7[b]	2555.7 ± 452.6[c]
				AUC Burst	95.2 ± 47.0[a]	277.9 ± 67.2[b]	238.1 ± 22.2[b]	613.0 ± 107.2[c]
				Maximum Intensity	11.2 ± 4.4[a]	34.2 ± 7.5[b]	51.4 ± 1.5[c]	79.3 ± 15.5[d]
				Final Intensity	6.2 ± 3.4[a]	8.4 ± 2.0[a]	10.0 ± 2.0[a]	15.4 ± 3.0[b]
83.049	83.049	$C_5H_7O^+$	(+) Methylfuran	*AUC*	1445.4 ± 199.9[a]	2142.2 ± 70.3[b]	3885.7 ± 171.3[c]	4935.9 ± 319.8[d]
				AUC Burst	220.1 ± 35.0[a]	589.6 ± 52.7[b]	1578.7 ± 97.0[c]	1735.0 ± 237.1[c]
				Maximum Intensity	21.6 ± 3.1[a]	70.9 ± 9.2[b]	151.8 ± 12.4[c]	236.3 ± 41.9[d]
				Final Intensity	15.0 ± 2.7[a]	18.2 ± 1.2[a]	15.0 ± 2.2[a]	26.1 ± 3.2[b]
101.058	101.06	$C_5H_9O_2^+$	(+) Pentanedione	*AUC*	3713.6 ± 436.3[a]	4278.6 ± 283.7[b]	5601.1 ± 253.3[c]	5812.7 ± 269.1[c]
				AUC Burst	580.9 ± 72.2[a]	763.3 ± 60.6[b]	630.2 ± 37.1[ab]	1223.0 ± 165.1[c]
				Maximum Intensity	57.5 ± 8.6[a]	74.8 ± 9.4[b]	104.2 ± 3.8[c]	135.7 ± 16.4[d]
				Final Intensity	39.3 ± 4.8[a]	42.9 ± 4.7[a]	37.0 ± 3.2[a]	50.5 ± 4.7[b]
111.041	111.044	$C_6H_7O_2^+$	(+) Methylfurfural	*AUC*	1535.4 ± 172.5[a]	2756.1 ± 509.5[b]	4588.2 ± 153.3[c]	6437.7 ± 547.9[d]
				AUC Burst	200.4 ± 24.8[a]	491.9 ± 145.5[b]	794.1 ± 58.4[c]	1378.7 ± 305.0[d]
				Maximum Intensity	22.4 ± 3.0[a]	45.7 ± 4.7[b]	85.6 ± 5.7[c]	173.1 ± 34.0[d]
				Final Intensity	16.6 ± 3.5[a]	24.9 ± 2.9[b]	24.1 ± 1.3[b]	44.0 ± 3.4[c]
111.078	111.080	$C_7H_{11}O^+$	(+) 2,3-Dimethyl-2-cyclopenten-1-one	*AUC*	348.5 ± 136.4[a]	660.3 ± 82.4[b]	1202.8 ± 51.3[c]	2166.5 ± 297.5[d]
				AUC Burst	46.1 ± 16.4[a]	141.4 ± 42.9[b]	253.4 ± 33.5[c]	463.8 ± 90.8[d]
				Maximum Intensity	6.6 ± 2.1[a]	15.2 ± 1.6[b]	30.2 ± 2.8[c]	59.3 ± 10.0[d]
				Final Intensity	4.0 ± 1.8[a]	6.0 ± 1.6[a]	5.4 ± 2.0[a]	13.6 ± 1.7[b]

Superscript annotations are used to display differences between coffees (Tukey's HSD, $p < 0.10$).
IC: instant cappuccino.
† IC-10: Instant cappuccino + microparticles with 10% (w/w) of roasted coffee oil in relation to total solids (oil + OSA-starch).
‡ IC-20: Instant cappuccino + microparticles with 20% (w/w) of roasted coffee oil in relation to total solids (oil + OSA-starch).
§ IC-30: Instant cappuccino + microparticles with 30% (w/w) of roasted coffee oil in relation to total solids (oil + OSA-starch).
* AUC: Area under the curve.
** AUC burst: Area under the curve of the burst.

The aroma compounds delivered to the headspace have a range of different physicochemical properties and consequently different release profiles are expected for each compound based on their properties. Such differences can be seen in Figure 1 for the six compounds selected in both products as example. While the concentration of maltol (Figure 1A) gradually increased during the 300 s of analysis, butanone, guaiacol, methylacetate (Figure 1A), furfural and acetic acid (Figure 1B) showed a rapid release on the first seconds of extraction, followed by a decreasing on release rate. This differential delivery rate may be due to the dissolution kinetics being attributed to solubility (water solubility and log K_{ow}) and volatility (vapor pressure and Henry's Law constant - HLC) of these compounds (CHARLES et al., 2015; ROBERTS et al., 2003; ROBERTS; POLLIEN; WATZKE, 2003).

Figure 1. Normalized intensity of selected compounds of (A) SC-30 and (B) IC-30 during the 300 seconds of analysis.

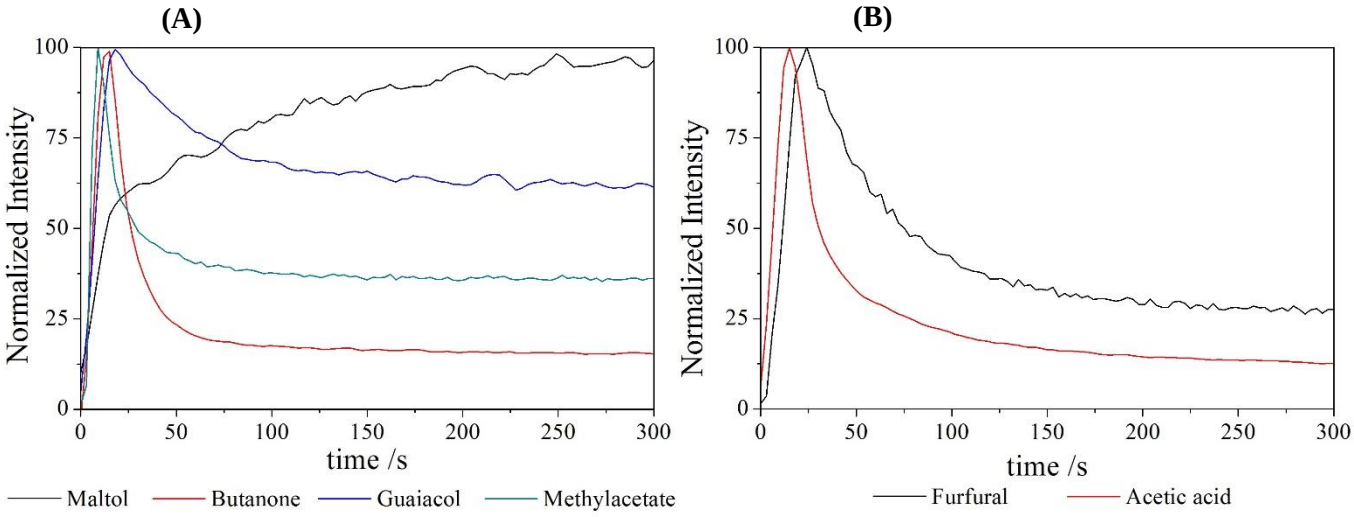

The partial vapor pressure considerably affected compound release during the preparation of soluble coffee. Maltol (Figure 1A) which presents very low vapor pressure (0.4×10^{-4} kPa (LÓPEZ et al., 2016)) was direct released upon water addition being later released on the headspace. On the other hand, volatile and poorly soluble compounds, such as butanone and methylacetate, presented a higher tendency to the gas phase, being extracted rapidly upon sample reconstitution (Figure 1A).

In addition to volatility, water solubility also affected aroma release from instant cappuccino. Once cappuccino is rich in fat milk, less polar compounds, for instance, furfural, whose water solubility is 77 g L^{-1}, was later delivered due to its partial dissolution in fat. On

the other hand, the release of compounds that have higher water solubility was favored, for example acetic acid (Figure 1B) (LÓPEZ et al., 2016; ROBERTS; POLLIEN; WATZKE, 2003).

In both products all aroma compounds reached maximum intensity after 24 s of extraction, although most of them were released in less than 18 s. Such different intensity rates provide information on how the compounds are extracted: a fast decrease implies that the compound is extracted quickly, while a slow decrease implies that the extraction lasted longer (SÁNCHEZ-LÓPEZ et al., 2014; YU et al., 2012). Upon sample reconstitution, the solubilization of instant coffee and hydration of the microparticles will depress the Tg and moves the matrix from a rigid glassy state to a softened rubbery state, leading to a rapid increase in diffusion of flavor compounds out of the food matrix releasing of the aroma into the headspace (UBBINK, KRÜGGER, 2006; SARAGONI, AGUILERA, BOUCHON, 2007).

3.1 AREA UNDER THE CURVE

The area under the curve (AUC) is proportional to the average concentration of flavor released (NORMAND, AVISON, PARKER, 2004) (Figure 2). Therefore, it represents an important parameter to describe the aroma intensity on headspace, from the preparation of brew until its consumption.

The addition of SC-10 in soluble coffee did not significantly increased AUC of most of the selected compounds (Table 1), probably because the concentration of oil in the microparticle was not enough to promote any difference in this parameter. However, the addition of SC-20 and SC-30 to soluble coffee increased the AUC for pyridine, methylfuran, furfural, pentanedione, benzaldehyde, dimethylpyrazine, methylfurfural, trimethylpyrazine, guaiacol, and furfurylacetate (Table 1). The other compounds could be present in low concentration in the oil or lost during the spray drying process by evaporation or thermal degradation (FREIBERGER et al., 2015). It is important to note that even though this increasing in aroma intensity also occurs with compounds of negative sensory effect, once as suggested by Kalschne et al. (2018) the balanced profile of negative and positive impact compounds is important for global sensory acceptance.

The addition of microparticles loaded with 30% of roasted coffee oil did not mean higher coffee aroma intensity, once the AUC of the sample SC-30 was only higher than SC-20 AUC for pyridine (responsible for a positive tosted flavor impact), dimethylpyrazine

(nutty flavor, positive impact) and trimethylpyrazine (sulfurous flavor, negative impact) (Table 1) (FLAMENT, 2002; KALSCHNE et al., 2018), due to the limiting amount of core material to produce microparticles. Above this limiting amount, encapsulation efficiency decreases, increasing the concentration of unprotected oil on the surface of the microparticles (JAFARI et al., 2008; REINECCIUS, YAN, 2016).

Figure 2. Upper graphs are presented the integrated intensity over time for (A) pyridine and (B) dimethylpyrazine for the four samples of soluble coffee analyzed (soluble coffee, SC-10, SC-20, SC-30 (Soluble coffee + microparticles with 10%, 20% and 30% (w/w), respectively, of roasted coffee oil in relation to total solids (oil + OSA-starch)). The two figures below are presented the integrated intensity over time for (C) methylfurfural and (D) butanone for the four samples of the instant cappuccino analyzed (instant cappuccino, IC-10, IC-20, IC-30 (Instant cappuccino + microparticles with 10%, 20% and 30% (w/w), respectively, of roasted coffee oil in relation to total solids (oil + OSA-starch)).

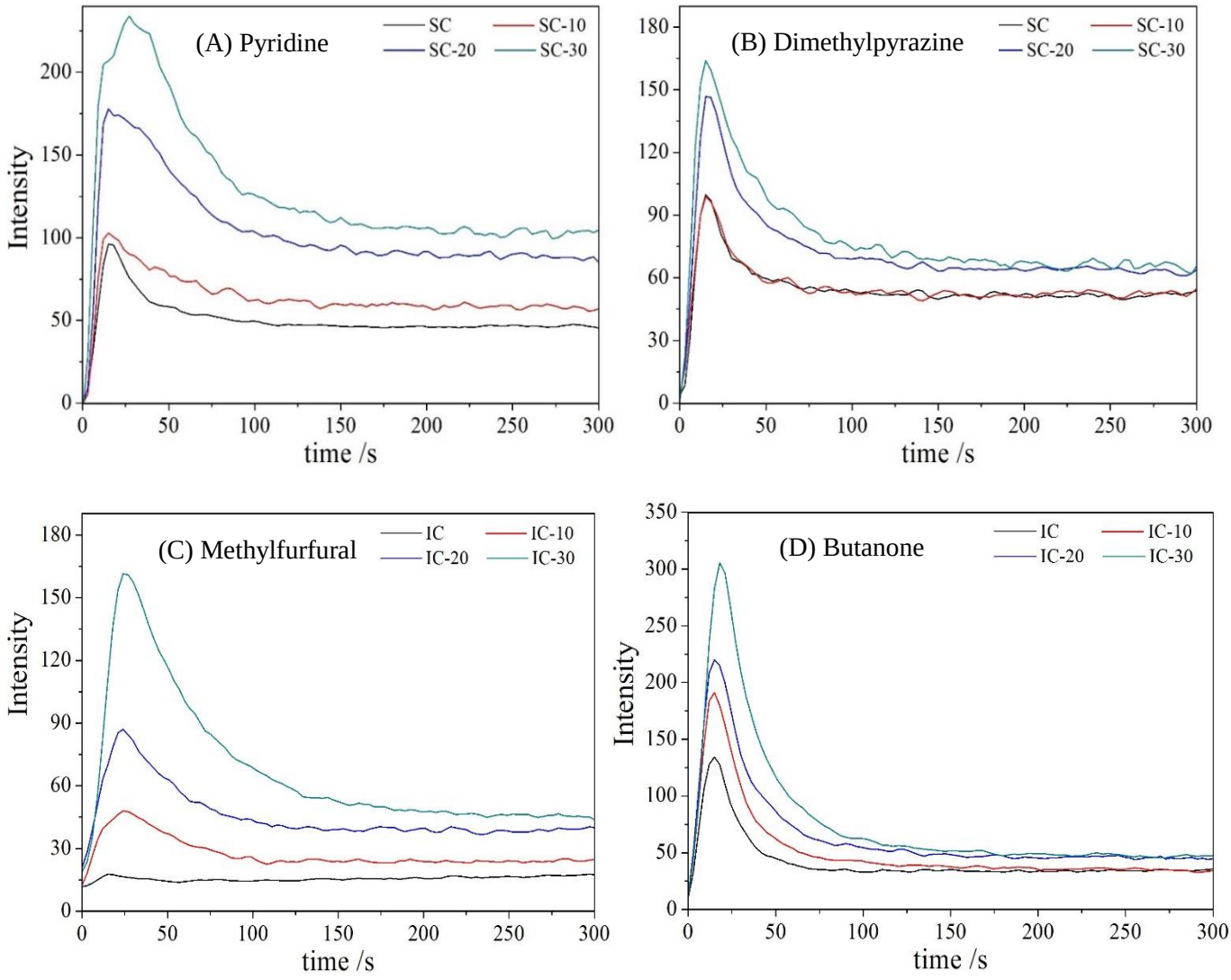

In contrast, for instant cappuccino that present other ingredients in its composition, such as sugar, milk, powder chocolate, and consequently less coffee fraction, the addition of all microparticles increased the AUC of pentanedione and methylfurfural, compounds that conferred positive sensory effect; and butanone, furfural, methylfuran, and 2,3-dimethyl-2-cyclopenten-1-one, compounds responsible for negative sensory impact (Figure 2C and 2D and Table 2).

The intensity of acetic acid and butanedione were not affected by microparticles, due to their high volatility and water solubility; in other words, they could have migrated to the water phase and been lost by evaporation during the encapsulation process (REINECCIUS et al., 2016; LÓPEZ et al., 2016; SANDER, 2015).

3.2 BURST EFFECT

Analyzing Figure 3, it is possible to observe a sudden increase on the intensity of compounds within a short time known as "burst effect", in which there is an instantaneous release of aroma compounds trapped in the sample structure upon sample reconstitution. Such phenomenon happens in a very short time compared to the entire release process (FLORES, KONG, 2017; YE, KIM, PARK, 2010). Upon contact with water and agitation, since OSA-starch is soluble in cold water and dissolution process is accelerated in hot water, the wall material dissolves and the core (roasted coffee oil) is burst-released into the medium (FLORES, KONG, 2017). This is an important parameter for instant and fast consumption products, because of the rapid increase in aroma intensity at the moment may improve the acceptability of the product (HUANG, BRAZEL, 2001).

The presence of microparticles with higher loads of oil in soluble coffee (SC-20 and SC-30) significantly increased the AUC burst for the most compounds monitored (Figure 3A and 3B).

The ratio "AUC burst/AUC" indicates the amount of aroma release during the first period of sample reconstitution. However, that ratio was similar in all samples of SC, showing that the addition of the microparticles increased the AUC of burst with no changes on the release profile. It is interesting to highlight that for most compounds the AUC burst accounted for about 23% of AUC, however, for butanone, methylfuran, and methylbutanal, the AUC burst represented 39%, 47% and 43%, respectively of total AUC (Figure 3A and 3B, and Table 1) that might be related to the fact that they are more volatile than the other compounds

and therefore quickly released to the headspace (FLORES, KONG, 2017; ROBERTS et al., 2003).

Figure 3. Upper graphs: Burst-effect profile of (A) trimethylpyrazine and (B) methylfuran during 150 seconds of analysis in soluble coffee. SC-10, SC-20, SC-30: Soluble coffee + microparticles with 10%, 20% and 30% (w/w), respectively, of roasted coffee oil in relation to total solids (oil + OSA-starch). Graphs below: Burst effect profile of (C) methylfurfural and (D) dimethylfuran during the first 150 seconds of analysis in instant cappuccino. IC-10, IC-20, IC-30: Instant cappuccino + microparticles with 10%, 20% and 30% (w/w), respectively, of roasted coffee oil in relation to total solids (oil + OSA-starch).

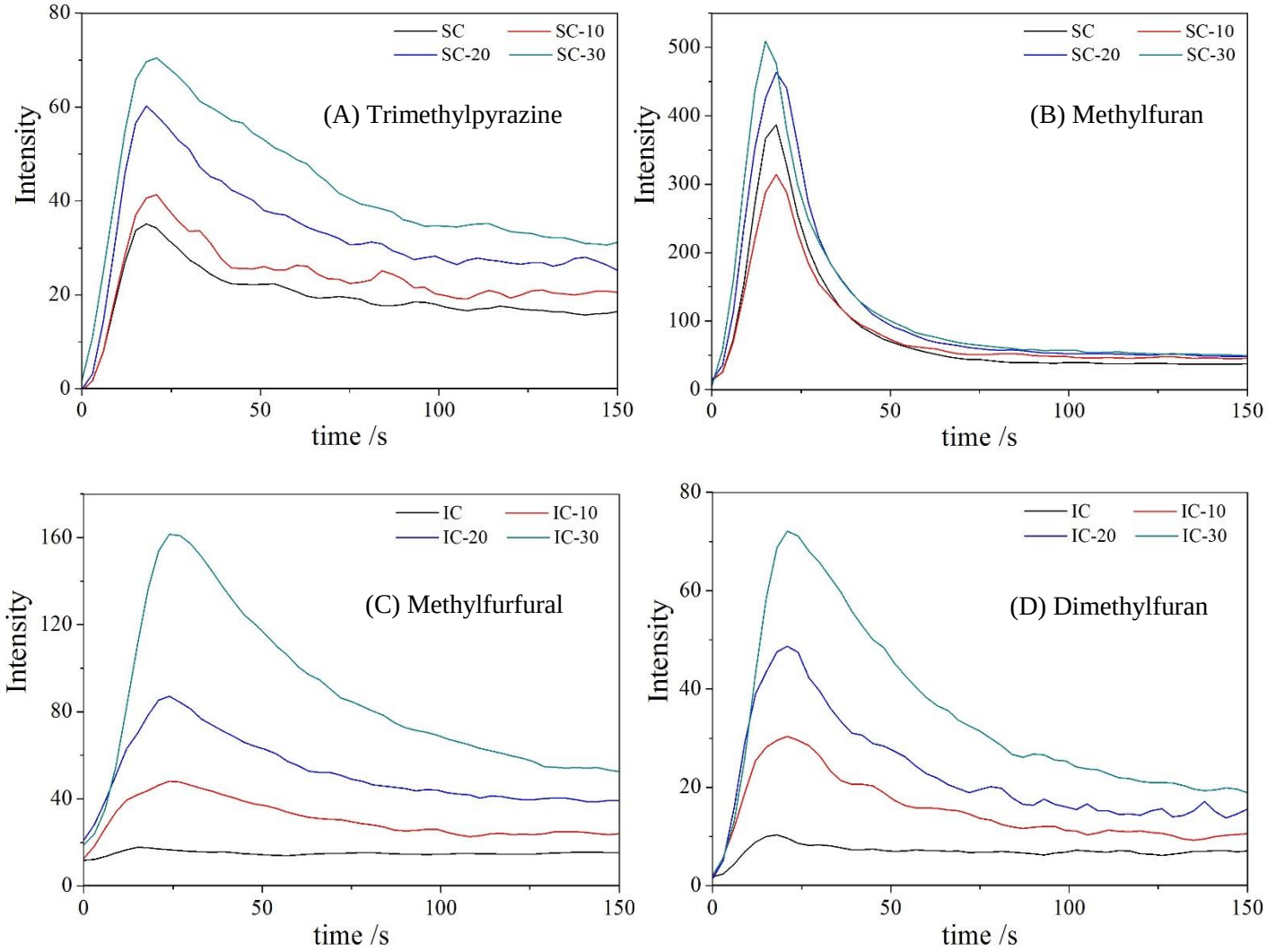

Similarly to the results for soluble coffee, the addition of microparticles of coffee oil in the instant cappuccino had a positive effect on AUC burst, once it was significantly increased for most compounds compared to the sample without microparticles (Figure 3C and 3D).

The presence of fat milk in cappuccino composition has a strong influence on aroma release once partially dissolve less polar compounds and retard their release, reducing the burst effect. Methylfurfural (Figure 3C) and dimethylfuran (Figure 3D) since present lower polarity were more retained in the brew and released over slightly longer times (MESTDAGH et al, 2014; ROBERTS et al., 2003, ROBERTS; POLLIEN; WATZKE, 2003).

3.3 MAXIMUM INTENSITY AND FINAL INTENSITY

Maximum intensity is related to the maximum concentration reached in the headspace. In general, the addition of microparticles with higher loads of roasted coffee oil to the soluble coffee increased the aroma intensity with the exception of acetic acid, methylacetate and butanedione (Table 1). As stated before these compounds could have been lost during the microencapsulation process by spray drying due their have high volatility (LÓPEZ et al., 2016; SANDER, 2015; REINECCIUS, 2004). The addition of SC-10 did not significantly increase this parameter in soluble coffee, due to the smaller amount of oil present in the microparticles. On the other hand, in a multicomponent matrix as instant cappuccino in which the quantity of coffee is lower, the presence of all microparticles (IC-10, IC-20 or IC-30) increased this parameter for all compounds in relation to the instant cappuccino without microparticles (Table 2).

The intensity at the end of the analysis (final intensity) was determined in order to verify if the addition of microparticles prolonged the higher intensity of aroma in the products by a considerable time (CHARLES et al., 2015). However, the release occurs within the first few seconds of preparation of the beverage and does not show a clear significant difference at the end of the preparation (Table 1 and 2). Since both samples are instant products, therefore quickly prepared and consumed, it is expected that aroma is released at the time of preparation. Even though, for the two products studied with the addition of microparticles at higher oil content (30%), the final intensity was significantly higher than the other samples (Table 1 and 2).

4. CONCLUSIONS

This study proposed the addition of spray dried microparticles of roasted coffee oil in instant coffee products and the use of PTR-ToF-MS in order to better understanding the

evolution of flavor release during brew preparation. The coffee aroma intensity in soluble coffee and instant cappuccino was increased by adding microparticles of roasted coffee oil but did not affect the release profile. In general, higher loads of roasted coffee oil in microparticles provide higher intensities of coffee aroma in soluble coffee while in instant cappuccino even the lowest concentration of roasted coffee oil (10%) was enough in promoting coffee aroma improvement. These results open new perspectives for the development of instant coffee products with higher coffee aroma intensity. Further experimentation is needed to determine the relationship between aroma release and sensory response.

REFERENCES

BAKRY, A. M.; ABBAS, S.; ALI, B.; MAJEED, H.; ABOUELWAFA, M. Y.; MOUSA, A.; LIANG, L. Microencapsulation of Oils: A Comprehensive Review of Benefits, Techniques, and Applications. **Comprehensive Reviews in Food Science and Food Safety**, v. 15, n. 1, p. 143–182, 2016.

BHUMIRATANA, N.; ADHIKARI, K.; IV, E. C. Evolution of sensory aroma attributes from coffee beans to brewed coffee. **LWT - Food Science and Technology**, v. 44, p. 2185–2192, 2011.

BIASIOLI, F.; GASPERI, F.; YERETZIAN, C.; MÄRK, T. D. PTR-MS monitoring of VOCs and BVOCs in food science and technology. **TrAC - Trends in Analytical Chemistry**, v. 30, p. 968–977, 2011.

BUFFO, R. A.; CARDELLI-FREIRE, C. Coffee flavour: An overview. **Flavour and Fragrance Journal**, v. 19, n. 2, p. 99–104, 2004.

CALLIGARIS, S.; MUNARI, M.; ARRIGHETTI, G.; BARBA, L. Insights into the physicochemical properties of coffee oil. **European Journal of Lipid Science and Technology**, v. 111, n. 12, p. 1270–1277, 2009.

CARRAPISO, A. I. Effect of fat content on flavour release from sausages. **Food Chemistry**, v. 103, p. 396–403, 2007.

CHARLES, M.; ROMANO, A.; YENER, S.; BARNABÀ, M.; NAVARINI, L.; MÄRK, T. D., BIASIOLI, F.; GASPERI, F. Understanding flavour perception of espresso coffee by the combination of a dynamic sensory method and in-vivo nosespace analysis. **Food Research International**, v. 69, p. 9–20. 2015.

DORDEVIC, V.; BALANC, B.; BELSCAK-CVITANOVIC, A.; LECIV, S.; TRIFKOVIC, K.; KALUSEVIC, A.; KOSTIC, I.; KOMES, D.; BUGARSKI, B.; NEDOVIC, V. Trends in Encapsulation Technologies for Delivery of Food Bioactive Compounds. **Food Engineering Reviews**, v. 7, n. 4, p. 452–490, 2014.

ELLIS, A. M.; MAYHEW, C. A. PTR-MS in the Food Sciences. In: **Proton Transfer**

Reaction Mass Spectrometry. Principles and Applications. [s.l: s.n.]. p. 221–265.

FLAMENT, I. From the raw bean to the roast coffee. In: FLAMENT, I. (Ed.). . **Coffee Flavour Chemistry**. Chichester: John Wiley & Sons, 2002. p. 37–52a.

FLAMENT, I. The individuals consituents: structure, nomenclature, origin, chemical and organoleptics properties. In: FLAMENT, I. (Ed.). . **Coffee Flavour Chemistry**. Chichester: John Wiley & Sons, 2002. p. 81–396b.

FLORES, F. P.; KONG, F. In Vitro Release Kinetics of Microencapsulated Materials and the Effect of the Food Matrix. **Annual Review of Food Science and Technology**, v. 8, p. 237–259, 2017.

FRASCARELI, E. C.; SILVA, V. M.; TONON, R. V.; HUBINGER, M. D. Effect of process conditions on the microencapsulation of coffee oil by spray drying. **Food and Bioproducts Processing**, v. 90, n. 3, p. 413–424, 2012.

FREIBERGER, E. B.; KAUFMANN, K. C.; BONA, E.; ARAÚJO, P. H. H.; SAYER, C.; LEIMANN, F. V.; GONÇALVES, O. H. Encapsulation of roasted coffee oil in biocompatible nanoparticles. **LWT - Food Science and Technology**, v. 64, n. 1, p. 381–389, 2015.

GETACHEW, A. T.; CHUN, B. S. Optimization of coffee oil flavor encapsulation using response surface methodology. **LWT - Food Science and Technology**, v. 70, p. 126–134, 2016.

GLÖESS, A. N.; VIETRI, A.; WIELAND, F.; SMRKE, S.; SCHÖNBÄCHLER, B.; LÓPEZ, J. A. S.; PETROZZI, S.; BONGERS, S.; KOZIOROWSKI, T.; YERETZIAN, C. Evidence of different flavour formation dynamics by roasting coffee from different origins: On-line analysis with PTR-ToF-MS. **International Journal of Mass Spectrometry**, v. 365–366, p. 324–337, 2014.

GROSCH, W. Flavour of coffee. A review. **Food/Nahrung**, v. 42, p. 344–350, 1998.
HUANG, X.; BRAZEL, C. S. On the importance and mechanism of burst release in matrix controlled drug delivery systems. **Journal of Controlled Release**, v. 73, p. 121–136, 2001.

HURTADO-BENAVIDES, A.; DORADO, D. A.; SÁNCHEZ-CAMARGO, A. D. P. Study of the fatty acid profile and the aroma composition of oil obtained from roasted Colombian coffee beans by supercritical fluid extraction. **Journal of Supercritical Fluids**, v. 113, p. 44–52, 2016.

JAFARI, S. M.; ASSADPOOR, E.; HE, Y.; BHANDARI, B. Encapsulation Efficiency of Food Flavours and Oils during Spray Drying. **Drying Technology**, v. 26, n. 7, p. 816–835, 2008.

KALSCHNE, D. L.; VIEGAS; M. C., DE CONTI; A. J., CORSO; M. P., BENASSI, M. T. Steam pressure treatment of defective Coffea canephora beans improves the volatile profile and sensory acceptance of roasted coffee blends. **Food Research International**, v. 105, 393–402, 2018.

KAUR, R.; KUKKAR, D.; BHARDWAJ, S. K.; KIM, K. H.; DEEP, A. Potential use of

polymers and their complexes as media for storage and delivery of fragrances. **Journal of Controlled Release**, v. 285, p. 81–95, 2018.

LINDINGER, W.; HANSEL, A.; JORDAN, A. On-line monitoring of volatile organic compounds at pptv levels by means of proton-transfer-reaction mass spectrometry (PTR-MS) medical applications, food control and environmental research. **International Journal of Mass Spectrometry and Ion Processes**, v. 173, n. 3, p. 191–241, 1998.

LÓPEZ, J. A. S.; WELLINGER, M.; GLOESS, A. N.; ZIMMERMANN, R.; YERETZIAN, C. Extraction kinetics of coffee aroma compounds using a semi-automatic machine: On-line analysis by PTR-ToF-MS. **International Journal of Mass Spectrometry**, v. 401, p. 22–30, 2016.

MESTDAGH, F.; DAVIDEK, T.; CHAUMONTEUIL, M.; FOLMER, B.; BLANK, I. The kinetics of coffee aroma extraction. **Food Research International**, v. 63, p. 271–274, 2014.

NAZARZADEH, E.; SAJJADI, S. Thermal effects in nanoemulsification by ultrasound. **Industrial and Engineering Chemistry Research**, v. 52, p. 9683–9689, 2013.

NORMAND, V.; AVISON, S.; PARKER, A. Modeling the kinetics of flavour release during drinking. **Chemical Senses**, v. 29, p. 235–245, 2004.

REINECCIUS, G. A. The spray drying of food flavors. **Drying Technology**, v. 22, n. 6, p. 1289–1324, 2004.

REINECCIUS, G. A.; YAN, C. Factors controlling the deterioration of spray dried flavourings and unsaturated lipids. **Flavour and Fragrance Journal**, v. 31, p 5–21, 2016.

ROBERTS, D. D.; POLLIEN, P.; ANTILLE, N.; LINDINGER, C.; YERETZIAN, C. Comparison of Nosespace , Headspace , and Sensory Intensity Ratings for the Evaluation of Flavor Absorption by Fat. **Journal of Agricultural and Food Chemistry**, v. 51, p. 3636–3642, 2003.

ROBERTS, D. D.; POLLIEN, P.; WATZKE, B. Experimental and Modeling Studies Showing the Effect of Lipid Type and Level on Flavor Release from Milk-Based Liquid Emulsions. **Journal of Agricultural and Food Chemistry**, v. 51, 189–195, 2003.

ROMANO, A.; CAPPELLIN, L.; TING, V.; APREA, E.; NAVARINI, L.; GASPERI, F.; BIASIOLI, F. Nosespace analysis by PTR-ToF-MS for the characterization of food and tasters : The case study of coffee. **International Journal of Mass Spectrometry**, v. 365–366, p. 20–27, 2014.

SÁNCHEZ-LÓPEZ, J. A.; ZIMMERMANN, R.; YERETZIAN, C. Insight into the time-resolved extraction of aroma compounds during espresso coffee preparation: Online monitoring by PTR-ToF-MS. **Analytical Chemistry**, v. 86, n. 23, p. 11696–11704, 2014.

SANDER, R. Compilation of Henry's law constants (version 4.0) for water as solvent. **Atmospheric Chemistry and Physics**, v. 15, n. 8, p. 4399–4981, 2015.

SANZ, C.; CZERNY, M.; CID, C.; SCHIEBERLE, P. Comparison of potent odorants in a

filtered coffee brew and in an instant coffee beverage by aroma extract dilution analysis (AEDA). **European Food Research and Technology**, v. 214, n. 4, p. 299–302, 2002.

SARAGONI, P.; AGUILERA, J. M.; BOUCHON, P. Changes in particles of coffee powder and extensions to caking. **Food Chemistry**, v. 104, n. 1, p. 122–126, 2007.

SILVA, E. K.; GOMES, M. T. M. S.; HUBINGER, M. D.; CUNHA, R. L.; MEIRELES, M. A. A. Ultrasound-assisted formation of annatto seed oil emulsions stabilized by biopolymers. **Food Hydrocolloids**, v. 47, p. 1–13, 2015.

TAYLOR, A. J.; LINFORTH, R. S. T. Understanding flavour release : the key to better food flavour ? **Nutrition & Food Science**, v. 98, n. 4, p. 202–206, 1998.

UBBINK, J.; KRÜGER, J. Physical approaches for the delivery of active ingredients in foods. **Trends in Food Science and Technology**, v. 17, n. 5, p. 244–254, 2006.

WANG, X.; YUAN, Y.; YUE, T. The application of starch-based ingredients in flavor encapsulation. **Starch/Staerke**, v. 67, n. 3–4, p. 225–236, 2015.

YE, M.; KIM, S.; PARK, K. Issues in long-term protein delivery using biodegradable microparticles. **Journal of Controlled Release**, v. 146, n. 2, p. 241–260, 2010.

YU, T.; MACNAUGHTAN, B.; BOYER, M.; LINFORTH, R.; DINSDALE, K.; FISK, I. D. Aroma delivery from spray dried coffee containing pressurised internalised gas. **Food Research International**, v. 49, p. 702–709, 2012.

ZELLER, B.; GAONKAR, A.; CERIALI, S.; WRAGG, A. Novel Microencapsulation System to Improve Controlled Delivery of Cup Aroma During Preparation of Hot Instant Coffee Beverages. In: GAONKAR, A. G. et al. (Eds.). **Microencapsulation in the Food Industry**. [s.l: s.n.]. p. 455–468.

CONCLUSÃO GERAL

Neste trabalho foi estudada a microencapsulação de óleo de café torrado por *spray drying* utilizando o ultrassom como método de emulsificação. As microcápsulas obtidas foram adicionadas em café solúvel e cappuccino instantâneo e foram avaliados o aumento da intensidade de aroma de café assim como os perfis de liberação de aroma.

A aplicação do Delineamento Central Composto Rotacional (DCCR) permitiu avaliar o efeito dos parâmetros da emulsificação assistida por ultrassom, potência e temperatura, sobre as características de tamanho de gotícula e viscosidade de emulsão, bem como sobre as características das micropartículas de *spray drying*. Foram obtidas emulsões estáveis com distribuição de gotículas monomodal e devido a esta estabilidade da emulsão, as micropartículas tiveram uma alta eficiência de encapsulação.

O aparato que simula a dissolução de café instantâneo e o *Proton Transfer Reaction - Time-of-Flight - Mass Spectrometry* (PTR-ToF-MS) permitiram uma abordagem eficiente da cinética de liberação dos compostos de aroma, que podem ser divididas em 1) efeito burst, 2) dissolução completa da matriz e 3) partição ar-líquido. A volatilidade é a propriedade físico-química que determina o perfil de liberação dos voláteis em café solúvel, enquanto que no cappuccino instantâneo, por este apresentar outros componentes em sua composição (gordura, açúcar, chocolate etc.), além da volatilidade, a polaridade influencia a liberação dos voláteis.

As discussões sobre como o processo de ultrassom, as características físico-químicas dos compostos, o amido OSA como material de parede e o mecanismo de difusão dos aromas através da parede da micropartícula afetaram balanço da composição de aroma de café são inéditas de acordo com a literatura consultada.

As microcápsulas produzidas por *spray drying* e adicionadas em produtos instantâneos de café aumenta a intensidade da maioria dos compostos monitorados sem alteração do perfil dessa liberação.

O trabalho desenvolvido abre novas perspectivas para o desenvolvimento de produtos de café com maior intensidade de aroma.